

**ROLE OF p38 MITOGEN-ACTIVATED PROTEIN KINASE SIGNALING  
AND THE DNA DAMAGE RESPONSE IN THE DEVELOPMENTAL  
TOXICITY INDUCED BY HYDROXYUREA**

by

Serena Banh

A thesis submitted to the Faculty of Graduate Studies and Research of McGill University in  
partial fulfillment of the requirements for the degree of Master of Science

February 2013

Department of Pharmacology and Therapeutics

McGill University

Montreal, Quebec

© Copyright by Serena Banh (2013)

## ABSTRACT

Hydroxyurea is commonly used to treat myeloproliferative diseases and sickle cell anemia. It is also a potent teratogen, inducing severe developmental malformations in many animal models after *in utero* exposure. The administration of hydroxyurea to CD1 mice during organogenesis causes predominantly hindlimb, tail, and neural tube defects. Hydroxyurea inactivates ribonucleotide reductase, inhibiting DNA replication and leading to DNA replication stress and cell death. Hydroxyurea exposure during embryo development also induces oxidative stress and p38 mitogen-activated protein kinase (p38 MAPK) signaling. My goal was to test the hypothesis that hydroxyurea-induced p38 MAPK activation, DNA damage, and cell death are spatially related to the malformations observed in organogenesis-stage embryos.

Hydroxyurea (400 or 600 mg/kg) or saline was given intraperitoneally to CD1 mice on gestation day 9. Dams were euthanized and whole embryos collected at 0.5, 3 and 6 hours post-treatment. Whole embryo protein extracts were used to examine the protein expression and activation levels of the p38 MAPK pathway using Western blots. Five regions of the embryos, including the rostral and caudal neuroepithelium, neural tube, somites and heart, were selected to determine the localization of proteins and DNA damage, using immunofluorescence and confocal microscopy. Subsequently, quantification of protein expression and DNA damage in the embryo at the subcellular level was determined using 3D imaging software.

Hydroxyurea treatment (400 or 600 mg/kg) induced the activation of mitogen-activated protein kinase kinases 3/6 (MEK-3/6), upstream MAP2K3 kinases; phospho-MEK-3/6 immunoreactivity was widespread throughout the embryo after hydroxyurea exposure. Downstream phospho-p38 MAPK was increased in the rostral and caudal neuroepithelium and the neural tube, but not in the somites or heart. Nuclear translocation of phospho-p38 MAPK was

significantly elevated in the rostral and caudal regions of embryos 3 hours after hydroxyurea treatment. Hydroxyurea exposure increased DNA damage, as assessed by the formation of  $\gamma$ -H2AX foci, throughout the embryo; the volume of  $\gamma$ H2AX foci peaked in the caudal neuroepithelium 3 hours post-treatment with hydroxyurea. Pyknotic nuclei and cell fragmentation increased 3 and 6 hours following hydroxyurea exposure in all regions of the embryo except the heart. These data suggest that the p38 MAPK nuclear signaling and DNA damage response triggered by hydroxyurea exposure play key roles in mediating the caudal malformations that are observed. Further work is needed to evaluate these two stress response pathways in order to elucidate the mechanism of embryonic responses to a teratogenic insult.

## RÉSUMÉ

L'hydroxyurée est un médicament couramment utilisé pour traiter les maladies myéloprolifératives et l'anémie falciforme. Il a cependant un puissant effet tératogène, causant de graves malformations congénitales chez de nombreux modèles animaux lorsqu'administré durant la grossesse. Le traitement de souris CD1 avec de l'hydroxyurée pendant la période de l'organogénèse provoque principalement des malformations au niveau des membres postérieurs, de la queue et des anomalies du tube neural. L'hydroxyurée inactive la ribonucléotide réductase ce qui diminue la réplication de l'ADN, et mène à la mort cellulaire. Une exposition à l'hydroxyurée au cours du développement embryonnaire induit également un stress oxydatif et active la voie de signalisation p38 mitogen-activated protein kinase (MAPK p38). Mon objectif était de tester l'hypothèse selon laquelle les malformations observées suite à une exposition à l'hydroxyurée lors de l'organogénèse sont colocalisées avec une activation de MAPK p38, des dommages créés à l'ADN et une mort cellulaire.

Au jour 9 de la gestation, des souris CD1 ont été injectées avec de l'hydroxyurée (400 ou 600 mg / kg) ou une solution saline par voie intrapéritonéale. Les mères ont été euthanasiées et les embryons prélevés à 0,5, 3 et 6 heures post-traitement. L'expression de protéines et des niveaux d'activation de la voie de signalisation MAPK p38 ont été quantifiée par western blot réalisé sur des extraits protéiques entiers de l'embryon. Les protéines et les dommages créés à l'ADN ont été localisés par microscopie confocale et immunofluorescence dans cinq régions de l'embryon comprenant le neuroépithélium rostrale et caudale, le tube neural, les somites et le cœur. Leur localisation au niveau subcellulaire a ensuite été déterminée en utilisant un logiciel d'imagerie 3D.

L'hydroxyurée (400 ou 600 mg / kg) induit l'activation des kinases activées par les mitogen-activated protein kinase kinase 3/6 (MEK-3/6) de la catégorie des MAP2K3 kinases; Les embryons provenant des groupes traités à l'hydroxyurée démontrent une immunoréactivité positive de phospho-MEK-3/6 détectée dans les cinq régions analysées de l'embryon. L'expression de phospho-p38 MAPK, la cible cellulaire de MEK-3/6, est élevée dans le neuroépithélium rostrale et caudale et le tube neural, mais pas dans les somites ou les cellules cardiaques. De plus, une translocation nucléaire de phospho-p38 MAPK est significativement induite dans les régions rostrales et caudales des embryons collectés 3 heures après le traitement à l'hydroxyurée. L'exposition à l'hydroxyurée est associée avec une augmentation des dommages créés à l'ADN, telle que démontrée par la formation de foyers de  $\gamma$ H2AX dans les cinq régions étudiées de l'embryon. . Le nombre maximal de foyers  $\gamma$ H2AX est observé dans le neuroépithélium caudale, 3 heures après l'exposition à l'hydroxyurée. Une augmentation du nombre de noyaux pycnotiques et de cellules avec une ADN fragmentée est détectée 3 à 6 heures après l'exposition à l'hydroxyurée dans toutes les régions de l'embryon à l'exception du cœur. Ces données suggèrent que l'activation de la voie de signalisation MAPK p38 nucléaire et les conséquences des dommages créés à l'ADN provoquées par une exposition à l'hydroxyurée jouent un rôle clé dans l'induction des malformations caudales observées. Des études supplémentaires sont néanmoins nécessaires afin d'investiguer ces deux voies de réponse au stress et ce, dans un but d'élucider les mécanismes de défenses embryonnaire face à un tératogène.

## TABLE OF CONTENTS

ABSTRACT .....	i
RÉSUMÉ.....	iii
TABLE OF CONTENTS .....	v
LIST OF FIGURES .....	viii
LIST OF TABLES .....	x
ABBREVIATIONS .....	xi
ACKNOWLEDGEMENTS.....	xiv
PREFACE.....	xvi

### Chapter One: Introduction

1.1 Hydroxyurea .....	- 2 -
1.1.1 Mechanism of Action .....	- 2 -
1.1.2 Hydroxyurea developmental toxicity .....	- 4 -
1.2 Redox Homeostasis and Oxidative Stress .....	- 5 -
1.2.1 Pro-oxidative mechanisms .....	- 6 -
1.2.2 Anti-oxidative defense mechanism .....	- 7 -
1.2.3 Cellular responses to oxidative stress.....	- 8 -
1.2.4 Developmental consequences of redox alterations .....	- 10 -
1.3 Redox Control during Embryo Development.....	- 11 -
1.3.1 Normal mouse embryo development .....	- 11 -
1.3.2 Reactive Oxygen Species (ROS) signaling during embryogenesis .....	- 13 -
1.3.3 Embryonic antioxidative capacity during organogenesis .....	- 14 -
1.3.4 ROS-mediated teratogenesis .....	- 15 -
1.4 p38 mitogen-activated protein kinases (p38 MAPK).....	- 17 -
1.4.1 The p38 MAPKs family .....	- 18 -
1.4.2 Regulation of p38 MAPKs in cellular processes .....	- 18 -
1.4.3 Cellular localization .....	- 21 -
1.4.4 Role of p38 MAPKs in stress responses.....	- 23 -
1.4.4.1 Apoptosis.....	- 23 -

1.4.4.2	Cell Cycle Checkpoints.....	- 24 -
1.4.4.3	Survival .....	- 26 -
1.4.5	p38 MAPK in embryo development .....	- 27 -
1.5	The DNA damage response pathway.....	- 28 -
1.5.1	DNA Double Strand Breaks (DSBs).....	- 29 -
1.5.2	DNA Replication Stress.....	- 29 -
1.5.3	DNA Damage Recognition.....	- 31 -
1.5.3.1	Role of $\gamma$ H2AX in DDR signaling .....	- 32 -
1.5.3.2	$\gamma$ H2AX foci .....	- 33 -
1.5.3.3	Spatiotemporal dynamics of $\gamma$ H2AX.....	- 34 -
1.5.4	DNA repair.....	- 35 -
1.5.4.1	Double-Strand Break Repair .....	- 36 -
1.5.4.2	DNA Repair during <i>in utero</i> development.....	- 37 -
1.6	Hypothesis.....	- 38 -

Connecting Text.....	- 40 -
----------------------	--------

**Chapter Two: Hydroxyurea Exposure Triggers Tissue Specific Activation of p38 Mitogen-Activated Protein Kinase Signaling and the DNA Damage Response in Organogenesis Stage Mouse Embryos**

Introduction .....	- 43 -
Materials and Methods.....	- 45 -
Results .....	- 52 -
Discussion.....	- 56 -
Figures and Legends .....	- 60 -
Supplementary Data Figure Legends and Tables .....	- 70 -

**Chapter Three: Discussion**

3.1	Summary .....	- 83 -
3.2	Role of p38 MAPKs in hydroxyurea induced developmental toxicity .....	- 83 -
3.3	DNA damage response in hydroxyurea induced developmental toxicity .....	- 86 -

3.4	The role of oxidative and replication stress in hydroxyurea induced developmental toxicity	- 90 -
3.5	Conclusions	- 92 -
	References	- 94 -

## LIST OF FIGURES

Figure 1.1 Molecular structure of hydroxyurea .....	- 2 -
Figure 1.2 The univalent path for oxygen reduction and formation of ROS. ....	- 7 -
Figure 1.3 ROS detoxification by antioxidative enzymes.....	- 8 -
Figure 1.4 Overview of the p38 MAPK signaling pathway.....	- 21 -
Figure 1.5 The role of p38 MAPKs in the G1/S and G2/M checkpoints.....	- 25 -
Figure 1.6 Structure of replicating DNA contributing to genomic instability.....	- 31 -
Figure 2.1 HU induced activation of MEK-3/6 .....	- 60 -
Figure 2.2 The localization of activated MEK-3/6 in GD 9 embryos exposed to HU.....	- 61 -
Figure 2.3 Intensity means of phospho-MEK-3/6 in different regions of GD 9 embryos .....	- 62 -
Figure 2.4 HU induced activation of p38 MAPK.....	- 63 -
Figure 2.5 The localization of phospho-p38 MAPK in GD 9 embryos exposed to HU.....	- 64 -
Figure 2.6 Total intensity means of phospho-p38 MAPK in different regions of GD 9 embryos... .....	- 65 -
Figure 2.7 Nuclear intensity means of phospho-p38 MAPK in different regions of GD 9 embryos .....	- 66 -
Figure 2.8 $\gamma$ H2AX staining in GD9 embryos exposed to HU .....	- 67 -

Figure 2.9 $\gamma$ H2AX focal volumes in different regions of GD 9 embryos .....	- 68 -
Figure 2.10 Pyknotic nuclei in different regions of the GD 9 embryos exposed to HU. ....	- 69 -
Figure S1. Animation movie of nuclear quantification by IMARIS.....	- 70 -
Figure S2. The five different regions of the whole embryo targeted for quantitative analysis.-	71 -
Figure S3. Basal level expression of markers in saline-treated embryos in the five different regions targeted for analysis. ....	- 72 -
Figure S4. Original images of $\gamma$ H2AX staining of GD 9 embryos .....	- 73 -

## LIST OF TABLES

Table S1: Summary of immunofluorescence analysis of phospho-MEK-3/6..... - 74 -

Table S2: Summary of immunofluorescence analysis of total phospho-p38 MAPK..... - 76 -

Table S3: Summary of immunofluorescence analysis of nuclear phospho-p38 MAPK ..... - 78 -

Table S4: Summary of immunofluorescence analysis of  $\gamma$ H2AX foci volume ..... - 80 -

## ABBREVIATIONS

ANOVA	analysis of variance
APH	aphidicolin
AP-1	activator protein-1
ASK1	apoptosis signal-regulating kinase 1
ATM	ataxia-telangiectasia mutated kinase
ATR	ATM- and Rad3-related
Bax	Bcl-2-associated X protein
CAT	catalase
DNA-PK	DNA dependent protein kinase
dNTP	deoxyribonucleoside triphosphate
DDR	DNA damage response
DSBs	DNA double strand breaks
ERK	extracellular-regulated protein kinase
Gadd45 $\alpha$	growth arrest and DNA damage inducible 45 $\alpha$
GAPDH	glyceraldehyde-3-phosphate dehydrogenase
GD	gestational day
GSH	reduced glutathione
GSSG	oxidized glutathione
h	hour
HIF-1	hypoxia inducible factor-1

HR	homologous recombination
HU	hydroxyurea
IRIF	ionizing radiation-induced foci
JNK	c-Jun N-terminal protein kinase
Mdm2	murine double minute 2
MAPK	mitogen-activated protein kinase
MAPKAP	mitogen-activated protein kinase-activated protein
MAP2K	mitogen-activated protein kinase kinase
MAP3K	mitogen-activated protein kinase kinase kinase
MEKK1	MAPK/ERK kinase kinase 1
MKP	mitogen-activater protein kinase phosphatase
MK2	MAPKAP kinase-2
NBS1	Nijmegen breakage syndrome 1
NF- $\kappa$ B	nuclear factor kappa B
NHEJ	nonhomologous end-joining
PBN	$\alpha$ -phenylbutyl nitron
PBS	phosphate buffered saline
PFA	paraformaldehyde
PI3K	phosphatidyl-inositol-3-kinase
PP	protein phosphatase
PPAR	peroxisome proliferator-activated receptor

PTP	protein tyrosine phosphatase
RNR	ribonucleoside diphosphate reductase
ROS	reactive oxygen species
S.E.M	standard error of the mean
SOD	superoxide dismutase
TAB-1	TAK-1 binding protein
TAK-1	transforming growth factor $\beta$ -activated kinase-1
TAO	thousand-and-one amino acid
TNF $\alpha$	tumour necrosis factor alpha
Trx	thioredoxin
Wnt	wingless/Int (mouse mammary tumour virus integration site)
Xpd	xeroderma pigmentosum complementation group D
4-HNE	4-hydroxynonenal
8-oxoG	8-oxoguanine

## ACKNOWLEDGEMENTS

First and foremost, I would like to thank my thesis supervisor, Dr. Barbara Hales, for giving me this opportunity and opening my eyes to the world of embryos and teratology. Her guidance and impeccable work ethics were essential to my learning for the past years.

I would like to thank Chunwei Huang for her assistance in all the tedious and laborious trouble shooting and general management of the lab. Without her, the environment of the laboratory would not have been as comforting.

I would also like to specially thank Ava Schlisser who is my mentor and team partner. Her patience and guidance in teaching me various valuable techniques, stimulating discussion and feedback were indispensable.

I would like to thank all the senior members of the Dr. Barbara Hales and Dr. Bernard Robaire labs, including research associates, post-doctoral fellows and PhD students, for their support and always being available to discuss thoughts; most importantly, for their valuable friendships.

I would like to thank all my companions, Thomas Nardelli, Anne Marie Downey, France-Hélène Paradis, Stephen Nagy and Vinidhra Vaitheeswaran for all the memorable times in- and outside of the lab, for their encouragement and irreplaceable friendship.

I would like to thank the Imaging Facility Team, Aleksandrs Spurmanis and Claire Brown for their diligent efforts and guidance in using the IMARIS software and Jacynthe Laliberté for her assistance with confocal microscopy.

I would like to thank my academic committee, Dr. Terry Hébert, Dr. Dusica Maysinger, and Dr. Bruce Allen for their advice, discussion and suggestions throughout my graduate studies.

This work was supported by a grant through the Canadian Institute for Health Research. I would like to thank the CIHR training program in Reproduction, Early Development, and the Impact on Health (REDIH), for providing scholarship, valuable training, mentorship and feedbacks throughout my graduate studies. I would also like to thank Fonds de la recherche en santé Québec (FRSQ) for the Master fellowship.

## **PREFACE**

### **Format of the thesis**

This is a manuscript-based thesis, which conforms to the “Thesis Preparation and Submission Guideline” of the Faculty of Graduate Studies and Research at McGill University. The thesis consists of three chapters: Chapter One, Introduction provides an overview of the model teratogen, hydroxyurea, and oxidative stress. Stress response pathways including the p38 mitogen-activated protein kinase (MAPK) and DNA damage response pathway are also reviewed. Lastly, the hypothesis and objectives are presented in this chapter as well.

Chapter Two, the data chapter, is published in *Toxicological Sciences* 2013 (doi: 10.1093/toxsci/kft069). This chapter includes detailed methodology.

Chapter Three provides a general discussion of the results and suggestions for future studies in addition to the final conclusion. References are provided at the end of the thesis.

### **Contribution of Authors**

All the experiments presented in this thesis were performed by the candidate.

## **Chapter One**

### **Introduction**

## 1.1 Hydroxyurea

Hydroxyurea (HU) ( $\text{CH}_4\text{N}_2\text{O}_2$ ) is a simple organic compound currently used clinically for the treatment of sickle cell anemia (Walker et al., 2011), myeloproliferative diseases such as chronic myelogenous leukemia (Kennedy, 1972), and solid tumours (Madaan et al., 2012).

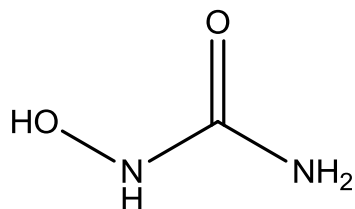


Figure 1.1 Molecular structure of hydroxyurea

HU is easily soluble in water and is rapidly distributed throughout the total body water. Following intraperitoneal administration of HU to pregnant rats during organogenesis, the half-life of HU has been reported to be 15 minutes in the maternal plasma and about 60-85 minutes in the embryo. Moreover, at 1 h post-treatment, the concentration of HU in the embryos exceeded that in plasma (Wilson et al., 1975).

### 1.1.1 Mechanism of Action

HU is a potent DNA synthesis inhibitor *in vitro* and *in vivo* and is selectively toxic to proliferating cells which are in the S-phase. It directly inhibits the enzyme ribonucleoside diphosphate reductase (RNR) by destroying a tyrosyl free radical in the catalytic center of the R2 unit of the enzyme (Krakoff et al., 1968). This hinders the reductive conversion of ribonucleotides to deoxyribonucleotides and thus limits *de novo* synthesis of the deoxyribonucleoside triphosphates (dNTPs) necessary for DNA synthesis (Sneeden and Loeb, 2004). Alterations and imbalances in the dNTP pools affect replication dynamics by impeding

fork progression, leading to replication stress (Poli et al., 2012). This causes the destabilization or “collapse” of the replication forks at specific regions of the chromosomes where fragility occurs, leading to chromosome breakage (Feng et al., 2011). Exposure to HU induces DNA double strand breaks, and triggers phosphorylation of H2AX and the formation of H2AX foci at the arrested replication forks (Ward and Chen, 2001).

HU also exhibits another apparently independent action, which is the rapid killing of cells. The appearance of frank cellular necrosis within embryos is extremely rapid. between 30-90 minutes after administration of the drug (Balaban et al., 2005). However, the manifestation of inhibited DNA synthesis, as measured by effects on 3H-thymidine incorporation, did not occur until 3-5 hrs after the drug was administered (DeSesso and Goeringer, 1990). Moreover, in an early study of the mechanism of toxicity of HU, the addition of exogenous dNTPs failed to protect the cells from HU (Berlett and Stadtman, 1997). Therefore, the ability for HU to inhibit RNR could explain the inhibition of DNA synthesis, but it does not explain the ability to kill cells rapidly. With such observations, these had led investigators to assume that HU acts through a common mechanism which not only will inhibit RNR but also will attack other cell components.

The chemical structure of HU contains a hydroxylamine group (-HNOH; Figure 1), which has the potential to react with oxygen in biological fluids and generate low levels of reactive oxygen species, including the highly reactive hydroxyl radical and hydrogen peroxide. Free radicals typically undergo chain reactions; therefore, the low levels of hydroxyl radicals can be readily propagated in aqueous solutions, thereby attaining biologically effective concentrations. The biological impact of these radical reactions is both rapid and devastating. Due to the extreme reactivity and non-specificity of the hydroxyl radical, it could inflict great

damage within cells, including cross-linking and inactivating enzymes and macromolecules (lipids, proteins, nucleic acids) within both the cytoplasmic and nuclear compartments, as well as initiating lipid auto-oxidation in cell membranes (DeSesso, 1979). The production of reactive oxygen species can induce oxidative stress, which can render cellular metabolism ineffective, leading to cell cycle arrest and cell death. DeSesso et al., (1979) therefore proposed that reactive oxygen species produced by HU are responsible for the rapid cell death induced in embryos and play a role in teratogenic insult. In support of this hypothesis, when antioxidants or a free-radical scavenger pre-treatment is administered prior to HU, the outcome is a delayed onset of embryonic cell death and a lowered incidence of malformations (Desesso et al., 1994). However, the underlying role of oxidative stress in mediating HU-induced developmental toxicity remains elusive.

### 1.1.2 Hydroxyurea developmental toxicity

The administration of HU at specific stages of pregnancy has been shown to cause fetal abnormalities in many different animal models. For instance, given in single intraperitoneal doses to the pregnant rat from gestation day 9 through 12, fetuses at 21 days exhibited malformations. These malformations included severe and characteristic injury to the fetal brain, such as exencephaly and encephalocele, cleft palate and lip, clubbed and retarded appendages, ectro- and polydactyl, as well as short and kinked tail (Hempstock et al., 2003). When HU was injected into the yolk sac of a 4 day chick embryo, it increased the incidence of micromelia in surviving chick embryos at 18 days (Kennedy, 1972). In a recent study, when organogenesis stage mouse embryos were exposed to HU *in utero*, mouse fetuses exhibited growth retardation and external malformations such as short and curly tail, spina bifida, hypoplastic limbs and

hydrocephaly. Double-stained skeletons of the fetuses displayed severe skeletal and vertebral defects, predominantly in the lumbosacral region and hindlimbs (Yan and Hales, 2006).

Increased frequencies of congenital anomalies have also been reported among the offspring of other animals, including rabbits, hamsters, cats, dogs and rhesus monkeys, when treated with HU doses that are equivalent to 2-25 times those used clinically in humans (Lee et al., 2005; Li et al., 2006; Madaan et al., 2012).

The potential teratogenicity caused by HU discourages women who take this drug from becoming pregnant. Therefore, developmental toxicity studies in human are often based on a small sample size and not controlled. One clinical case report studied and evaluated the outcome of 32 pregnancies among women with haematological conditions who were exposed to HU. Teratogenic effects were evaluated after first trimester exposures; no major malformations were described after HU exposure during this period or among the 24 liveborns. However, there were 2 *in utero* fetal deaths and 1 spontaneous abortion. Among the liveborn infants, 9 were premature, 5 presented with neonatal respiratory distress and 3 had minor abnormalities such as hip dysplasia, unilateral renal dilation and pilonidal sinus (Khera, 1979). Although these complications might be attributed to the underlying haematological condition, nevertheless, this report indicates that HU is a possible developmental toxicant and should be avoided whenever possible until more data has accumulated.

## **1.2 Redox Homeostasis and Oxidative Stress**

The normal development of an embryo is a complex process that constitutes a series of regulatory events that underlie precise spatial and temporal control. Throughout development, the embryo encounters ever changing environments which challenge its metabolism. Oxygen is

vital for embryogenesis, but under specific conditions, it can give rise to unstable molecules such as reactive oxygen species (ROS). If produced excessively, ROS can be hazardous and alter biological functions. Under normal conditions, cellular antioxidant or defense systems detoxify ROS and prevent their toxicity. Therefore, redox homeostasis plays an important role in the regulation of cellular gene expression. It is defined by the equilibrium between pro- and anti-oxidative processes. Both sides of the redox equilibrium equation involve enzymatic and non-enzymatic processes and their proper balance is of major biological importance. This section gives a brief review of the regulatory principles of redox homeostasis by characterizing the most important pro- and anti-oxidative reactions, their regulatory importance and cellular responses to oxidative stress.

### 1.2.1 Pro-oxidative mechanisms

Molecular dioxygen ( $O_2$ ) has a fairly stable electron configuration and is not particularly reactive. This is also the case for its 4 electron reduction product, water ( $H_2O$ ). However, if the dioxygen is not completely reduced to water, it can lead to the production and activation of ROS, including superoxide ( $\bullet O_2^-$ ), hydrogen peroxide ( $H_2O_2$ ), or the hydroxyl radical ( $\bullet OH$ ) (Figure 1.2). Due to the presence of an unpaired electron, ROS is highly reactive; the hydroxyl radical is considered to be the most toxic ROS. *In vivo*, it has a half life of  $10^{-9}$  s and may react with the first molecule it encounters, including proteins, lipids and nucleic acids. This could lead to deleterious effects such as cell membrane peroxidation, protein inactivation and degradation (El-Benna et al., 2009), as well as DNA base oxidation and strand breaks (Farber and Baserga, 1969). The majority of ROS is formed via mitochondrial electron transport; leakage occurs at intermediate steps during the process of ATP production, leading to single-electron reductions of

oxygen. It is estimated that about 1-2% of the total molecular dioxygen respired is converted into ROS (D'Autreaux and Toledano, 2007). Moreover, a variety of enzymatic reactions, such as NADPH oxidase, cytochrome P450 isoforms and cyclooxygenases, may contribute to cellular ROS formation (DeSesso, 1979; 1981; DeSesso and Jordan, 1977). In addition to cellular metabolism, ROS is also generated by the induction of environmental stimuli such as irradiation or xenobiotics.

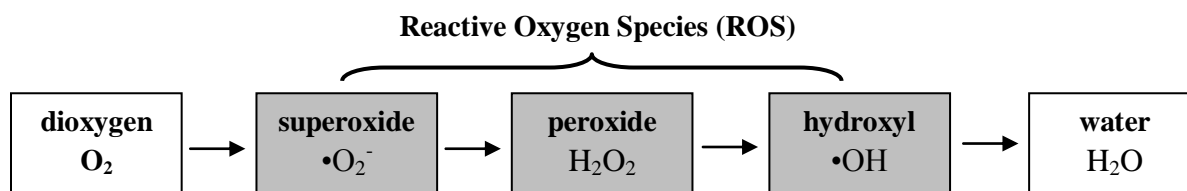


Figure 1.2 The univalent path for oxygen reduction and formation of ROS. Sequential one electron reduction of molecular dioxygen leads to the formation of ROS. Modified from (Dennery 2007).

### 1.2.2 Anti-oxidative defense mechanism

To avoid excessive damage from ROS, a complex antioxidant defense system has evolved to overcome this challenge. It consists of both non-enzymatic antioxidants (ascorbic acid, tocopherols and bililrubin) and antioxidative enzymes, such as superoxide dismutase, catalases, the glutathione (GSH) system and others. Superoxide dismutase (SOD) plays an important role in the antioxidant defense system; it catalyzes the conversion of superoxide to water and hydrogen peroxide.  $H_2O_2$  is then broken down by catalase (CAT) into water and less reactive oxygen molecules (Feng et al., 2011). The glutathione system includes glutathione, glutathione reductase and glutathione peroxidase . Using glutathione as a substrate, glutathione peroxidase catalyzes the breakdown of hydrogen peroxide and organic hydroperoxides. The cycle continues

as oxidized glutathione (GSSG) is converted back to reduced glutathione (GSH) by glutathione reductase with the use of NADPH as a cofactor (Fig 1.3). Altogether, non-enzymatic antioxidants and antioxidative enzymes detoxify ROS and maintain cellular redox status.

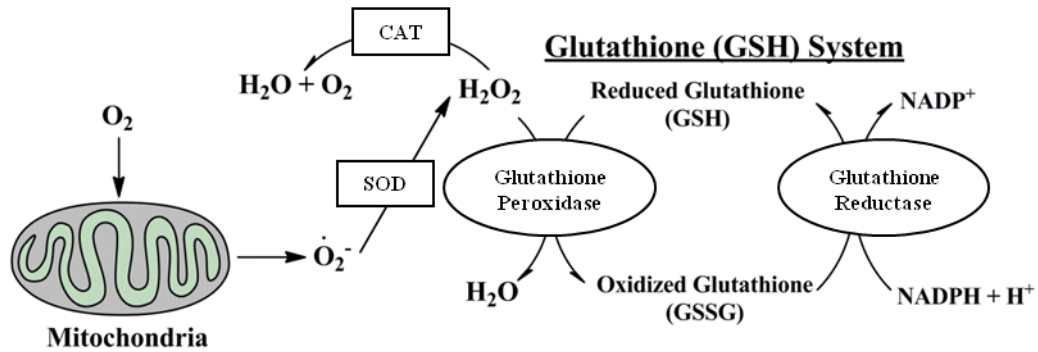


Figure 1.3 ROS detoxification by antioxidative enzymes. The major source of superoxide is the mitochondria. Anti-oxidative enzymes, including superoxide dismutase (SOD),; catalase (CAT),; and the glutathione system (GSH) help to sequester and eliminate ROS. Modified from(Gaetani, Ferraris et al. 1996).

### 1.2.3 Cellular responses to oxidative stress

Due to the high reactivity of ROS and their ability to modify biological components, these modifications can often lead to deleterious effects. The survival of cells, therefore, depends on the ability of cells and tissues to adapt to or to resist oxidative stress, and repair or remove damaged molecules or cells. In response to oxidative insults, numerous stress response pathways have evolved and are rapidly activated, thereby influencing cell survival and death. These pathways exert their influences largely through the modulation of transcription factor activities, which change the pattern of gene expression.

Mitogen-activated protein kinases (MAPKs) encompass a large number of

serine/threonine kinases and are one of the major pathways that mediate the activation of transcription factors in response to oxidative stress. These kinases mediate signal transduction from the cell surface to the nucleus, which in turn leads to changes in gene expression by mediating their effects through phosphorylation of transcription factors. Based on structural differences, these kinases are categorized into three subfamilies, including the extracellular signal-regulated kinases (ERK), c-Jun N-terminal kinases (JNK) and p38 MAPKs. All three subfamilies have been shown to be activated in response to oxidant injury. Therefore, they could all potentially influence the ability of cells to survive or die. Maternal exposure to HU, in particular, was shown to induce oxidative stress which activates JNK and p38 MAPK in embryos (Yan and Hales, 2008). In addition, MAPK pathways play crucial roles during embryo development. The extent to which these pathways mediate teratogen-induced abnormal development remains elusive.

Numerous transcription factors are phosphorylated by MAPK in response to oxidative stress, including activator protein-1 (AP-1) and p53 (Bulavin et al., 1999; Filosto et al., 2003). AP-1 is an early response redox-sensitive transcription factor and with both pro- and anti-apoptotic functions. In response to oxidative stress, AP-1 regulates cell cycle checkpoint, antioxidant defense and apoptosis (Karin and Shaulian, 2001; Pinkus et al., 1996). The binding of AP-1 to DNA allows it to directly regulate gene expression; for example, activation of AP-1 has been implicated in regulating p53 expression levels (Schreiber et al., 1999). In previous studies, HU exposure induces AP-1 DNA binding activity in organogenesis-stage embryos and yolk sacs at early time points (Yan and Hales, 2005). This suggests the possibility of using AP-1 DNA binding activity as an efficient measure to screen potential developmental toxicants.

DNA damage caused by ROS activates p53 a universal sensor of genotoxic stress. In addition, p53 is activated by p38 MAPK and JNK signaling pathways (Bulavin et al., 1999; Buschmann et al., 2001). Furthermore, optimal induction and activation of p53 require the activation of ataxia-telangiectasia mutated (ATM) kinase, a pathway essential in coordinating the detection of DNA damage and DNA repair (Shackelford et al., 2001). In the absence of functional ATM, cells show disruption in G1/S and G2/M cell cycle checkpoints, rendering them hypersensitive to oxidative damage (Lavin and Shiloh, 1997). Therefore, ATM serves a protective role in response to oxidative stress via activation of downstream effectors involved in cell cycle checkpoint functions and DNA damage detection, thus allowing cells the time to repair oxidative damage.

Overall, ROS elicit a wide spectrum of responses that are dependent upon the severity of the oxidative damage. ROS can directly or indirectly modulate proteins, specifically transcription factors, and trigger a multitude of signaling cascades, as discussed. Ultimately, these signal transduction pathways result in changes of gene expression, influencing cellular outcome.

#### 1.2.4 Developmental consequences of redox alterations

Precise control of cellular redox homeostasis is essential for normal cell function and is of particular importance for developmental processes such as embryogenesis. During development, the embryo encounters variable levels of ROS. These reactive intermediates originate not only from the developing embryo itself, but also from maternal metabolism. ROS produced by the mother can cross the placental barrier and act as a signal transducer to modify embryonic processes. Redox alterations can pose complex consequences to biological systems, but the main effects include changes to cellular energy metabolism and gene expression.

Regulation of gene expression takes place at various levels of the expression cascade and redox changes can affect epigenetic, transcriptional, and post-transcriptional mechanisms. AP-1, hypoxia inducible factor-1 (HIF-1), nuclear factor  $\kappa$ B (NF- $\kappa$ B), wingless and integration site for mouse mammary tumor virus (Wnt) and peroxisome proliferator-activated receptor (PPAR) are included among the many transcription factors that are redox-sensitive. These are important players in transcriptional regulation and are vital to cell signalling pathways that dictate proliferation, differentiation, and apoptosis. Thus, they can mediate significant effects in embryonic development.

### **1.3 Redox Control during Embryo Development**

The redox system must be tightly controlled for normal embryogenesis; a dysregulated redox equilibrium can severely hamper embryo development. At certain developmental stages, embryos are especially susceptible to redox alterations and at these stages the antioxidant defense system of the embryo is of particular importance. This section gives a brief overview of normal mouse embryogenesis, the redox control and antioxidative capacity exhibited by the embryo during this sensitive period, as well as documented teratogenicity that is mediated by ROS and dysregulated redox equilibrium.

#### **1.3.1 Normal mouse embryo development**

The gestation period of mice lasts 18 to 19 days (gestation day (GD) 18 and 19) following the fertilization of an oocyte and a spermatozoon (gestation day 0) (Dennery, 2007). Mouse embryos can be staged according to a variety of criteria, including somite number, cell number and crown rump length (Sauer et al., 2000b). The ages of the embryos can also be given based on the days after conception abbreviated to 'dpc' or days post-conception.

Many of the events in embryo development occur after the embryos implant in the wall of the uterus (Ruiz-Gines et al., 2000). Gastrulation occurs at 6.5-7 dpc, in which the primitive groove can be clearly seen, and provides the first evidence of an embryonic axis. Over the period between 7.5-8.5 dpc, neurulation and early organogenesis begin. The neural folds form on either side of the embryonic axis and become elevated. This process of primary neurulation forms the primitive neural tube; it initiates the development of central nervous system and continues throughout the entire life of the organism. Similarly, the cardiogenic plate is first seen at this stage, when it starts to differentiate into the heart, initiating the development of the cardiovascular system and erythropoiesis (Ruiz-Gines et al., 2000).

At 8.5 dpc, the embryo undergoes the process of 'turning', during which the configuration of the embryonic axis changes. This process converts the embryo from being inside-out to adopting the familiar 'fetal' position. At the same time, the embryo is completely surrounded by its amnion and yolk sac. The rostral neuropore also closes at this time to form the rostral neural tube and optic vesicles; these vesicles are a developmental hallmark for embryos at 9 dpc. Once the embryo has 'turned', it develops rapidly. Over the period from 8.5-13 dpc, the principal features of each of the various body systems become established; these include the hindlimbs, lungs, salivary glands, gut and liver (Dennerly, 2007). The period between 13.5 dpc and birth is when embryo begins to display fine structural detail of each system as it grows and becomes functional. As all components of the skeletal system are readily formed, the developmental age can now be established by analyzing ossification centers (Sastre et al., 1996a).

### 1.3.2 Reactive Oxygen Species (ROS) signaling during embryogenesis

A variety of basic cellular processes, such as metabolism, proliferation, differentiation and apoptosis, are affected by the cellular redox equilibrium. Proliferating mammalian cells exhibit a broad spectrum of responses to oxidative stress. The effects of ROS are variable and are dependent on the cell type, on the metabolic state of the embryos, and on the intensity and duration of the stimulus. For example, when cells were incubated with glucose oxidase, an enzyme that generates hydrogen peroxide continuously, proliferation of bovine aortic endothelial cells was found to be significantly increased (Yarbro, 1968). Moreover, proliferation was suppressed with the overexpression or administration of an antioxidant enzyme, such as catalase or superoxide dismutase (Ferm, 1966). These observations demonstrated the essential role of ROS as second messengers in cell proliferation and cell growth. On the other hand, high concentrations of hydrogen peroxide lead to permanent cell growth arrest, cell disintegration and necrosis in mammalian fibroblasts (Sastre et al., 1996b).

During embryogenesis, cell differentiation and maturation are an integral part of this process and complete arrest of differentiation in early embryogenesis is lethal. Embryonic stem cells differentiate within a certain lineage, resulting in the formation of highly specialized cell types. These differentiation processes are characterized by major metabolite alterations and are critically dependent on the intracellular redox state. Previous studies have demonstrated the crucial role of ROS in driving cardiac and osteoclast differentiation by regulating cell-type specific transcription factors (Bard, 1994; Davison and Baldock). On the other hand, an overexpression of antioxidant enzymes or deregulated exposure of embryonic stem cells to ROS

can induce marked alterations in the differentiation pattern, such as an inhibition of cardiomyogenesis and vasculogenesis (Kaufman, 1992).

Apoptosis, or programmed cell death, also plays an essential role during embryogenesis in sculpting embryonic structures. In mouse embryos, developmental apoptosis and ROS formation appears to be spatially correlated; the necrotic zones of developing limbs represent a classic example. During embryonic limb development, high levels of ROS are present in the interdigital regions of primitive limbs and, simultaneously, pronounced cell death and downregulated antioxidative enzymes are detected in these areas (Schnabel et al., 2006). Moreover, the addition of an antioxidant prevents digit individualization as well as interdigital cell death (Salas-Vidal et al., 1998). Similarly, neuronal apoptosis correlates with high ROS levels in a time-dependent manner and is also prevented by antioxidants during embryonic development of the central nervous system (Sanchez-Carbente et al., 2005). These data suggest that an increased formation of ROS is a primary process required for induction of apoptosis during mouse embryonic development.

### 1.3.3 Embryonic antioxidative capacity during organogenesis

In the uterus, during the early post-implantation period, maternal arterial blood flow to the placenta is not fully established (Wilson et al., 1975). Therefore, oxygen flow to the embryo is limited and the embryo resides in an environment that is relatively hypoxic. The placental circulation is established between the embryo and mother at around GD 9 in mice, during organogenesis. The yolk sac of the placenta regresses and the allantoic placenta begins to provide nutrients and establish respiratory exchange. This results in a sudden acute exposure to higher concentrations of oxygen in the embryo. The embryo makes a rapid transition from

anaerobic to aerobic metabolism, which is referred to as redox switching (Dennery, 2007; Sneed and Loeb, 2004). The mother provides low molecular weight antioxidants (GSH, vitamin C, and vitamin E) to the embryos to protect them from oxidative damage, unfortunately, the enzymatic activity of embryonic antioxidative enzymes is much lower than that of the mother (Wiese et al., 1995). Thus, during organogenesis, embryos are particularly sensitive to oxidative damage. Concomitantly, the embryo is most susceptible to induction of malformations by developmental toxicants at this stage since the basic structures of major organs are being formed during this period.

#### 1.3.4 ROS-mediated teratogenesis

Teratogenesis includes developmental retardation, organ malformation and functional deficiencies, which are commonly a result of dysregulation of embryogenesis. Embryonic redox homeostasis is an important factor of teratological risk, and both embryonic and maternal ROS formations have been implicated. Although the major source of ROS originates from the mitochondria, ROS can be generated by xenobiotics as well. Approximately 2500 chemicals have been identified as potential teratogens in humans (Hansen, 2006), and many of these compounds, such as thalidomide, phenytoin, ethanol and tobacco smoke are also capable of inducing ROS production (Ornoy, 2007; Peng et al., 2005; Sauer et al., 2000a; Winn and Wells, 1995). With bioactivation during maternal metabolism, a number of proteratogens generate reactive radicals, which can be transferred to the embryo (Wells and Winn, 1996) and induce embryopathies. Many of these toxicants can often induce multiple malformations, including neural tube and limb defects (Fantel and Person, 2002). Interestingly, treatment with antioxidants

can partially or completely prevent oxidative damage and teratogenicity caused by these development toxicants (Kim et al., 1997).

One of the most notorious and best studied human teratogens is thalidomide. The primary outcome of thalidomide exposure during a critical window in development was the induction of cell death in limbs, leading to limb truncations (phocomelia) (Lenz and Knapp, 1962). These malformations have been related to oxidative stress in experiments using limb bud cells removed from rat and rabbit embryos (Hansen et al., 2002). This appears to have resulted from the depletion of glutathione, DNA oxidation, and the activation of redox sensitive transcription factors, such as AP-1 and NF- $\kappa$ B, through the signaling of MAPKs (Hansen and Harris, 2004; Hansen et al., 2002; Knobloch et al., 2007). Moreover, co-administration of the free radical trapping agent,  $\alpha$ -phenylbutyl nitron (PBN), attenuated thalidomide-induced DNA oxidation as well as the manifestation of phocomelia (Hansen et al., 1999). Similarly, pre-treatment with antioxidants prior to HU treatment delayed the onset of embryonic cell death and lowered the incidence of malformations, specifically limb defects (Desesso et al., 1994).

Previous studies from our laboratory investigated the underlying mechanism of oxidative stress and HU-induced teratogenicity. HU treatment enhanced the production of 4-hydroxynonenal (4-HNE) protein adducts, a major end product of lipid peroxidation, in malformation sensitive regions of the embryos, namely the somites and caudal neural tube (Yan and Hales, 2006). Moreover, some of the major proteins that were modified by 4-HNE are involved in energy metabolism, including glyceraldehyde-3-phosphate dehydrogenase (GAPDH) and aldolase A1 (Schlisser et al., 2010). Furthermore, HU exposure also increased AP-1 DNA binding through the activation of p38 MAPK and JNK pathways (Yan and Hales, 2005; 2008). Most interestingly, selective inhibition of these MAPK pathways resulted in differential adverse

outcomes, suggesting that they play distinct roles in responding to oxidative stress. Altogether, these results suggest that ROS mediates teratogenicity induced by HU and that stress response pathways are activated in response to this teratogenic insult.

Several questions remain as to how p38 and JNK MAPKs mediate fetal death and hindlimb malformations respectively (Yan and Hales, 2008). Moreover, whether the other possible mechanism of action of HU, namely HU-induced replication stress, contributes to HU-induced teratogenicity remains elusive. The following section will review the importance of p38 MAPK signaling and DNA damage response (DDR) pathways, as well as the interplay between these two.

#### **1.4 p38 mitogen-activated protein kinases (p38 MAPK)**

With constant changes in the extracellular milieu, cells respond accordingly and have developed sophisticated mechanisms to receive and transmit signals. The MAPKs represent one of the major pathways that are involved in signal transduction. In particular, the p38 MAPK pathway is strongly activated by stress, but plays important roles in embryonic development as well. In previous studies, p38 MAPK has been found to be activated with HU exposure. Moreover, the inhibition of p38 MAPK with SB203508 enhanced HU-induced fetal death without affecting growth retardation or the incidence of deformities among surviving fetuses (Yan and Hales, 2008). Thus, the activation of p38 MAPK in response to HU may indicate a protective role in the embryo in response to insult. This section gives a brief review of the p38 MAPK pathway, focusing on its regulation, mechanisms and its role in stress response, as well as embryo development.

#### 1.4.1 The p38 MAPKs family

The p38 MAPK family was first identified during a pharmacological screen for compounds inducing the production of tumour necrosis factor alpha (TNF $\alpha$ ) (Han et al., 1994). Following this discovery, four isoforms of p38 MAPK ( $\alpha$ ,  $\beta$ ,  $\gamma$  and  $\delta$ ) have been described. They share more than 60% sequence homology and 90% identity in the kinase domain. Despite such similarity, these isoforms have notable differences with respect to tissue expression, upstream activators and downstream effectors. For example, p38 $\alpha$  and p38 $\beta$  are expressed ubiquitously in most tissues, whereas p38 $\gamma$  and p38 $\delta$  appear to be more tissue restricted, with p38 $\gamma$  in skeletal muscle and p38 $\delta$  in endocrine glands (Raman et al., 2007).

The specific function of each isoform has not been fully explored, but the use of pharmacological inhibitors, such as the SB family of drugs, has helped accelerated studies of p38 $\alpha$  and p38 $\beta$ . In contrast, p38 $\gamma$  and p38 $\delta$  appear to be insensitive to these agents (Kumar et al., 1997). Further structural and site-directed mutagenesis revealed structural differences between p38 $\alpha/\beta$  and p38 $\gamma/\delta$  underlying the basis of this inhibition (Young et al., 1997). To better understand the biological functions of each isoform, a genetic approach was used to inactivate genes encoding each isoform. In mice, genetic ablation of p38 $\alpha$  results in embryonic lethality due to defective placental angiogenesis and development of the yolk sac (Allen et al., 2000). However, disruption of p38 $\beta$ , p38 $\gamma$  or p38 $\delta$  results in fertile and viable mice with no discernible differences in phenotype (Beardmore et al., 2005).

#### 1.4.2 Regulation of p38 MAPKs in cellular processes

p38 MAPKs are strongly activated *in vivo* by environmental stresses and inflammatory cytokines. The activation of p38 MAPK requires dual phosphorylation on threonine and tyrosine

(Thr<sup>180</sup>/Tyr<sup>182</sup>) residues within the active site. Upon activation, the dually phosphorylated p38 MAPKs undergo conformational changes that relieve steric blocking, which facilitates substrate binding and enhances catalytic activity (Cuadrado and Nebreda, 2010). p38 MAPK is activated by upstream MAPK kinases (MAP2Ks), including MEK-3 and MEK-6, which are highly specific for p38 MAPKs and do not activate other MAPKs, such as JNKs or ERKs. MEK-6 can phosphorylate all four p38 MAPK isoforms, whereas MEK-3 activates only p38 $\alpha$ , p38 $\gamma$  and p38 $\delta$  (Enslin et al., 1998). Despite slight differences, both MAP2Ks are required for maximal activation of p38. The extent to which different MAP2Ks activate p38 MAPK may be affected not only by stimuli (Remy et al., 2010), but also by the cell type due to different expression levels of MAP2Ks (Brancho et al., 2003).

MEK-3 and MEK-6 are in turn activated and phosphorylated by MAPK kinase kinases (MAP3Ks) at two conserved serine/threonine sites of the activation loop. The MAP3Ks responsible for activating the p38 MAPK pathway also seem to be cell type and stimulus specific. Several MAP3Ks are implicated in the regulation of p38 MAPK, including apoptosis signal-regulating kinase 1 (ASK1), transforming growth factor  $\beta$ -activated kinase-1 (TAK-1), thousand-and-one (TAO) amino acid 1 and 2 and MAPK/ERK kinase kinase 1 (MEKK1). Many of these MAP3Ks have been linked to specific stimuli. For example, ASK1 has been shown to play a key role in activating p38 MAPK induced by oxidative stress (Noguchi et al., 2008). ROS, such as H<sub>2</sub>O<sub>2</sub>, are the most potent activators of ASK1. Thioredoxin (Trx) was identified as an ASK1-interactive molecule, which plays an important role in oxidative stress-induced regulation of ASK1 (Fujino et al., 2007). In resting cells, the reduced form of Trx binds non-covalently with ASK1 to form an inactive complex and inhibit ASK1 kinase activity. Under oxidizing condition, such as exposure to ROS, TRX becomes oxidized and dissociates from ASK1, allowing it to

activate p38 MAPK (Nishitoh et al., 1998). Thus, the ASK1-TRX complex is known as a redox sensor. The ROS-dependent dissociation of Trx from ASK1 serves as a molecular redox switch, converting oxidative stress to a kinase signaling.

On the other hand, downregulation of p38 MAPK is essential to regulate signal intensity and duration, which are critical determinants for specific biological effects. In mammalian cells, termination of the kinase catalytic activity involves several protein phosphatases which interact and inactivate the p38 MAPK pathway. Protein phosphatases such as protein phosphatase (PP) 2A and PP2C target the activation loop and dephosphorylate the serine/threonine residues, while protein tyrosine phosphatase (PTP) dephosphorylates the tyrosine residues (Takekawa et al., 1998). Dephosphorylation by these phosphatases would lead to the formation of monophosphorylated p38 MAPK forms, whose biological functions remain unknown. Biochemical studies have suggested that Thr<sup>180</sup> is essential for catalysis, and Tyr<sup>182</sup> is required for substrate recognition (Askari et al., 2009). p38 MAPK can also be downregulated by a family of MAPK phosphatases (MKPs), which dephosphorylate both tyrosine and threonine residues. Among the MKPs, MKP1 and 8 appear to be more specific to p38 MAPK than JNK (Franklin and Kraft, 1997; Vasudevan et al., 2005). Binding of p38 MAPKs to MPKs increases phosphatase activity and mediates the interaction of MAPK with its substrate. Interestingly, some MKPs have shown to be up-regulated transcriptionally, in order to limit the extent of MAPK activation (Owens and Keyse, 2007). MKP1-null mice display sustained levels of p38 MAPK and JNK activity in response to endotoxic shock, highlighting the importance of MKPs in modulating MAPK activation (Hu et al., 2007). Figure 1.4 provides an overview of the p38 MAPK signaling pathway.

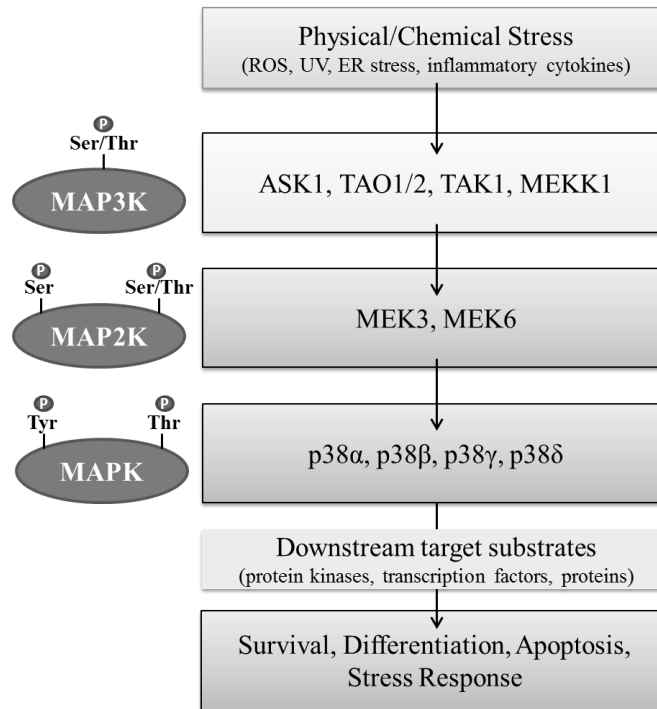


Figure 1.4 Overview of the p38 MAPK signaling pathway. The MAPK cascade is typically composed of three-tiered core kinases, including MAP3K, MAP2K and MAPK, that together establish a sequential activation pathway. p38 MAPKs are strongly activated by stress-inducing stimuli, including oxidative stress, UV irradiation, and inflammatory cytokines. p38 MAPKs phosphorylate downstream targets which in turn generate diverse biological responses. Modified from (Matsuzawa and Ichijo, 2008).

### 1.4.3 Cellular localization

Endogenous p38 MAPKs are distributed in both cytosol and nucleus in resting cells (Raugeaud et al., 1995). Contrary to other MAPKs, p38 MAPK has no nuclear localization signal. Therefore, the mechanism of subcellular translocation is far less known compared to the other two MAPKs. The subcellular localization varies depending on the activation stimulus. Ultimately, stimulation of the intracellular redistribution of p38 MAPK is an important aspect as it allows p38 MAPK to fulfill its cellular functions, through targeting different substrates in the cytoplasm and nucleus. It has been estimated that p38 MAPKs have more than 200 substrates,

that compromise protein kinases, nuclear proteins such as transcription factors, chromatin remodelling regulators, as well as cytosolic proteins regulating protein degradation, mRNA stability, cytoskeleton dynamics and cell migration (Cuadrado and Nebreda, 2010).

It has been reported that p38 MAPKs are exported from the nucleus to the cytosol in 293T cells following treatment with arsenite (Ben-Levy et al., 1998). This translocation mirrors that of MAPK-activated protein kinase-2 (MAPKAP kinase-2/MK2), a p38 MAPK substrate. Upon phosphorylation of MK2 by p38 MAPK in the nucleus, the p38-MK2 complex is exported from the nucleus. This allows p38 MAPK to activate cytosolic targets, such as the cytoskeletal protein stathmin, which has been linked to microtubule dynamics (Parker et al., 1998), as well as other proteins such as the metabolic enzymes, glycogen synthase and cytosolic phospholipase A2 (Dean et al., 1999; Kuma et al., 2004). It has also been shown that TAK-1-binding protein (TAB-1) binds to p38 MAPK, disrupting its interaction with MEKs and preventing the nuclear localization of p38 MAPK (Lu et al., 2006).

However, other studies have shown that p38 MAPKs translocate into the nucleus upon activation by stimuli that induce DNA double strand breaks (Wood et al., 2009). This could be relevant to its role in the regulation of cell-cycle arrest, as well as DNA repair. Nuclear translocation of p38 MAPKs is induced by a conformational change triggered by the dual phosphorylation on the activation loop. Since phosphorylation triggers the nuclear accumulation of p38 MAPK in response to DNA damage, but not in response to other stimuli, it is postulated that DNA damage signals also specifically induce nuclear shuttling. Therefore, nuclear translocation of p38 MAPK requires not only the activation of kinase, but also an active nuclear shuttling partner. Alternatively, DNA damage signals could potentially cause the release of TAB-1 from p38 MAPK, allowing its nuclear translocation.

#### 1.4.4 Role of p38 MAPKs in stress responses

The extent and duration of p38 MAPK activation that is induced by stress stimuli can initiate a multitude of responses with well-recognized roles in cell fate, including differentiation and cell death. More recently, emerging new biological roles involved in cell cycle regulation and cell survival have also been described.

##### 1.4.4.1 Apoptosis

While early and transient activation of p38 MAPK can induce differentiation (Roulston et al., 1998), it has been reported that sustained activation of p38 by oxidative stress induces apoptosis (Tobiume et al., 2001). As mentioned previously, oxidative-stress induced p38 activation is mediated by the ASK1-Trx complex. In ASK1-deficient mice, mouse embryonic fibroblasts (MEFs) were significantly resistant to oxidative stress-induced apoptosis and p38 MAPK activation was dramatically diminished (Tobiume et al., 2001). Therefore, ROS-mediated apoptosis is driven by the ASK1-p38 axis, whereby prolonged exposure of ROS induces excess damage to cells and eventually leads to cell death.

The mechanism by which p38 MAPK contributes to the induction of apoptotic cell death has been described. Kang and Lee (2008) showed that ROS-mediated mitochondrial cell death was associated with an activation of p38 MAPK that induced the activation of Bcl-2-associated X protein (BAX). BAX is a pro-apoptotic protein and is found in the cytosol in resting cells. Upon initiation of apoptotic signaling, BAX undergoes conformational changes and inserts itself into organelle membranes, primarily the outer mitochondrial membranes (Wolter et al., 1997). This results in the release of cytochrome c and pro-apoptotic factors, which leads to the activation of caspases and initiates apoptosis. In the presence of the p38 MAPK inhibitor,

PD169316, mitochondrial translocation of Bax was completely suppressed and mitochondrial membrane potential loss was effectively attenuated (Kang and Lee, 2008). Another important target of p38 MAPK that regulates apoptosis is the tumor suppressor protein p53. p53 is implicated in the induction of apoptosis in both the extrinsic and intrinsic pathway; both pathways lead to the activation of caspases. In the extrinsic pathway, p53 induces the transcription of genes encoding transmembrane proteins such as Fas and DR5 (Wu et al., 1997). These cell surface receptors are key components of the extrinsic death pathway and promote cell death through caspase-8 activation (Nagata and Golstein, 1995). Intrinsically, p53 activates Bax and, as described above, induces apoptosis through mitochondrial membrane disruption.

#### 1.4.4.2 Cell Cycle Checkpoints

The classical role of p38 MAPK as a stress kinase and its ability to regulate apoptosis and growth inhibition have been very well established. More recently, alternative and non-classical functions of p38 MAPK, including in the cell cycle checkpoint and survival, have also been described.

In response to stress stimuli that cause DNA damage, p38 MAPK plays a role in cell cycle checkpoints, both G1/S and G2/M, to allow time for DNA repair. Double strand DNA breaks (DSBs) activate p38 MAPK, which then phosphorylates p53 and activates the p53-dependent G2/M checkpoint (Bulavin et al., 1999). Phosphorylation of p53 induces its dissociation from Murine double minute 2 (Mdm2). In resting cells, Mdm2 interaction with p53 promotes p53 ubiquitination and degradation. Therefore, disruption of this interaction leads to p53 accumulation. The activation and stabilization of p53 by p38 MAPK induces transcription of p53-targeted genes, such as growth arrest and DNA damage inducible 45 $\alpha$  (Gadd $\alpha$ ), p21 and 14-

3-3. All of these genes enforce the G2/M checkpoint by inactivating cdk2/cyclinB complex, which is a major driver of the G2 to M phase of the cell cycle (Morris et al., 2000; Zhan et al., 1999).

Consistent with its role as a master cell cycle regulator, p53 can also regulate the progression from G1 to S phase. p38 MAPK activation of p53 leads to the activation of p21, which then inactivates cdk2 to establish a G1/S checkpoint (Kishi et al., 2001). p38 MAPK can also mediate the G1/S checkpoint by up-regulating p16INK4a and p19ARF gene expression (Bulavin et al., 2004). The encoded proteins can both promote the G1/S checkpoint; p16 inhibits Cdk4/6, the major driver of G1 to S phase progression, whereas p19 regulates p53 activation and inhibits cdk2 activity (Tao and Levine, 1999). Altogether, p38 MAPK can regulate the induction of G2/M and G1/S checkpoints by multiple distinct mechanisms (Figure 1.5).

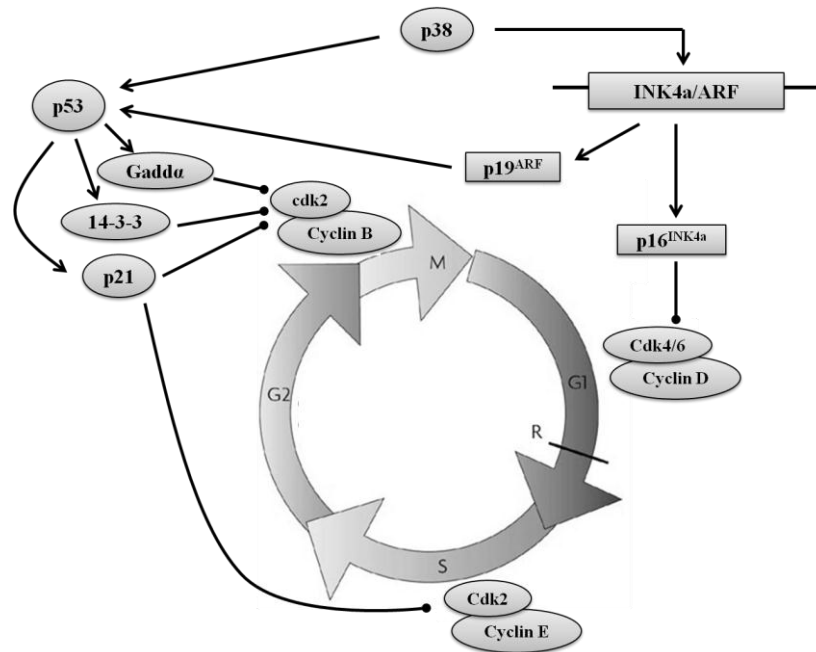


Figure 1.5 The role of p38 MAPKs in the G1/S and G2/M checkpoints. The cell cycle is regulated by the oscillating activity of cyclin-dependent kinases (Cdks), which are positively regulated by cyclins and negatively regulated by Cdk inhibitors (Guardavaccaro and Pagano, 2006).

#### 1.4.4.3 Survival

Depending on the extent of cell damage and the efficacy of DNA repair, instead of promoting cell death, p38 MAPK can enhance survival. Activation of p38 MAPK and cell death were observed in Jurkat T cells upon treatment with 8-methoxypsoralen, a chemotherapeutic cancer drug. However, instead of preventing cell death, inhibition of p38 MAPK by SB203580 increased death in these cells in a dose-dependent manner (Cappellini et al., 2005). Similarly, in utero exposure to HU activates p38 MAPK in embryos and induces skeletal malformations in fetuses, but pharmacological inhibition of this pathway enhances fetal mortality (Yan and Hales, 2008). Thus, in response to cell damaging stimuli, p38 MAPK activation increases cell survival. This could be a defense mechanism that cells develop to overcome the cytotoxic effects caused by drugs. The mechanism by which p38 MAPK directly mediates cell survival is not very clear. A recent study has shown a novel mechanism by which p38 MAPK directly inactivates GSK3 $\beta$ , an inhibitor of cell survival (Thornton et al., 2008). Phosphorylation of GSK3 $\beta$  inhibits its activity, which leads to the accumulation of  $\beta$ -catenin, a transcription factor known to promote survival by regulating the expression of other survival genes such as c-myc (He et al., 1998). Interestingly, p38 MAPK-mediated inactivation of GSK3 $\beta$  seems to be tissue-specific, predominantly in the brain.

In summary, in addition to its well-characterized role in cell death, p38 MAPK signaling in stress responses also contributes to cell cycle checkpoints and survival. As p38 MAPK has opposing roles in mediating cell fate, biological outcomes might depend on the level of damage to the cells and the extent to which p38 MAPK is activated. Additional studies are needed to define the specific mechanism used by p38 MAPK to discriminate its targets to mediate cell death, from those that mediate cell survival.

#### 1.4.5 p38 MAPK in embryo development

The role of p38 MAPK in embryonic development has been explored extensively *in vivo* in many different organisms. During embryogenesis, the four different p38 MAPK isoforms are expressed in different sets of tissues. MAPK p38 $\alpha$  is preferentially expressed in the somites, branchial arches, limb buds, heart and placenta (Adams et al., 2000), while MAPK p38 $\delta$  is expressed in the foregut, liver, kidney, adrenal gland, small and large intestine, as well as the epidermis (Hu et al., 1999). Studies have characterized distinct developmental roles for each of the p38 MAPK isoforms. However, because only MAPKs p38 $\alpha$  and p38 $\beta$  are sensitive to pharmacological inhibitors, in this regard MAPKs p38 $\gamma$  and p38 $\delta$  have much less well-characterized developmental functions.

During mammalian embryogenesis, the disruption of the p38 $\alpha$  MAPK gene results in homozygous embryonic lethality beginning at GD10.5 (Allen et al., 2000). This is because p38 $\alpha$  MAPK is essential for normal placental development, specifically diploid trophoblast development and placental vascularization (Mudgett et al., 2000). As a consequence of defective placental development, p38 $\alpha$ <sup>-/-</sup> embryos died of suffocation and starvation. In contrast, embryos lacking MAPKs p38 $\beta$ , p38 $\gamma$  and p38 $\delta$  are viable without any obvious developmental defects. This suggests that p38 MAPK isoforms have redundant roles; however, embryonic lethality has impeded attempts to establish their distinct developmental roles *in vivo*.

Using tissue-specific genetic loss-of-function studies, Greenblatt et al. (2010) revealed that *in vivo* MAPKs p38 $\alpha$  and p38 $\beta$  are essential for skeletogenesis and bone homeostasis. Mice displayed profound reduction in bone mass, secondary to defects in osteoblast differentiation after the deletion of any of the p38 MAPK pathway member-encoding genes in osteoblasts, including MEK-3, MEK-6, p38 $\alpha$  and p38 $\beta$  (Greenblatt et al., 2010). Most interestingly, p38 $\alpha$  and

p38 $\beta$ -deficient osteoblasts displayed distinct phenotypes. In conclusion, each isoform plays a fundamentally different role in osteoblast development, with p38 $\alpha$  affecting early osteoblast differentiation and p38 $\beta$  affecting the late stage osteoblast differentiation.

More recently, the role of p38 MAPK in sex determination has been evaluated in vivo (Warr et al., 2012). The loss of *Gadd45 $\gamma$*  and *Mek4* causes mouse embryonic XY gonadal sex reversal due to disruption of the testis-determining gene, *Sry*. Sex reversal in these mutants is associated with reduced activation of p38 MAPK. Furthermore, MAPK p38 $\alpha$  and p38 $\beta$ -deficient embryos also exhibit XY gonadal sex reversal. Taken together, these data suggest a novel developmental function of p38  $\alpha/\beta$  MAPK in gonadogenesis, specifically testis determination.

## **1.5 The DNA damage response pathway**

Damage to our DNA is an ongoing threat and maintaining genomic integrity is essential to our survival, as well as to the faithful transmission of genetic information to offspring. To overcome these threats, the DNA damage response (DDR) has evolved to protect DNA from damage induced by environmental agents or generated spontaneously during DNA metabolism. The DDR is a complex network which senses DNA damage and influences cellular response, including DNA repair and chromatin remodeling. These activities must be tightly regulated, both spatially and temporally, in order to optimize repair and prevent unnecessary alterations to the DNA structure. Besides being activated by DNA damaging agents, the DDR also plays an essential role in surveying the quality of DNA replication. The following section will focus on the mechanisms that govern DNA double-strand breaks, DNA repair and the regulatory functions of DDR.

### 1.5.1 DNA Double Strand Breaks (DSBs)

There are many forms of DNA damage, ranging from innocuous single base or nucleotide modifications and single-strand breaks to highly cytotoxic lesions such as double strand breaks (DSBs) and interstrand crosslinks. The former types of lesions occur spontaneously during the normal cell cycle and are rapidly repaired without eliciting a full activation of the DDR network. This phenomenon appears to be restricted to massive replication problems or the presence of DSBs, which are considered to be the most destructive form of DNA damage (Wyman and Kanaar, 2006). DSBs are formed as a result of two-single stranded nicks in opposing DNA strands. They arise from numerous endogenous and exogenous sources, such as ionizing radiation, oxidative stress and the replication of damaged DNA. In addition, DSBs also occur intentionally during genetically programmed processes such as meiotic recombination and V(D)J recombination in precursor lymphocytes (Grawunder et al., 1998). Unrepaired DSBs can lead to detrimental effects, including gene mutations, chromosomal deletions and translocations, which altogether can induce genomic instability and increase susceptibility to diseases such as cancer (Khanna and Jackson, 2001).

### 1.5.2 DNA Replication Stress

During the S-phase of the cell cycle, the genome is particularly at risk due to the fragile replication forks, which are prone to collapse during DNA replication. The stalling or collapse of a replication fork is known as DNA replication stress, which can lead to detrimental effects. Failure to restart the fork can lead to incomplete chromosome duplication, which cause mitotic catastrophe, complex chromosome rearrangements and cell death (Ciccia and Elledge, 2010). Duplication of the genome depends largely on a balanced supply of dNTPs. The activity of RNR

must be tightly coordinated with DNA synthesis for faithful duplication. Upon entry into the S-phase, the dNTP pool is increased by three-fold in comparison to G1 phase (Chabes et al., 2003). Replication inhibitors, such as mitomycin, HU and aphidicolin (APH) reduce dNTP production by inhibiting RNR. With reduced or imbalanced dNTP pools, fork progression is impeded and mutagenesis is induced in human cells (Bester et al., 2011).

Due to the unique structure of replicating DNA molecules, DNA replication stress can cause DNA damage and lead to genomic instability at replication forks (Figure 1.6). Normally, when single-strand lesions occur in non-replicating DNA, the overall integrity of chromosomes is maintained by hydrogen bond base-pairing on either side of the lesions. In contrast, replicating chromosomes contain single-stranded DNA that is unwound from the double-strand template. These single strands on each arm of the replication fork no longer base-pair to each other, but instead base-pair to the newly synthesized DNA molecules. Consequently, DSBs are produced if lesions occur within the unwound and replicating strand (Figure 1.6). DSBs occurring at replication fork can be triggered spontaneously by ROS, which induce single-strand lesions. Therefore, checkpoint functions are extremely crucial to stabilize stalled replication fork, blocking entry or progression through S-phase in cells that have suffered DNA damage (Burhans and Weinberger, 2007).

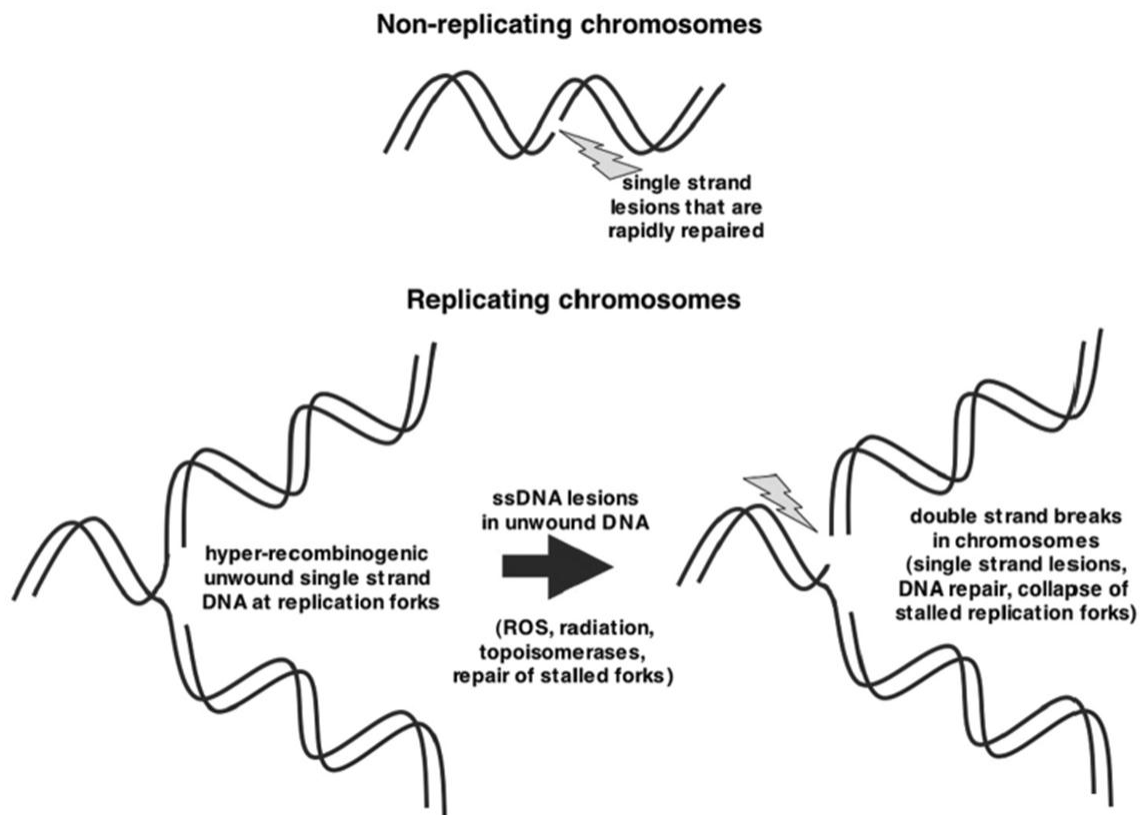


Figure 1.6 Structure of replicating DNA contributing to genomic instability. The integrity of non-replicating chromosomes is maintained by hydrogen bond base pairing on either side of the single strand lesion. In contrast to replicating chromosomes, single strand lesions encountered by replication fork can be converted into DSBs during DNA synthesis, thus inducing fork collapse. Obtained from (Burhans and Weinberger, 2007)

### 1.5.3 DNA Damage Recognition

Chromatin organization can be affected by genotoxic stress and induce histone alterations, nucleosome repositioning or changes in higher-order folding of the chromatin fiber. To begin DNA repair, DDR factors must first be localized to sites of DNA damage, forming an affinity platform known as Ionizing Radiation-Induced Foci (IRIF). The assembly of these factors is dependent on post-translational chromatin modifications, including phosphorylation,

ubiquitination, sumoylation, poly(ADP-ribosylation), acetylation, and methylation (Bergink and Jentsch, 2009; Kleine and Luscher, 2009). A wide variety of proteins specifically recognize these modifications, many of which initiate the recruitment of DDR factors to DNA damage sites. The following section focuses on a specific post-translation chromatin modification in response to DNA DSBs: the phosphorylation of histone.

#### 1.5.3.1 Role of $\gamma$ H2AX in DDR signaling

The assembly of DDR proteins into IRIF at the DSB-flanking chromatin occurs in a highly regulated and hierarchical fashion. A critical aspect of the formation of IRIF involves the phosphorylation of Ser139 on a specialized histone, H2AX, to form  $\gamma$ H2AX (Rogakou et al., 1998). Members of the phosphatidylinositol-3-kinase (PI3K) protein kinase family, including ataxia telangiectasia mutated (ATM), DNA dependent protein kinase (DNA-PK), and ATM- and Rad3-related (ATR) are all thought to contribute to H2AX phosphorylation in vivo (Stiff et al., 2004). This phosphorylation event is one of the most extensively characterized chromatin modifications and is considered the most proximal marker of IRIF formation in response to DNA DSBs.

The key function of  $\gamma$ H2AX is to create an epigenetic signal that is recognized by specific domains of downstream DDR proteins. Specifically, it provides a high-affinity binding site for MDC1 protein, which in turn orchestrates the recruitment of all downstream IRIF-associated factors at the DNA ends. In addition to serving as a direct binding partner of  $\gamma$ H2AX, the interaction of MDC1 and  $\gamma$ H2AX prevents dephosphorylation of the histone, which helps to extend the assembly of IRIF (Stucki et al., 2005). Besides recruitment,  $\gamma$ H2AX also plays an essential role in DSB rejoining.  $\gamma$ H2AX helps to anchor broken ends together by repositioning

nucleosomes at damaged sites and reduces chromatin density, which helps to increase DNA accessibility for DDR factors (Xie et al., 2004). Furthermore, cohesins are recruited to the regions of DNA damage to keep broken ends at close proximity during post-replicative repair, preventing the loss of large chromosomal regions (Unal et al., 2004). In addition,  $\gamma$ H2AX modulates cell cycle checkpoints, allowing time for DNA to be repaired. Mice lacking H2AX manifest a G2/M checkpoint defect. However, this appears to be true only at relatively low levels of DNA damage (Fernandez-Capetillo et al., 2002). Finally,  $\gamma$ H2AX has been shown to be of key importance for faithful DNA repair. H2AX null or haploinsufficient mice have impeded DSB repair efficacy, requiring more time for repair. They are also more sensitive to damage induced by irradiation, displaying numerous morphological abnormalities in addition to chromosome and mitotic defects and defective G2/M cell cycle kinetics (Celeste et al., 2002). Collectively, this evidence demonstrates that H2AX performs a vital role in the identification and efficient repair of damaged genomes, thereby maintaining genome stability that could otherwise manifest into cancers.

#### 1.5.3.2 $\gamma$ H2AX foci

$\gamma$ H2AX can be visualized by fluorescence microscopy, appearing as bright speckles or discrete nuclear “foci” as a result of H2AX phosphorylation. Two distinct yet highly discernible  $\gamma$ H2AX focal populations have been observed; these are a large population of small foci and a small population of larger amorphous foci that co-localize with various DNA DSB repair proteins (McManus and Hendzel, 2005).

Unlike previous methods for the detection of DSBs, such as constant or pulsed field gel electrophoresis, that only detect DSBs after large doses of ionizing radiation (IR) (5-50Gy),

detection of breaks using  $\gamma$ H2AX foci-based detection is 100-fold more sensitive, enabling measurements of radiation doses as low as 1mGy (Mah et al., 2010). Foci formation has been observed to have a strong linear dose response relationship. After the induction of DSBs, the numbers of  $\gamma$ H2AX foci formed are proportional to the numbers of DSBs incurred, with each focus corresponding to each break (Sedelnikova et al., 2002). As  $\gamma$ H2AX foci are formed *de novo*, they are also a more reliable detection of DSBs than other repair proteins which are present in resting cells regardless of DNA damage (Ayoub et al., 2008).

For all these reasons, fluorescence visualization of  $\gamma$ H2AX foci has become a gold standard for DSB detection (Fernandez-Capetillo et al., 2002). Using anti-  $\gamma$ H2AX antibodies, the size and number of  $\gamma$ H2AX foci can be measured. The discovery of  $\gamma$ H2AX foci at DSB sites permits the study of cellular mechanisms of DDR after DNA damage.

#### 1.5.3.3 Spatiotemporal dynamics of $\gamma$ H2AX

The detection of  $\gamma$ H2AX allows the distinction of spatial and temporal distribution of DSB formation. H2AX phosphorylation is tightly constrained spatially, being confined to sections of the damaged chromosome and not spreading throughout the nucleus (Rogakou et al., 1999). Although only a few base pairs may be implicated in DSBs, there is significant signal amplification.  $\gamma$ H2AX can spread from the sites of DSB into mega base-sized domains of surrounding chromatin flanking each lesion in the mammalian cell. It is estimated that there are approximately 2000 H2AX molecules phosphorylated per DSB, producing highly amplified nuclear micro-domains (Rogakou et al., 1999). Moreover, high resolution chromatin immunoprecipitation studies of  $\gamma$ H2AX have shown that  $\gamma$ H2AX is absent from areas directly

opposed to the DSB and that the distribution of foci along the chromatin is non-homogenous (Savic et al., 2009).

Initial phosphorylation of H2AX occurs within minutes after the induction of DSBs and continues to increase rapidly until a plateau is reached within 30 to 60 minutes after irradiation (Rogakou et al., 1998). At the early stages, small foci are formed and gradually increased in size as the DDR progresses. Finally,  $\gamma$ H2AX must be dephosphorylated to restore the epigenome to its pre-damage status. While the plateau phase lasts for approximately 60 minutes, the number of foci begins to decrease with a half-life of several hours (Keogh et al., 2006). It has been proposed that the loss of  $\gamma$ H2AX reflects the completion of DNA repair (Bouquet et al., 2006). However, this is only true at relatively low levels of DNA damage. In cases with more severe damage, the number of foci decreases but the global expression of  $\gamma$ H2AX still remains unchanged. This is counterbalanced by the increase in size of the foci instead, hence not affecting the total  $\gamma$ H2AX signal (Bouquet et al., 2006).

#### 1.5.4 DNA repair

In order to overcome DNA damage, repair mechanisms specific for different types of lesions have evolved. During DNA repair, a plethora of enzymatic activities are carried out to chemically modify DNA lesions and repair the damage. These repair tools are tightly regulated in order to preserve the integrity of the genome. Here, this section describes the cellular mechanisms that regulate DNA repair for DSBs specifically and the capability of DNA repair in embryos.

#### 1.5.4.1 Double-Strand Break Repair

DSBs are extremely toxic lesions whose repair is promoted by an intricate network of multiple DNA repair pathways. The two major pathways in mammalian cells that govern DSB healing include homologous recombination (HR) and nonhomologous end-joining (NHEJ). The main difference between these pathways is that HR uses information from the undamaged sister chromatid, while NHEJ uses no or little sequence homology to rejoin broken ends (Brugmans et al., 2007).

HR is a highly accurate repair mechanism, relying on the presence of a homologous DNA fragment as a template. Free DNA ends at the site of DSBs are first recognized and processed into 3' single-stranded tails. Following end processing, single-stranded DNA ends are coated with replication protein A (RPA), which helps to recruit other HR mediators, such as Brca2 and Rad. Altogether, these HR mediators help to load Rad51 onto the single-stranded DNA and replace RPA (Sung, 1997). From an intact sister chromatid, Rad51 searches for homologous DNA and creates a joint molecule between the damaged and undamaged strands. Following Rad51-dependent strand invasion into homologous sequences of the sister chromatid, the 3' single strand tails can be extended by using the undamaged sister strand as a template.

In contrast to HR, NHEJ does not require sequence homology at all to repair DSBs. This pathway is not only used to repair classic DSBs induced by exogenous agents, but also is required during V(D)J recombination (Karran, 2000). During NHEJ, DSBs are rapidly bound by the Ku heterodimer (Ku70 and Ku80). The Ku proteins have high affinity to DNA ends, localizing within seconds to DSBs and activate the catalytic subunit of DNA-PKcs to initiate repair (Mahaney et al., 2009). Through a series of phosphorylation reactions, DNA-PKcs stabilize DSB ends and recruit XRCC4/LIG4, promoting the re-ligation of broken ends. However,

if DNA ends contain non-ligatable end groups, DNA-PKcs will recruit end processing enzymes, such as Artemis, APLF nuclease and PNK kinase, prior to DNA ligation (Mahaney et al., 2009).

#### 1.5.4.2 DNA Repair during *in utero* development

*In utero* exposure to environmental genotoxicants can result in the induction of DNA damage and formation of somatic mutations in the developing fetus or newborn (Perera et al., 1999). In embryos, cell proliferation is enhanced with the increase in DNA replication necessary for tissue development. Moreover, the cell cycle is much shorter in embryos compared to adult (Mac Auley et al., 1993). A shorter cell cycle increases the chance for DNA lesions to escape cell cycle checkpoints and repair mechanisms, thereby increasing susceptibility to mutation and cancer initiation. In fact, it is estimated that 25-30% of all birth defects are due to gene mutations and chromosomal abnormalities (Beckman and Brent, 1984). Of the many factors that may contribute to the increase in *in utero* susceptibility to genotoxicants, DNA repair is a crucial determinant of whether or not exposure to these toxicants leads to immediate or long-term health effects.

Studies with DNA repair gene knock-out mouse strains have provided insight regarding embryonic DNA repair capabilities. Based on these models, DNA repair activities during development vary widely depending on the development stage of the conceptus, leading to specific periods of development that appear to be more sensitive to genotoxic stress. For example, loss of *Xrcc4* gene leads to embryonic lethality by GD16.5 (Barnes et al., 1998), whereas xeroderma pigmentosum complementation group D (*Xpd*) null-embryos die before implantation (de Boer et al., 1998). Additional clues to the role of DNA repair enzymes were obtained from null-mutant embryos that were viable. *ATM* null-embryos displayed growth retardation, neurological abnormalities and infertility (Lee et al., 2000); while the loss of checkpoint and

DNA repair gene, Nijmegen breakage syndrome 1 (*NBS1*), led to viable but immunodeficient fetuses with microcephaly (Vinson and Hales, 2002). Not only do these mutant animals for DNA damage responsive genes demonstrate how essential DNA repair pathways are to the survival of the embryo, but also they illustrate their additional role in non-repair pathways that are crucial for proper tissue and embryonic development.

Embryoprotective DNA repair genes during development are highlighted by in studies where dams were exposed to genotoxicants. 8-Oxoguanine glycosylase, encoded by *Ogg1*, is involved in base-excision repair by excising 8-oxoguanine (8-oxoG) from DNA. With the loss of *Ogg1*, *in utero* exposure to methamphetamine increased oxidative damage in fetal brains compared to wild type littermates, as measured by the increase in 8-oxoG. Moreover, high dose methamphetamine also increased susceptibility to postnatal neurodevelopmental deficits in female mutant mice (Wong et al., 2008). As mentioned previously, *p53* is a master regulator of cell cycle checkpoints, thereby facilitating DNA repair. Several studies have provided data that suggest that the *p53* gene is the “guardian of the babies”, as it protects against limb malformations and eye defects induced by alkylating agents, 4-hydroperoxycyclophosphamide (Moallem and Hales, 1998) and 2-chloro-2-deoxyadenosine (Wubah et al., 1996), respectively. In summary, DNA repair genes in embryos are crucial not only for protection against exposure to teratogens and genotoxicants but also for the normal development of the embryo and its survival.

## **1.6 Hypothesis**

We hypothesize that oxidative stress is involved in HU-induced developmental toxicity. We propose that HU-induced oxidative stress activates the p38 MAPK pathway and induces DNA damage in embryos during organogenesis.

CD1 mice were chosen as the animal model to test these hypotheses; these mice are easy to breed, have a low spontaneous malformation rate and large litter size, which are appropriate to explore the impact of teratogens. Moreover, these mice are outbred, reflecting the general human population. On GD9, timed-pregnant mice were administered HU by intraperitoneal injection. This is the period when organogenesis is occurring and when embryos undergo the switch from anaerobic to aerobic metabolism, making them highly susceptible to oxidative stress and developmental toxicity.

Three specific objectives were addressed through several studies:

Objective 1: To elucidate the role of p38 MAPKs by examining the protein expression and activation of MEK-3/6 and p38 MAPK in whole embryos in response to maternal exposure to HU.

Objective 2: To investigate the localization of MEK-3/6 and subcellular localization of p38 MAPKs in whole embryos in response to maternal exposure to HU.

Objective 3: To elucidate the DDR response in HU-induced developmental toxicity by examining the expression and localization of  $\gamma$ H2AX in whole embryos.

## **Connecting Text**

The following chapter, “Hydroxyurea Exposure Triggers Tissue Specific Activation of p38 Mitogen-Activated Protein Kinase Signaling and the DNA Damage Response in Organogenesis Stage Mouse Embryos” has been submitted for publication to Toxicological Sciences. This is a data chapter, which includes detailed methodology, addressing the objectives and hypothesis of this study.

## **Chapter Two**

### **Hydroxyurea Exposure Triggers Tissue Specific Activation of p38 Mitogen-Activated Protein Kinase Signaling and the DNA Damage Response in Organogenesis Stage Mouse Embryos**

## Abstract

Hydroxyurea (HU) is commonly used to treat myeloproliferative diseases and sickle cell anemia. The administration of HU to gestation day 9 CD1 mice causes predominantly hindlimb, tail, and neural tube defects. HU induces oxidative stress and p38 mitogen-activated protein kinase (MAPK) signalling in embryos. HU also inactivates ribonucleotide reductase, leading to DNA replication stress and DNA damage response signalling. We hypothesize that HU exposure induces p38 MAPK activation and DNA damage response signalling during organogenesis preferentially in malformation-sensitive tissues. HU treatment (400 or 600 mg/kg) induced the activation of MEK3/6, upstream MAP2K3 kinases, within 30 min; phospho-MEK3/6 immunoreactivity was increased throughout the embryo. Activation of the downstream p38 MAPK peaked 3 h post-HU treatment. At this time, phospho-p38 MAPK immunoreactivity was enhanced in the cytoplasm and nucleus of cells in the rostral and caudal neuroepithelium and neural tube; significant increases in p38 MAPK signalling were not observed in the somites or heart. Interestingly, the DNA damage response, as assessed by the formation of  $\gamma$ -H2AX foci, was increased at 3 h in HU-exposed embryos in all tissues examined, including the somites and heart. Increases in pyknotic nuclei and cell fragmentation were observed in all tissues except the heart, an organ that is relatively resistant to HU-induced malformations. Thus, although HU induces a widespread DNA damage response, the activation of p38 MAPK is localized to the rostral and caudal neuroepithelium and neural tube, suggesting that p38 MAPK pathways may play a role in mediating the specific malformations observed after HU exposure.

## Introduction

The p38 mitogen-activated protein kinases (MAPKs) ( $\alpha$ ,  $\beta$ ,  $\gamma$  and  $\delta$ ) are members of a highly conserved superfamily of MAPKs. This family of kinases is of fundamental importance in mediating cellular responses to a wide variety of signals, including cellular stressors such as oxidative stress, UV radiation, cytokines and DNA damage (She et al., 2000; Uhlik et al., 2003; Wood et al., 2009). In response to stress, p38 MAPKs are activated by phosphorylation on threonine and tyrosine (Thr<sup>180</sup>/Tyr<sup>182</sup>) residues within the active site. This phosphorylation is mediated primarily by two upstream dual specificity kinases, MEK3 and MEK6, that are highly specific for p38 MAPKs (Enslin et al., 2000). Activated p38 MAPKs phosphorylate a broad range of substrates, both in the cytosol and nucleus. Nuclear shuttling of p38 MAPK has been reported to be triggered specifically by DNA damage inducing stimuli (Wood et al., 2009). Substrates of p38 MAPKs include nuclear proteins, such as transcription factors and regulators of chromatin remodelling, and cytosolic proteins implicated in the regulation of cell differentiation and fate (Cuadrado and Nebreda, 2010).

p38 MAPKs play critical roles in numerous biological processes, including cell growth, proliferation, differentiation, death, and cell cycle checkpoints (Deacon et al., 2003; Kurosu et al., 2005; Puri et al., 2000). The role of p38 MAPKs in embryonic development has been investigated extensively in many model organisms, including flies, sea urchins, frogs and mice. Studies have demonstrated that p38 MAPKs play important roles during oocyte maturation, embryonic cleavage, and axial specification (Bradham and McClay, 2006; Suzanne et al., 1999). During murine embryogenesis, the p38 MAPK pathway is essential for skeletogenesis, bone homeostasis, and cardiovascular and placental development (Greenblatt et al., 2010; Mudgett et al., 2000; Tamura et al., 2000). The biological impact of the activation of p38 MAPKs is

dependent not only on the stimulus but also on the cellular context. Thus, it is important to understand how an insult to the embryo may trigger activation of the p38 MAPKs and alter cell fate determination. The role of p38 MAPK signaling in mediating teratogen-induced abnormal development remains to be elucidated.

HU, an antineoplastic drug commonly used to treat sickle cell anemia and myeloproliferative diseases, has been studied extensively as a model teratogen. The recommended therapeutic doses of hydroxyurea are in the range of 15 mg/kg/day for sickle cell anemia and 80 mg/kg once every three days for chronic myelogenous leukemia. HU is a potent DNA synthesis inhibitor; it directly inhibits ribonucleoside diphosphate reductase and hinders the reductive conversion of ribonucleotides to deoxyribonucleotides, resulting in rapid inhibition of DNA replication (Sneeden and Loeb, 2004). In mice, thymidine <sup>3</sup>H incorporation into DNA in the skin and thymus is decreased to 5% of control at 0.5 h and 1 h after an intraperitoneal injection of 100 mg/kg HU; DNA synthesis in the liver is reduced to 20-40% of control at this time (Smith et al., 1968). In rabbits, DNA synthesis in the embryos is reduced 10-fold 2 h after a subcutaneous injection of 650 mg/kg HU (DeSesso and Goeringer, 1990). During this replication stress, DNA is prone to breakage and the genome is unstable (Chan et al., 2009).

HU also induces the generation of reactive oxygen species (ROS). The hydroxylamine group in HU interacts with oxygen in biological tissues to produce the highly reactive hydroxyl radical and hydrogen peroxide (DeSesso, 1979). The production of ROS induces oxidative stress, adversely affecting cellular metabolism and leading to cell cycle arrest and cell death (DeSesso, 1979). Thus, HU induces both oxidative and replication stress, modifying macromolecules such as DNA, proteins, and lipids in the embryo. In previous studies, we have shown that *in utero* exposure to HU increases the formation of 4-hydroxynonenal protein adducts in embryos and

induces caudal skeletal defects (Yan and Hales, 2006). Previous studies have also revealed that MAPK signaling is activated in HU-exposed organogenesis stage mouse embryos; moreover, inhibition of p38 MAPK activation increases fetal death in HU-exposed embryos (Yan and Hales, 2008), demonstrating that p38 MAPK signaling plays an essential role in the survival of the conceptus after insult with this teratogen.

We hypothesize that HU exposure triggers oxidative stress, inducing p38 MAPK activation, and replication stress, inducing DNA damage response signalling, and that these responses are enhanced in the organogenesis-stage embryo in malformation-sensitive tissues. To test this hypothesis, we examined the temporal and spatial localization of the activation of MEK3/6 and p38 MAPK and the DNA damage response, as assessed by the formation of nuclear  $\gamma$ H2AX foci, in HU-exposed embryos. We report that the HU-induced DNA damage response is ubiquitous; however, even in the presence of DNA damage, cell death was not increased in the heart, a relatively malformation-resistant organ. In contrast, activation of the p38 MAPK signaling pathway was region-specific and enhanced in malformation-sensitive tissues of the embryo.

## **Materials and Methods**

### **Animals, treatments and embryo collection**

All animal protocols were approved by the Animal Care Committee of McGill University (protocol #1825) in conformance with the guidelines outlined in the Guide to the Care and Use of Experimental Animals, prepared by the Canadian Council on Animal Care.

Timed-pregnant CD1 mice were purchased from Charles River Canada Ltd. (St. Constant, QC, Canada) and housed at the McIntyre Animal Resource Centre (McGill University, Montreal,

QC, Canada). Female virgin mice were mated between 8:00 AM and 10:00 AM on gestation day (GD) 0. On GD 9, saline (control) or hydroxyurea (HU, Aldrich Chemical Co., Madison, WI, 400 mg/kg or 600 mg/kg) was given to females by intraperitoneal injection at 9:00 AM. Dams were euthanized at 0.5, 3, or 6 h after treatment by CO<sub>2</sub> inhalation and cervical dislocation. The uteri were removed and embryos were dissected out in Hanks' balanced salt solution (Invitrogen Canada Inc., Burlington, ON, Canada) At the time of collection on GD 9, for each dosage group, 3-4 embryos from each litter were fixed in paraformaldehyde for immunofluorescence staining experiments. The remaining embryos from two litters were pooled together, snap frozen in liquid nitrogen, and stored at -80°C until later use for western blotting experiments.

### **Western Blotting**

Whole tissue lysates were prepared for MEK 3/6, phospho-MEK-3/6, p38 MAPK and phospho-p38 MAPK determinations. Samples, consisting of 10-18 embryos each (pooled from two litters), were placed in 60-100 µl of radioimmunoprecipitation assay buffer (150 mM NaCl, 1% Nonidet P-40, 0.5% deoxycholate, 0.1% SDS, and 50 mM Tris, pH 7.5) containing 10 µl/ml protease inhibitor cocktail and 20 µl/ml phosphatase inhibitor mix (Active Motif Inc., Carlsbad, CA). The samples were homogenized with an ultrasonicator (Sonics and Materials Inc., Newtown, CT) and centrifuged at 10,000g for 10 min at 4 °C. The supernatants were used for immunoblotting.

Total proteins from each sample were quantified using the spectrophotometric Bio-Rad Protein Assay (Bio-Rad Laboratories Ltd., Mississauga, ON, Canada). Proteins (15 µg from each sample) were separated with 10% SDS-polyacrylamide gel electrophoresis and then transferred onto equilibrated polyvinylidene difluoride membranes (Amersham Biosciences,

Buckinghamshire, UK). Membranes were blocked with 5% skim milk for 1 h at room temperature and then probed overnight at 4 °C with primary antibodies against MEK 3/6 (1:500, catalog number sc-13069, Santa Cruz Biotechnology Inc, Santa Cruz, CA), phospho-MEK-3/6 (1:2000, catalog number sc-8407, Santa Cruz Biotechnology), p38 MAPK (1:1000, catalog number #9212, Cell Signaling Technology Inc, Danvers, MA), phospho-p38 MAPK (1:1000, catalog number #4511, Cell Signaling Technology) and  $\beta$ -actin (1:5000, catalog number sc-1616, Santa Cruz Biotechnology).

Membranes were incubated with horseradish peroxidase-conjugated secondary antibodies (1:10,000; GE Healthcare, Buckinghamshire, UK) for 2 h at room temperature and proteins were detected by enhanced chemiluminescence (GE Healthcare). The bands were quantified by densitometric analysis using a ChemiImager 400 imaging system (Alpha Innotech, San Leandro, CA); the peak area represents the intensity of the band. Each experiment was replicated five to ten times with different pooled litters for each dosage group.

### **Immunofluorescence**

At the times of collection on GD 9, 3 to 4 embryos were collected from each litter and fixed for 4 h at 4°C in 4% paraformaldehyde. Embryos were then dehydrated in ethanol, embedded in paraffin, and serially sectioned (5  $\mu$ m sections) along the sagittal plane. Tissue sections were deparaffinized and re-hydrated with water. After rinsing twice for 2 min each with phosphate buffered saline (PBS), sections were subjected to antigen unmasking by incubating in sodium citrate buffer (10 mM sodium citrate trisodium salt dehydrate, pH 6.0) and microwaving at 100% power for 2 min and then 10% power for 10 min. Slides were allowed to cool at room temperature for 15 min and then rinsed in PBS for 5 min.

Phospho-MEK-3/6 immunoreactivity was detected using a M.O.M immunodetection kit (Vector Laboratories, Burlington, CA) as follows. Sections were incubated in the working solution of M.O.M mouse IgG blocking reagent for 1 h in a humidified chamber. After further rinses with PBS, two times for 2 min each, sections were incubated in the working solution of M.O.M diluents for 5 min. Solution was gently tipped off the slides and sections were then incubated for 30 min at room temperature with a mouse monoclonal anti-phospho-MEK-3/6 (Ser187/Ser209) (1:100, catalog number sc-8407, Santa Cruz Biotechnology Inc.) in M.O.M diluent. After washing two times for 2 min in PBS, the sections were incubated in the working solution of M.O.M biotinylated anti-mouse IgG reagent for 10 min, followed by washing twice for 2 min in PBS. The sections were stained with Fluorescein Avidin DCS for 5 min, washed three times for 5 min in PBS, mounted with Vectashield for fluorescence with DAPI mounting medium (Vector Laboratories) and covered with cover slips.

Phospho-p38 MAPK and  $\gamma$ H2AX immunoreactivity were detected as follows. Sections were incubated in blocking serum (0.5% BSA, 0.1% Triton X-100, 10 % goat serum in PBS) for 1 h at room temperature in a humidified chamber. Serum was gently tipped off the slides, primary antibody against phospho-p38 MAPK (1:50; catalog number #4511, Cell Signaling Technology) and  $\gamma$ H2AX (1:100; catalog number ab2893, Abcam, Cambridge, MA) were diluted in antibody diluent buffer (0.5% BSA, 0.1% Triton X-100, 1.5% goat serum in PBS), and sections were incubated overnight at 4°C or 1 h at room temperature, respectively. Sections were rinsed three times for 5 min in PBS and then incubated with secondary goat anti-rabbit IgG (1:100, catalog number A11008, Invitrogen), diluted in antibody diluent buffer for 1 h at room temperature. After washing three times for 5 min in PBS, sections were counterstained with propidium iodide (Sigma-Aldrich Co., St. Louis, MO) at 10  $\mu$ g/ml in antibody diluent buffer for

5 min at room temperature and then washed again with PBS, three times for 5 min each. Finally, slides were mounted with Vectashield mounting medium (Vector Laboratories, Inc.) and covered with cover slips.

All slides were stored at 4°C and visualized with a fluorescence or confocal microscope within two days. As a negative control for phospho-MEK-3/6, phospho-p38 MAPK and  $\gamma$ H2AX staining, the primary antibodies were preadsorbed with phospho-MEK-3/6 blocking peptide (Santa Cruz Biotechnology, Inc), phospho-p38 MAPK blocking peptide (Cell Signaling Technology, Inc) or  $\gamma$ H2AX blocking peptide (Abcam Inc.), respectively.

### **Fluorescence and Confocal Microscopy**

Phospho-MEK-3/6 immunoreactivity images were captured with a Leica DM LB2 fluorescence microscope (Leica Microsystems Inc, Concord, ON) using a 40x lens fitted with an Infinity-3 video camera (Lumenera Corp., Ottawa, ON).

Phospho-p38 MAPK and  $\gamma$ H2AX immunoreactivities were visualized using a Zeiss LSM 510 Axiovert 100M confocal microscope with a Plan-Apochromat x63/1.4 oil DIC objective (Supplementary data Fig. S4). All embryos were scanned at a 1.65  $\mu$ s pixel time speed with an optical slice of approximately 0.6  $\mu$ m, zoom factor equal to 0.7, and a pinhole setting of 96  $\mu$ m for phospho-p38 MAPK and  $\gamma$ H2AX and 88  $\mu$ m for propidium iodide. Z-stack images of five independent saline treated and HU-treated embryos from each group were acquired.

Optimal settings for fluorescence imaging were determined experimentally for all primary antibodies and maintained for all embryos. For whole embryo images, stained embryos were carefully traced and captured at 20x magnification with the fluorescence microscope and

images were stitched together using the Microsoft Image Composite Editor software (Microsoft Corporation, Albuquerque, NM).

### **Quantitative Analysis**

For quantitative analysis of phospho-MEK-3/6, saline and HU-treated embryos were analyzed using MetaMorph Image Analysis software (Molecular Devices, Sunnyvale, CA). Two regions of interest were randomly selected and created within an image by a 2D box of 200 x 200  $\mu\text{m}$ . Then the intensity means were analyzed in the cropped images. The unit of measure (N) was the number of saline or HU-treated pregnant females. For the control group, N=5 females, with 13, 14 and 13 embryos, were analyzed in the 0.5 h, 3 h and 6 h groups, respectively. For the low dose (400 mg/kg) HU-treated embryo groups, N=5 females, with 15, 14, 15 embryos, were analyzed at 0.5 h, 3 h and 6 h, respectively. For the high dose (600 mg/kg) HU-treated embryo group, N=5 females, with 15, 14, 14 embryos, were analyzed at 0.5 h, 3 h and 6 h, respectively (Supplementary data, Table S1).

Measurements of phospho-p38 MAPK and  $\gamma\text{H2AX}$  immunoreactivities were analyzed using Imaris Software (Bitplane AG, Zurich, Switzerland). For each image, two regions of interest were randomly selected and created by a 3D box of 50 x 50 x 14  $\mu\text{m}$ . 3D iso-surfaces of saline and HU-treated embryos were generated and total intensity means were measured for the staining of phospho-p38 MAPK. For the quantification of nuclear staining, a nuclear surface was first created from propidium iodide staining for each image; within that surface, phospho-p38 MAPK and  $\gamma\text{H2AX}$  were isolated. The nuclear intensity means were analyzed for phospho-p38 MAPK;  $\gamma\text{H2AX}$  foci were quantified based on their volume normalized to the nuclear volume. An animation of the nuclear quantification is included in the supplementary data (Supplementary

data, Fig. S1). For the analysis of phospho-p38 MAPK, the sample size for the control, low dose and high dose groups was N=5 females; 10 embryos were analyzed at each time point for each group (ie. 2 embryos/female). For the analysis of  $\gamma$ H2AX, the sample size for each dose group and time point was N=5 females; 13 to 15 embryos were analyzed for each group at each time point (2-3 embryos per female) (Supplementary data, Tables S2-4).

Images from  $\gamma$ H2AX staining were used to analyze pyknotic nuclei. Green channel ( $\gamma$ H2AX) was turned off and propidium iodide staining was isolated using IMARIS. The total numbers of nuclei and of pyknotic nuclei were counted in each image.

The five areas quantified for each embryo were the rostral neuroepithelium (RNE), caudal neuroepithelium (CNE), neural tube (NT), somite (S) and heart (H) (as indicated in Supplementary data, Fig. S2). To compare the intensity means and DNA damage between the HU-treated groups and the control group, the values for the control group were set to 1 and the fold differences from control were examined. All the immunofluorescence analyses for this study are summarized in supplementary data Tables S1-S4.

## **Statistical Analyses**

All statistical analyses were done by two-way ANOVA, using GraphPad Prism version 5.00 (GraphPad Software, San Diego, CA). Dunnett's test was done to analyze the drug effect between control and HU-treated embryos. Tukey's multiple comparison test was used to assess any differences in the intensity means of phospho-MEK-3/6 and phospho-p38 MAPK, as well as  $\gamma$ H2AX foci volume, among the five selected regions at 3 h in each treatment group. All values were reported as fold difference from the control group, set to  $1 \pm$  standard error of mean. The a priori level of significance was  $p < 0.05$ .

## Results

### **HU induced widespread activation of MEK-3/6 in GD 9 embryos.**

The expression of total and activated MEK-3/6 protein was determined in GD 9 embryos 0.5, 3 and 6 h post-treatment with saline (C), low (L: 400 mg/kg) or high (H: 600 mg/kg) dose HU. Total MEK-3/6 protein concentrations were not altered by HU treatment at 0.5, 3 or 6 h, compared with saline controls (Fig. 1A). However, HU exposure induced a dramatic increase in the activation of MEK-3/6 at 0.5, 3 and 6 h as detected by an increase in phospho-MEK-3/6 in Western blots (Fig. 1B). Therefore, *in utero* HU exposure triggered the activation of MEK 3/6.

The localization of activated MEK-3/6 in the embryo was assessed to determine the tissue specificity of the response to HU exposure. In saline treated embryos, low amounts of phospho-MEK-3/6 immunoreactivity (green color) were detected in the embryos (Fig. 2A and B). Exposure to HU increased the activation of MEK-3/6 as demonstrated by an increase in fluorescence intensity. Phospho-MEK-3/6 immunoreactivity was widespread and enhanced in HU-exposed embryos; activated MEK-3/6 was detected in the rostral neuroepithelium (RNE), caudal neuroepithelium (CNE), neural tube (NT), somites (S) and heart (H) (Fig. 2B). Quantitative analysis of the fluorescence in these regions using MetaMorph revealed a dose-dependent increase in phospho-MEK-3/6 total intensity in HU exposed embryos compared to control/saline treated embryos (Fig. 3). At 3 h post-treatment, a 3 fold increase in reactivity was observed in the rostral and caudal neuroepithelium and heart in the high dose HU group compared to the saline group (Fig 3). To determine if activated MEK-3/6 preferentially localized to a specific region within the embryo, Tukey's analysis was done to compare the five regions against each other within a treatment group (a total of 10 comparisons). There were no significant differences in p-MEK3/6 total mean intensities among the five regions in either the

saline or HU-treated embryos (Fig. 3F and Suppl. Data, Fig. S3A). Therefore, HU treatment induced a widespread activation of MEK-3/6 in embryos.

### **HU promoted localized activation and nuclear translocation of p38 MAPK.**

Since the upstream MEK3/6 kinases catalyze phosphorylation of the downstream p38 MAPKs, we determined the effects of HU exposure on the activation and localization of p38 MAPK. Western blot analysis showed that the total expression of p38 MAPK was not affected by HU treatment at 0.5, 3 or 6 h (Fig. 4A), but its activation was enhanced after exposure to increasing doses of HU (Fig. 4B). Exposure to high dose HU significantly increased the phosphorylation of p38 MAPK at 3 h post treatment compared to the saline group (Fig. 4B). The maximum amplitude of this increase (10.7 fold) exceeded that observed for phospho-MEK-3/6; the activation of p38 MAPK was transitory since by 6 h post-treatment HU exposed embryos did not differ significantly from controls. Phospho-p38 MAPK immunofluorescence staining was distributed globally in control embryos (Fig. 5A, Suppl. Fig. S3B); the total intensity increased with increasing HU dose (Fig. 5A and B). Similarly, Tukey's test was carried out to determine the region specificity of the distribution of phospho-p38 MAPK within the embryo. Contrary to the widespread MEK-3/6 activation observed in embryos, quantitative analysis of phospho-p38 MAPK immunoreactivity 3 h after HU treatment revealed that p38 MAPK was preferentially activated in the rostral neuroepithelium, caudal neuroepithelium and neural tube of HU-treated embryos (Fig. 6A-C). Although there was also an increase in total phospho-p38-MAPK in the somite and heart (Fig. 6E-F), the mean changes were not significant. Activated p38 MAPKs phosphorylate substrates in the cytoplasm and nucleus. Therefore, our next goal was to determine whether HU exposure altered the intracellular distribution of phospho-p38 MAPK in

embryos. We used confocal microscopy and IMARIS 3D imaging software surface rendering to assess phospho-p38 MAPK immunofluorescence in the cytosol and nucleus. This allowed the removal of cytosol staining, isolating the nuclear staining; cytosol and nuclear intensities were quantified separately (Suppl. Fig. S1). In control embryos, phospho-p38 MAPK was detected primarily in the cytosol, with low amounts in the nucleus and no region specificity (Fig. 5A and B; Suppl. Fig. S3C). Exposure to HU resulted in the nuclear accumulation of phospho-p38 MAPK (Fig. 5A and B; Fig. 7). HU exposure significantly increased the nuclear intensity of phospho-p38 MAPK in the rostral neuroepithelium, caudal neuroepithelium, neural tube and somite compared to the saline group (Fig. 7); peak amounts of nuclear phospho-p38 MAPK were observed in the neuroepithelium at 3 h. At this time, Tukey's analysis revealed that there was a significant region specific nuclear accumulation of phospho-p38 MAPK in the rostral and caudal neuroepithelium (Fig. 7F). While total phospho-p38 MAPK was expressed highly in the neuroepithelium and neural tube (Fig. 6F), nuclear phospho-p38 MAPK was preferentially localized to the neuroepithelium (Fig. 7F). Since the total protein expression of p38 MAPK was unaffected by HU treatment (Fig. 4A), the increase in nuclear expression of phospho-p38 MAPK was due to protein translocation rather than the translation of new protein. Thus, these results suggest that p38 MAPK is activated dramatically in response to HU insult; moreover, phospho-p38 MAPK is translocated into the nucleus in a region-specific manner within the embryo.

### **HU induced localized DNA damage and altered nuclear morphology**

Since DNA damage inducing stimuli trigger the nuclear translocation of phospho-p38 MAPK, we investigated the impact of HU treatment on DNA damage in embryos using  $\gamma$ H2AX as a marker for DNA double strand breaks (DSBs). Low numbers of  $\gamma$ H2AX foci were observed

in all regions of the control embryos (Fig. 8; Supp. Fig. S3D). HU-treated embryos exhibited a dramatic increase in the overall  $\gamma$ H2AX signal intensities and in the numbers of  $\gamma$ H2AX foci compared with the saline-treated embryos (Fig. 8). The foci in the high dose HU (HU600) group were so concentrated that they appeared as clusters within the nuclei. Therefore,  $\gamma$ H2AX focal volume was chosen as the parameter to be measured quantitatively. Comparisons of the mean volumes of  $\gamma$ H2AX foci indicated that a significant increase occurred in the HU-treated embryos in each of the five regions (Fig. 9). Temporally, this increase occurred as early as 0.5 h (neural tube) post-HU treatment; the response peaked at 3 h in all tissues. Spatially, the greatest increase in  $\gamma$ H2AX focal volumes within the embryos was observed in the caudal neuroepithelium, with up to a 13.5 fold increase compared to the saline-treated group. A comparison among the five regions indicated a significant difference in  $\gamma$ H2AX focal volumes in the caudal neuroepithelium of the embryos exposed to high dose HU (Fig. 9). Thus, the HU-induced activation of DNA damage signaling pathways in the embryo during organogenesis was enhanced in this malformation-sensitive tissue.

The nuclei of cells that are in the process of dying, by apoptosis or necrosis, display an irreversible condensation of chromatin known as pyknosis. The propidium iodide staining of the nuclei of saline-treated and HU-exposed embryos was detected in cells in the process of dying. Embryos exposed to saline showed normal nuclear morphology at all time points. However, pyknotic nuclei and cell fragmentation were observed in HU-treated embryos starting at 3 h post-treatment (Fig. 10). The numbers of pyknotic nuclei were increased in all affected regions at 6 h, reaching up to 41% (Fig. 10). It is interesting to note that pyknotic nuclei were observed in all regions of the embryo except the heart, even though  $\gamma$ H2AX foci were increased significantly in the heart (Fig. 9).

## Discussion

Maternal exposure to HU activated p38 MAPK and its upstream mediator, MEK3/6, in the organogenesis-stage embryo. MEK 3/6 is crucial in mediating the activation of p38 MAPK. Studies have shown that MEK3/6 double-knockout mice die during embryogenesis due to a placental defect (Mudgett et al., 2000), whereas mice deficient only in MEK 3 or MEK6 are viable but display a decrease in long bone mineralization and p38 MAPK activation (Greenblatt et al., 2010). Thus, the MEK3/6-p38 MAPK axis is a major mediator of skeletal mineralization. Both MEK3/6 and p38 MAPK were activated in embryos 0.5 h post-HU treatment, at a time when previous studies have shown that HU induces oxidative stress (Yan and Hales, 2006). This association suggests that free radical species may be one of the stimuli that triggers p38 MAPK signaling. Similarly,  $\gamma$ H2AX foci formation is observed as early as 0.5 h post-HU-treatment, suggesting that free radicals may directly attack DNA and cause strand breaks. Moreover, this direct free radical-induced damage to DNA may induce DNA damage signals which, in turn, activate the p38 MAPK pathway. Both the formation of  $\gamma$ H2AX foci and the activation of p38 MAPK peaked at 3 h post-HU treatment. We anticipate that DNA synthesis is still reduced at this time after HU treatment (DeSesso and Goeringer, 1990; Smith et al., 1968). Stalled replication forks lead to replication stress and further induce DNA strand breaks (Feng et al., 2011). Thus, HU-mediated embryotoxicity may be due to two mechanisms, oxidative stress and replication stress.

Interestingly, the localization of activated kinases in embryos was more region-specific for phospho-p38 MAPK, the downstream target kinase, than for MEK-3/6. MEK-3/6 activation was widespread in the embryo, whereas p38 MAPK activation was localized to the rostral and caudal neuroepithelium and neural tube. Phospho-p38 MAPK was found predominantly in the

cytoplasm in control embryos. Upon HU exposure, preferential translocation of phospho-p38 MAPK into the nucleus was observed in the rostral and caudal neuroepithelium. This nuclear translocation may be a specific response to stimuli that induce DNA double strand breaks while other exposures, such as to sodium arsenite, promote the cytoplasmic accumulation of phospho-p38 MAPK (Ben-Levy et al., 1998). The HU-induced nuclear accumulation of phospho-p38 MAPK will enable the activation of its nuclear substrates, such as MAPKAP kinase-2 (MK2) and p53, both of which induce cell cycle checkpoints and facilitate DNA repair (Bulavin et al., 2001). Activation of cell cycle checkpoints in response to DNA damage is essential for the maintenance of genomic stability. Reinhardt and colleagues (2007) have shown that down-regulation of MK2 caused regression of tumour cells *in vivo*, leading to mitotic catastrophe after treatment with DNA damaging agents. Since previous studies have shown that the inhibition of p38 MAPK enhanced fetal mortality after HU exposure (Yan and Hales, 2008), we propose that p38 plays a role in protecting the embryo from HU insult. Furthermore, the disruption of the p38 MAPK-MK2 axis may increase the sensitivity of embryos to HU by disrupting normal checkpoint functions and allowing cells with damaged DNA strands to enter mitosis, leading to mitotic catastrophe and resulting in an increase in apoptotic cell death. Therefore, in addition to its well-described role in apoptosis, p38 MAPK may also be important in mediating survival in embryos.

Caudal regions of the embryo are of special interest to us since caudal defects predominate in embryos exposed to HU on GD9. In this study, we report that the caudal neuroepithelium displayed the highest accumulation of phospho-p38 MAPK and  $\gamma$ H2AX foci in the nuclei. HU-induced damage in the caudal region of the embryo may exceed the repair capacity of cells in this area, leading to the induction of apoptosis as indicated by the increase in

pyknotic nuclei observed 6 h post-HU-treatment. Interestingly, the heart was the only region in which an increase in pyknotic nuclei was not observed. Cells in the heart have a longer cell cycle; the presence of fewer cells in S phase would be expected to result in fewer pyknotic nuclei after HU exposure. The heart is also an organ that is resistant to insult by a number of cytotoxic teratogens (Mirkes and Little, 1998). HU-induced nuclear phospho-p38 MAPK was relatively low in the heart. During limb development, p38 MAPK was activated where cell death occurs, in the interdigital tissue. Moreover, nuclear labeling of phospho-p38 MAPK increased during tissue regression, suggesting that p38 MAPK mediates the up-regulation of genes involved in programmed cell death (Zuzarte-Luis et al., 2004). Since the absence of cell death in the heart is accompanied by low levels of nuclear phospho-p38 MAPK, the expression of cell death genes regulated by p38 MAPK may be repressed in the heart.

The absence of cell death despite the formation of  $\gamma$ H2AX foci in the embryonic heart may also suggest that there is sufficient DNA repair to preserve chromatin architecture and, ultimately, cell survival in this organ. Immediate and efficient repair after the induction of DNA double strand breaks is important to restore and preserve the integrity and functionality of chromatin. Phosphorylation of H2AX is a key step in the DNA damage response, playing a role in signaling and initiating the repair of DNA double strand breaks (Celeste et al., 2002). The formation of  $\gamma$ H2AX foci represents an epigenetic signal that helps in the recruitment and accumulation of DNA damage response proteins at the sites of DNA strand breaks (Kinner et al., 2008). In parallel, p38 MAPK modulates the cell cycle checkpoint response, providing the time required for DNA repair. Interestingly, this appears to be true only at relatively low levels of DNA damage (Kinner et al., 2008). After higher levels of damage, extensive chromosome breakage results in cells that are incapable of resuming DNA synthesis (Feng et al., 2009). Since

the formation of  $\gamma$ H2AX foci is low in the heart compared to the caudal neuroepithelium, we predict that DNA damage in the heart is below a critical threshold, allowing this damage to be sufficiently repaired for cells to survive. In addition, it has been proposed that the cytoplasmic accumulation of p38 MAPK favours a survival response. Reinhardt et al. (2010) discovered a late cell cycle checkpoint that is controlled by cytoplasmic p38 MAPK (Reinhardt et al., 2010). It is possible that sustained cell cycle arrest is occurring in the heart, allowing this organ to undergo more efficient DNA repair.

The increases in activation of the p38 MAPK signaling and DNA damage response pathways as a result of HU-induced oxidative and replication stress suggest that these pathways may serve as intracellular effectors of the embryonic stress response. It is clear that the regulation of p38 MAPK signaling is complex. Further insight into the identification of p38 MAPK nuclear substrates in different regions of the embryo is a priority in understanding the decision of cells to execute different pathways, i.e. apoptosis in the caudal neuroepithelium versus cell survival and differentiation in the heart. In addition, the extent to which a teratogenic insult stimulates the DNA repair process in the embryo remains to be determined.

## Figures and Legends

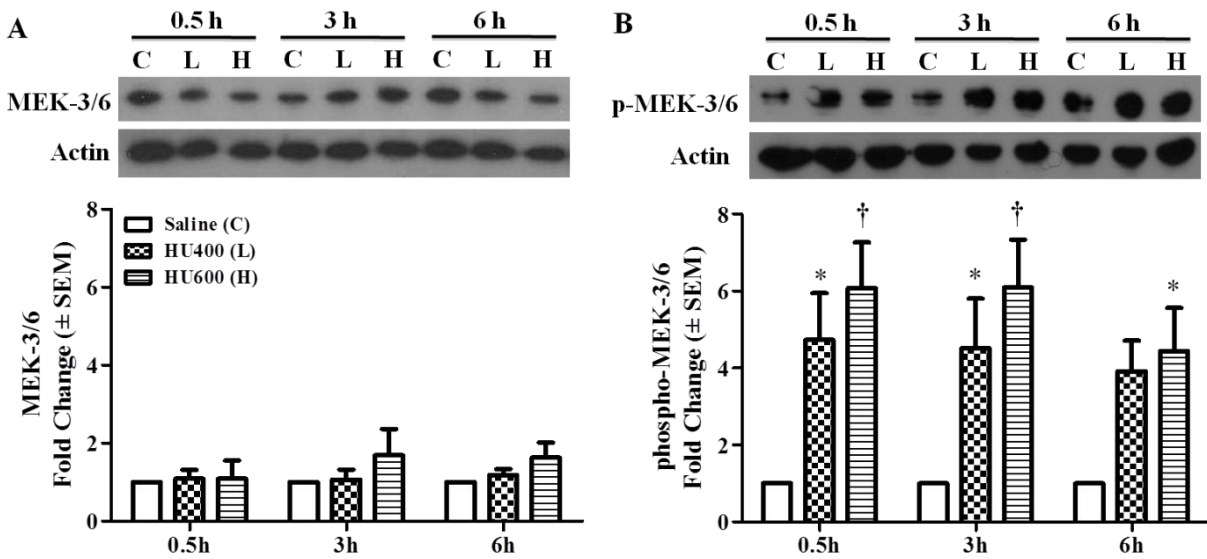


**Figure 2.1 HU induced activation of MEK-3/6**

A. Western blot analysis of total protein expression of MEK-3/6 at 0.5, 3, and 6 h after treatment with HU at 400 mg/kg (L) or 600 mg/kg (H) is shown in the upper panel. The lower panel shows the densitometry quantification of MEK-3/6. B. Western blot analysis of phospho-MEK-3/6 at 0.5, 3, and 6 h after treatment with HU at 400 mg/kg (L) or 600 mg/kg (H) is shown in the upper panel. The lower panel shows the densitometry quantification of phospho-MEK-3/6. Each bar (mean  $\pm$  S.E.M) represents embryos from five litters ( $n = 5$ ). \* and †, significantly different from saline (control) group at the same time point (\*,  $p < 0.05$ ; †,  $p < 0.01$ , Dunnett's test).

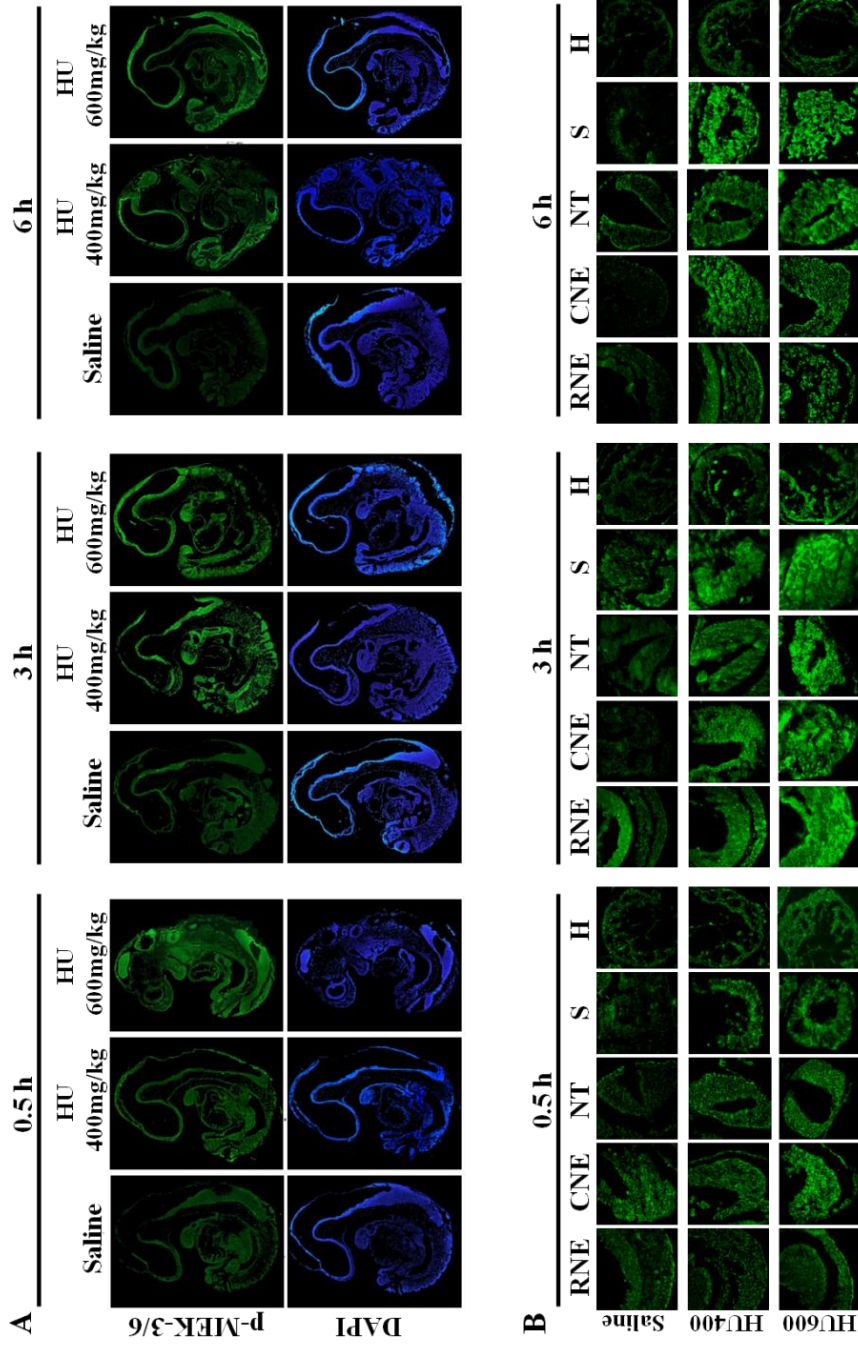


**Figure 2.2 The localization of activated MEK-3/6 in GD 9 embryos exposed to HU**

Timed-pregnant female mice received saline or HU at 400 mg/kg or 600 mg/kg on GD 9. Embryos were processed for immunofluorescence staining with an antibody against phospho-MEK-3/6 (in green) and counterstained with DAPI (in blue). A, Whole embryo views of phospho-MEK-3/6 immunoreactivity at 0.5, 3 and 6 h post-HU treatment. B, 40x magnification of the selected five regions in an embryo: rostral neuroepithelium (RNE), caudal neuroepithelium (CNE), neural tube (NT), somite (S) and heart (H).

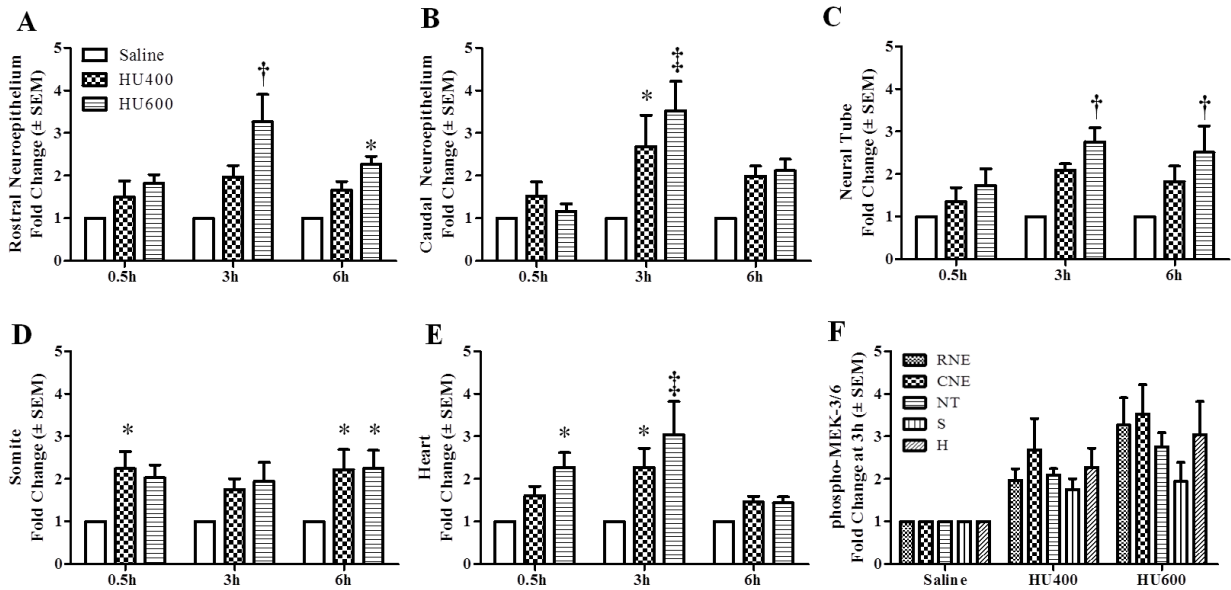


**Figure 2.3 Intensity means of phospho-MEK-3/6 in different regions of GD 9 embryos**

The quantification of phospho-MEK-3/6 immunoreactivity by intensity mean in GD 9 embryos exposed to saline or HU at 400 mg/kg or 600 mg/kg in different regions is presented in the rostral neuroepithelium (A), caudal neuroepithelium (B), neural tube (C), somite (D), and heart (E). Values were normalized to the corresponding saline control and expressed as fold changes.  $n = 5$ , Asterisks, daggers and double daggers denote a significant difference from saline control at the same time point (\*,  $p < 0.05$ ; †,  $p < 0.01$ ; ††,  $p < 0.001$ , Dunnett's test). F. Phospho-MEK-3/6 staining at 3 h post-HU treatment. There were no significant regional differences in phospho-MEK-3/6 staining within the embryo.

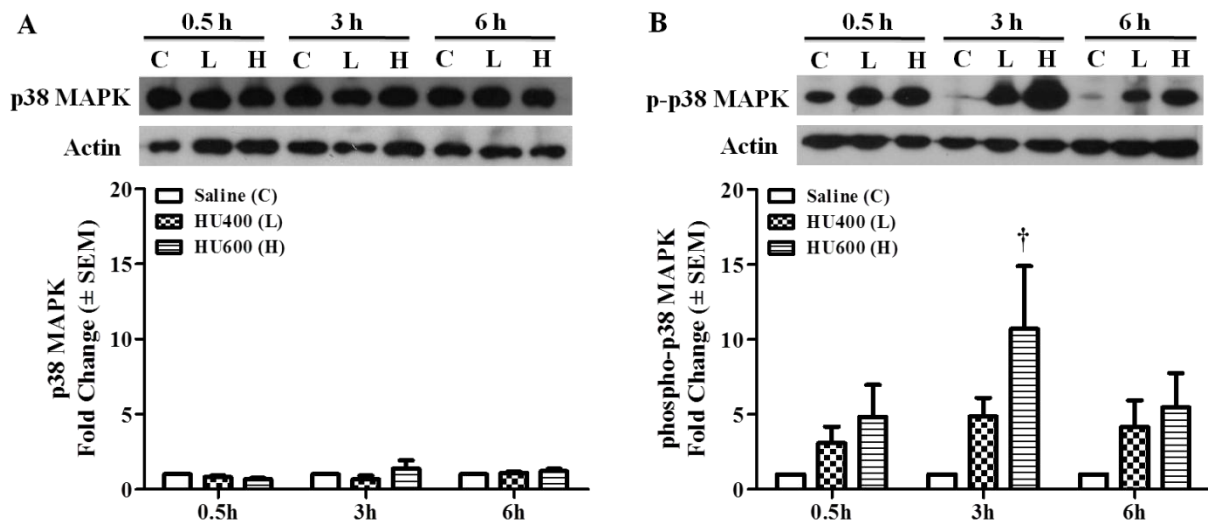


**Figure 2.4 HU induced activation of p38 MAPK**

A. Western blot analysis of total protein expression of p38 MAPK at 0.5, 3, and 6 h after treatment with HU at 400 mg/kg (L) or 600 mg/kg (H) is shown in the upper panel; the lower panel depicts the scan densitometry quantification of p38 MAPK. B. Western blot analysis of phosphorylated p38 MAPK at 0.5, 3, and 6 h after treatment with HU at 400 mg/kg (L) or 600 mg/kg (H) is shown in the upper panel; the lower panel depicts the scan densitometry quantification of phospho-p38 MAPK. Each bar (mean  $\pm$  S.E.M) represents embryos from six litters. \*, significantly different from saline (control) group at the same time point ( $\dagger$ ,  $p < 0.01$ , Dunnett's test).

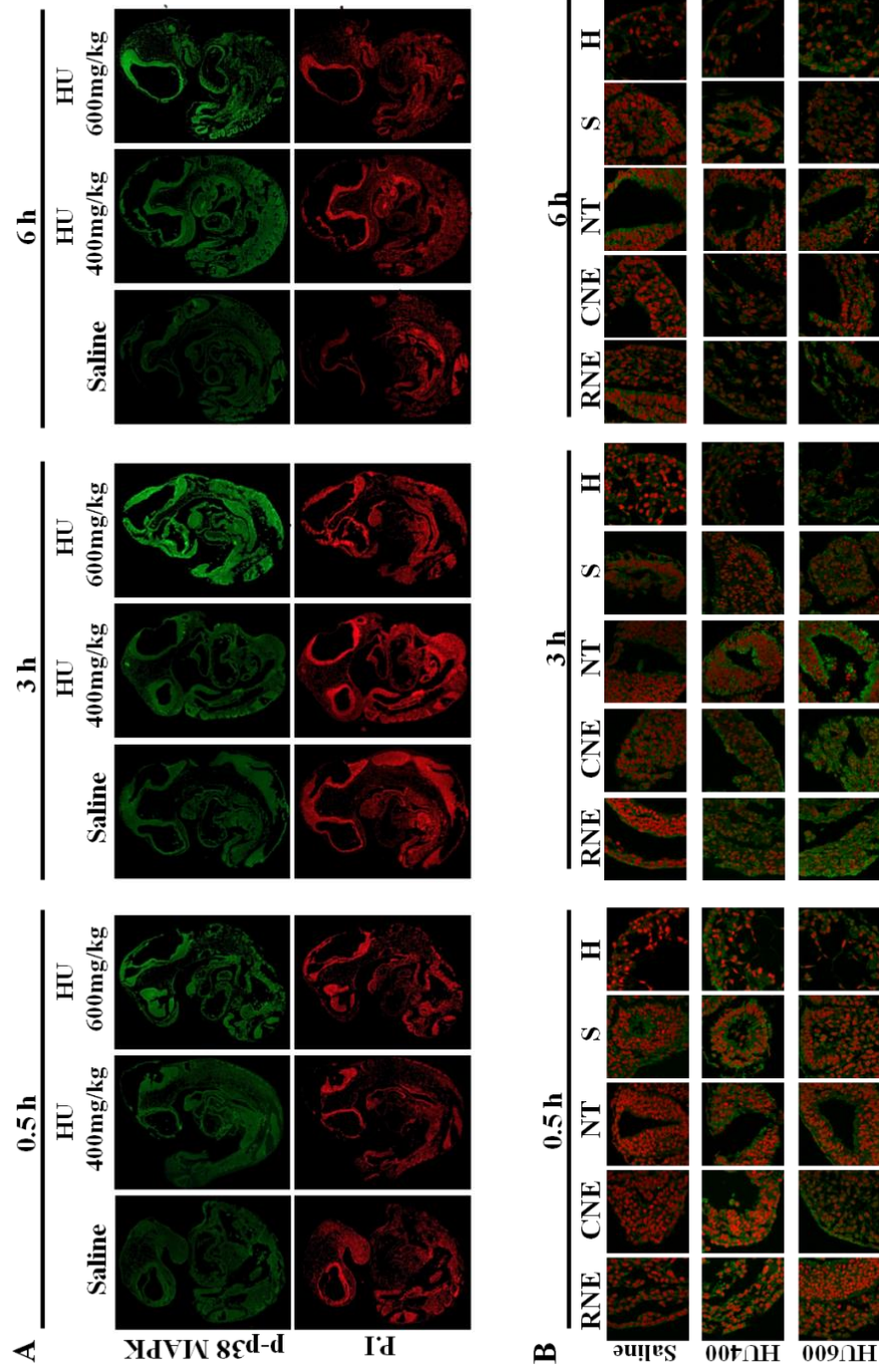


**Figure 2.5 The localization of phospho-p38 MAPK in GD 9 embryos exposed to HU**

Timed-pregnant female mice received saline or HU at 400 mg/kg or 600 mg/kg on GD 9. Embryos were processed for immunofluorescence staining with an antibody against phospho-p38 MAPK (in green) and counterstained with propidium iodide (in red). A, Whole embryo views of phospho-p38 MAPK immunoreactivity at 0.5, 3 and 6 h post treatment. B, 60x magnification views of the selected five regions in an embryo: rostral neuroepithelium (RNE), caudal neuroepithelium (CNE), neural tube (NT), somite (S) and heart (H).

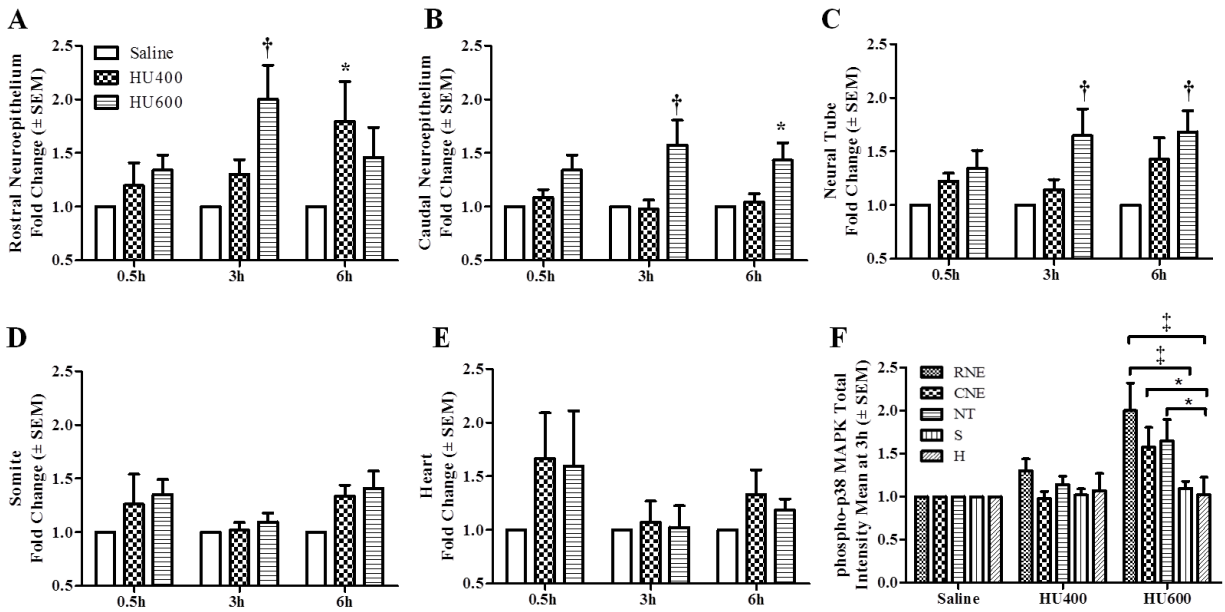


**Figure 2.6 Total intensity means of phospho-p38 MAPK in different regions of GD 9 embryos**

The quantification of total phospho-p38 MAPK immunoreactivity by intensity means in GD 9 embryos exposed to saline or HU at 400 mg/kg or 600 mg/kg in different regions is presented for the rostral neuroepithelium (A), caudal neuroepithelium (B), neural tube (C), somite (D) and heart (E). Values were normalized to the corresponding saline control and expressed as fold changes.  $n = 5$ , Asterisks, daggers and double daggers denote a significant difference from saline control at the same time point (\*,  $p < 0.05$ ; †,  $p < 0.01$ ; ‡,  $p < 0.001$ , Dunnett's test). F. Regional differences in total phospho-p38 MAPK reactivity in control and HU-exposed embryos. At 3 h post-treatment, RNE was significantly different than S and H (‡,  $p < 0.001$ ); CNE and NT were both significantly different than H (\*,  $p < 0.05$ , Tukey's multiple comparison test).

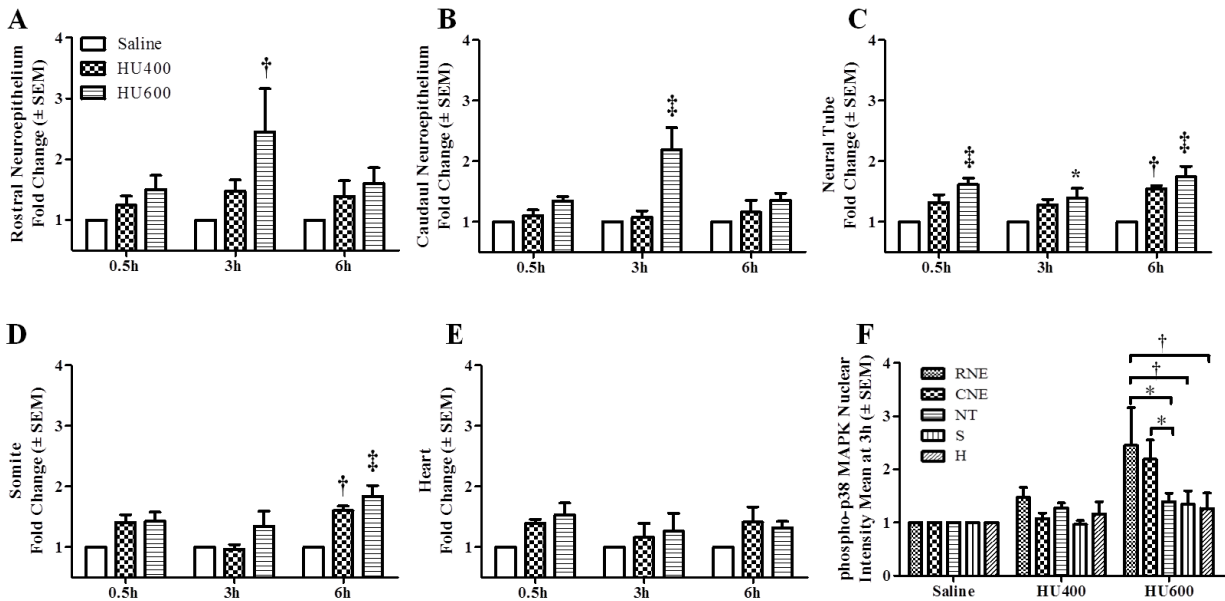


**Figure 2.7 Nuclear intensity means of phospho-p38 MAPK in different regions of GD 9 embryos**

The quantification of nuclear phospho-p38 MAPK immunoreactivity by intensity mean in GD 9 embryos exposed to saline or HU at 400mg/kg or 600mg/kg in different regions is presented for the rostral neuroepithelium (A), caudal neuroepithelium (B), neural tube (C), somite (D), and heart (E). Values were normalized to the corresponding saline control and expressed as fold changes.  $n = 5$ , Asterisks, daggers and double daggers denote a significant difference from saline control at the same time point (\*,  $p < 0.05$ ; †,  $p < 0.01$ ; ‡,  $p < 0.001$ , Dunnett's test). Panel F illustrates the regional differences in nuclear phospho-p38 MAPK expression found in RNE and CNE of embryos exposed to HU at 600mg/kg. RNE was significantly different than NT (\*,  $p < 0.05$ ), S and H (†,  $p < 0.01$ ); CNE was significantly different than H (\*,  $p < 0.05$ , Tukey's multiple comparison test).

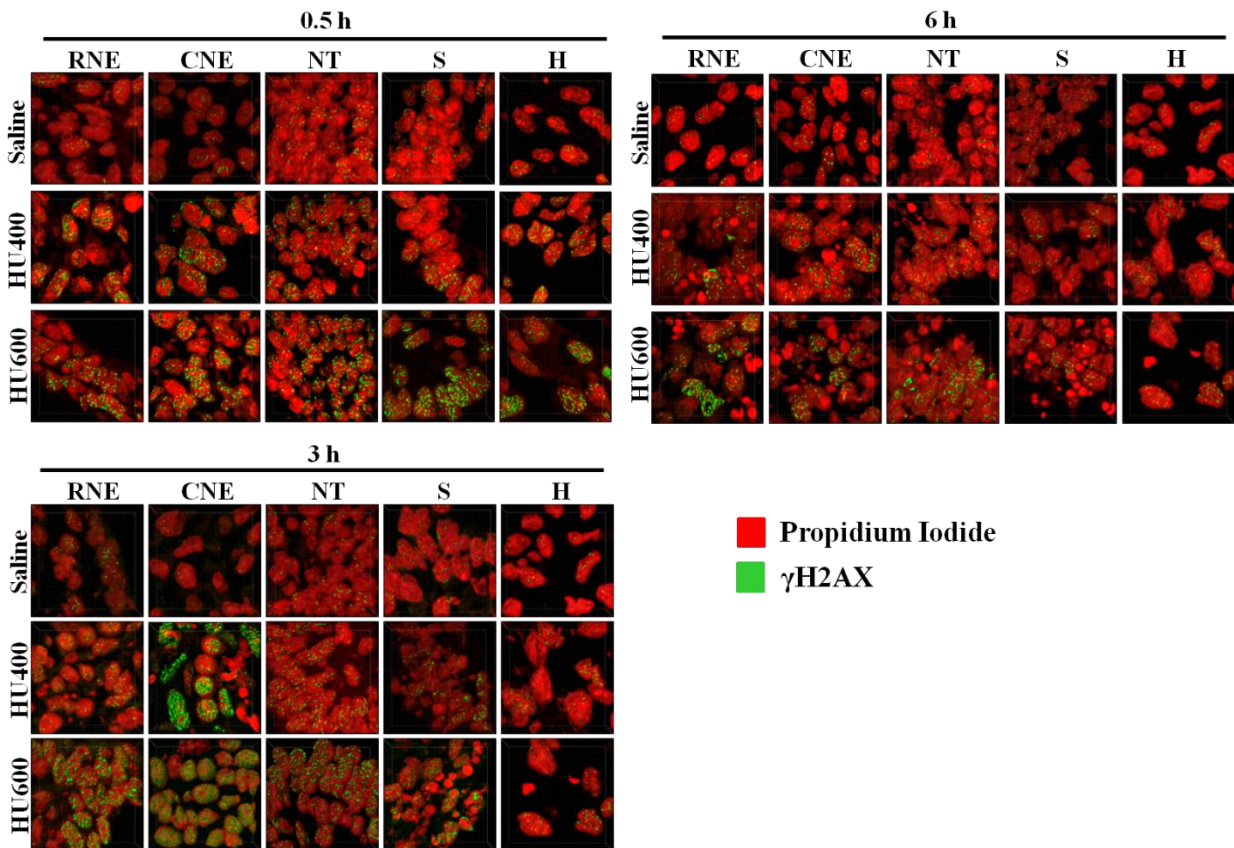


**Figure 2.8  $\gamma$ H2AX staining in GD9 embryos exposed to HU**

The detection of DNA double strand breaks with  $\gamma$ H2AX in saline and HU-exposed embryos in different regions. Immunodetection of  $\gamma$ H2AX is in green and nuclear propidium iodide in red.

Images display quantification regions (50 x 50 x 14 $\mu$ m) which were randomly selected from each structure taken at 63 x magnification (shown in Supplementary data Fig. S4).

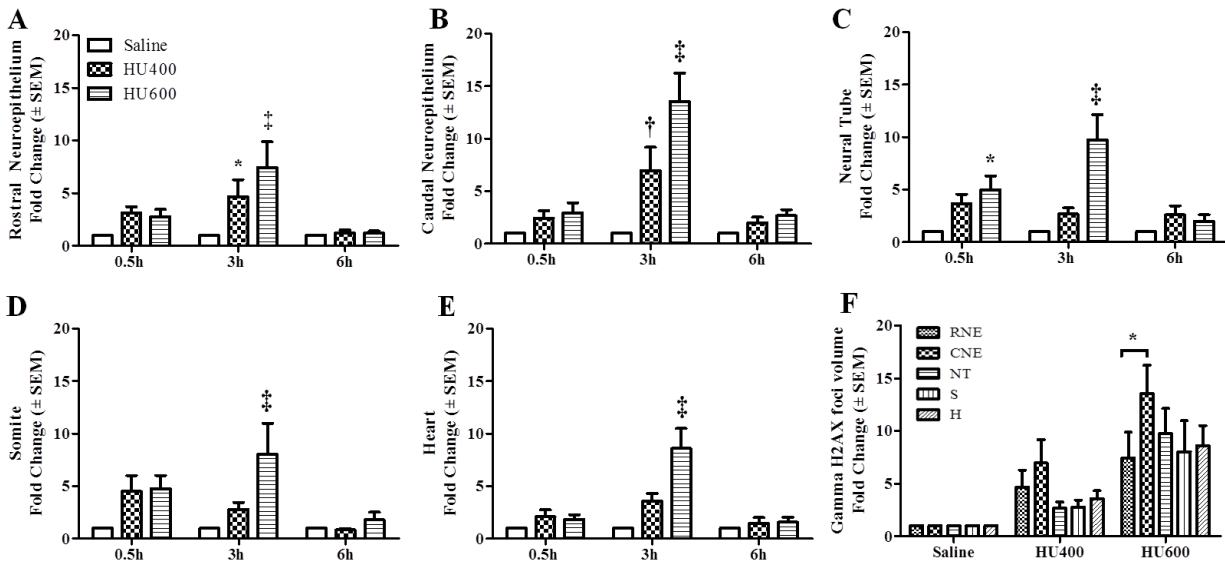


**Figure 2.9  $\gamma$ H2AX focal volumes in different regions of GD 9 embryos**

The quantification of  $\gamma$ H2AX focal volumes in different regions of the GD 9 embryos exposed to saline or HU at 400 mg/kg or 600 mg/kg is presented for the rostral neuroepithelium (A), caudal neuroepithelium (B), neural tube (C), somite (D), and heart (E). Values were normalized to the corresponding saline controls and expressed as fold changes.  $n = 5$ , Asterisks, daggers and double daggers denote a significant difference from saline controls at the same time point (\*,  $p < 0.05$ ; †,  $p < 0.01$ ; ‡,  $p < 0.001$ , Dunnett's test). F. The regional differences in  $\gamma$ H2AX focal volumes found in the CNE of embryos exposed to HU at 600 mg/kg. CNE was significantly different than RNE (\*,  $p < 0.05$ , Tukey's multiple comparison test).

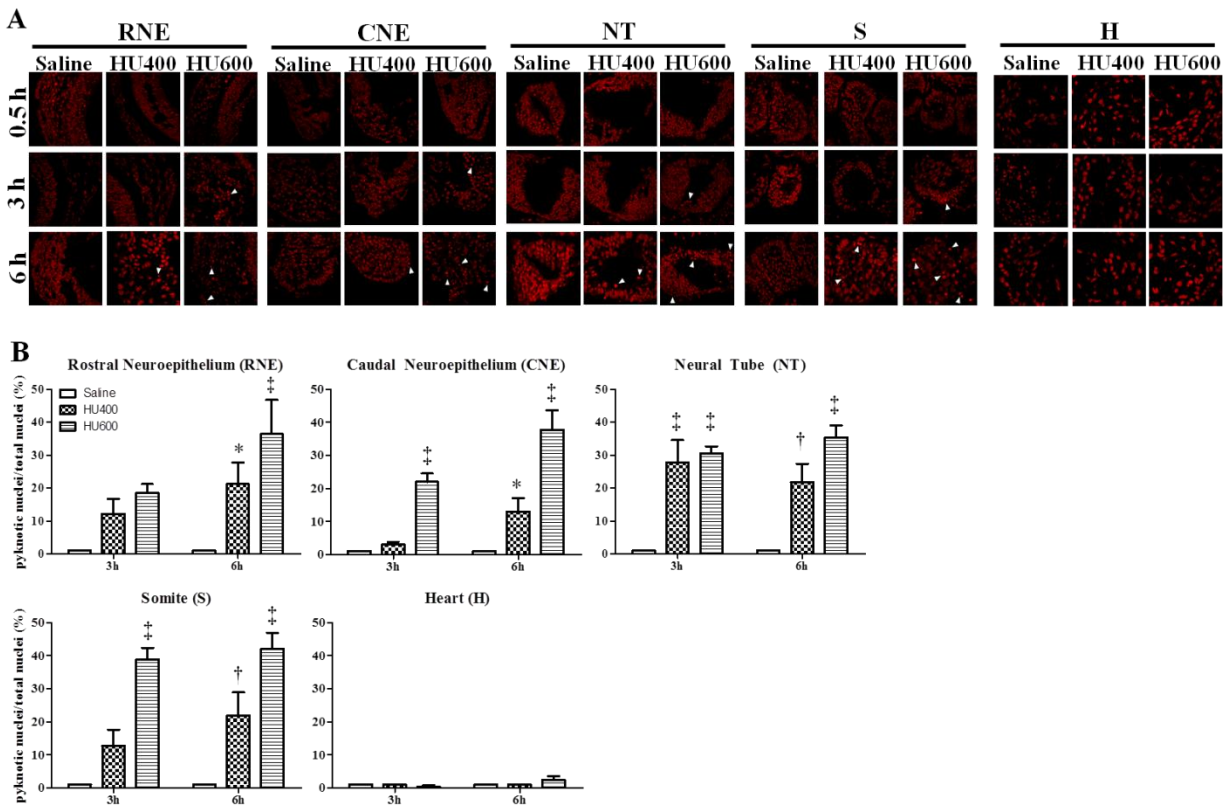


**Figure 2.10 Pyknotic nuclei in different regions of the GD 9 embryos exposed to HU.**

A, Propidium iodide staining of the rostral neuroepithelium (RNE), caudal neuroepithelium (CNE), neural tube (NT), somite (S), and heart (H) in saline and HU-exposed embryos at 0.5, 3 and 6 h post-treatment. The arrowheads indicate pyknotic nuclei. B, Quantification of pyknotic nuclei by IMARIS. Each bar (mean  $\pm$  S.E.M) represents the percentage of pyknotic nuclei. Embryos from five litters per treatment group were analyzed. Asterisks, dagger and double dagger denote a significant difference from saline control at the same time point (\*,  $p < 0.05$ ; †,  $p < 0.01$ ; ††,  $p < 0.001$ , Dunnett's test).

## Supplementary Data Figure Legends and Tables

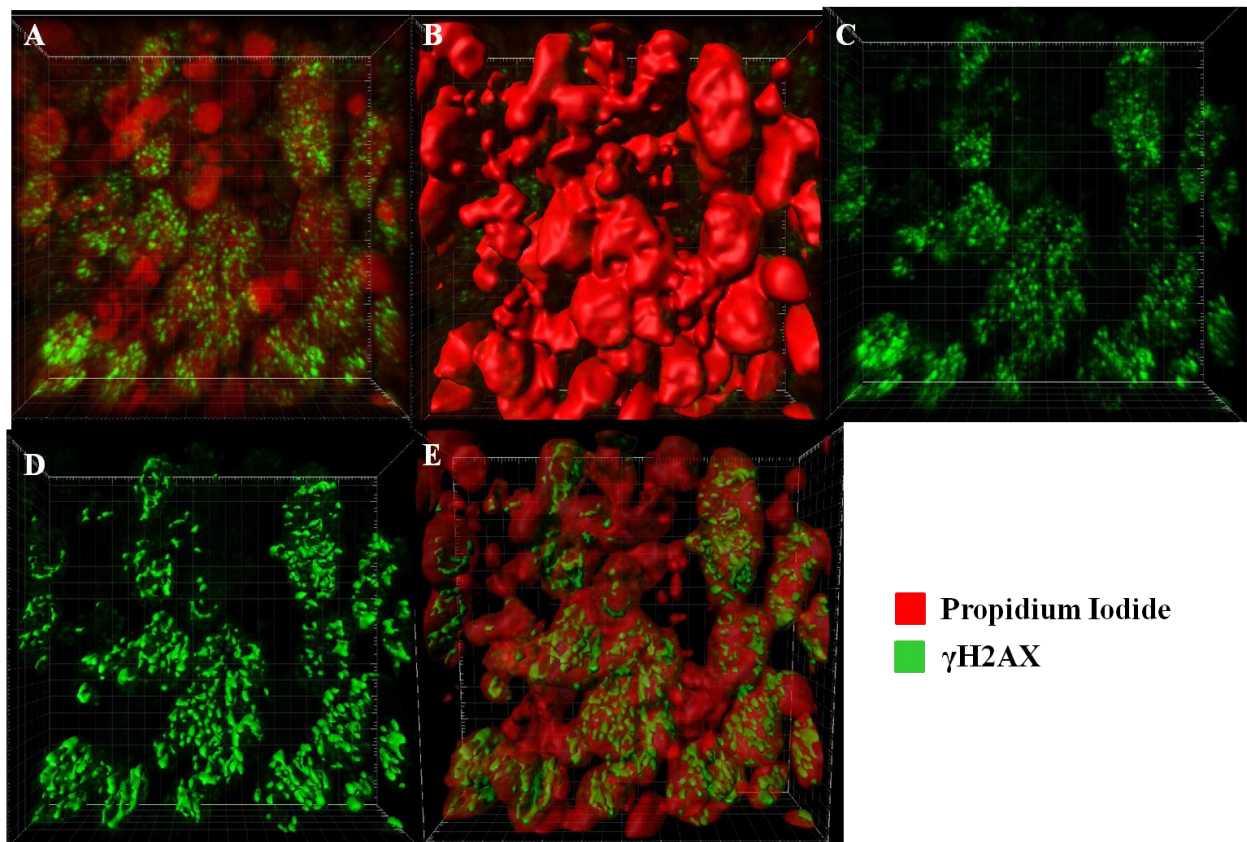


**Figure S1. Animation movie of nuclear quantification by IMARIS.**

Red: Propidium Iodide, Green:  $\gamma$ H2AX (or phospho-p38 MAPK). Using the IMARIS 3D surface rendering technique on the original confocal z-stack image (A), nuclei are first isolated by propidium iodide staining (B). Nuclear  $\gamma$ H2AX or phospho-p38 MAPK was isolated (C) and different parameters, such as intensity, area, or cell counts, were measured by masking the green channel within the nuclei (D-E).

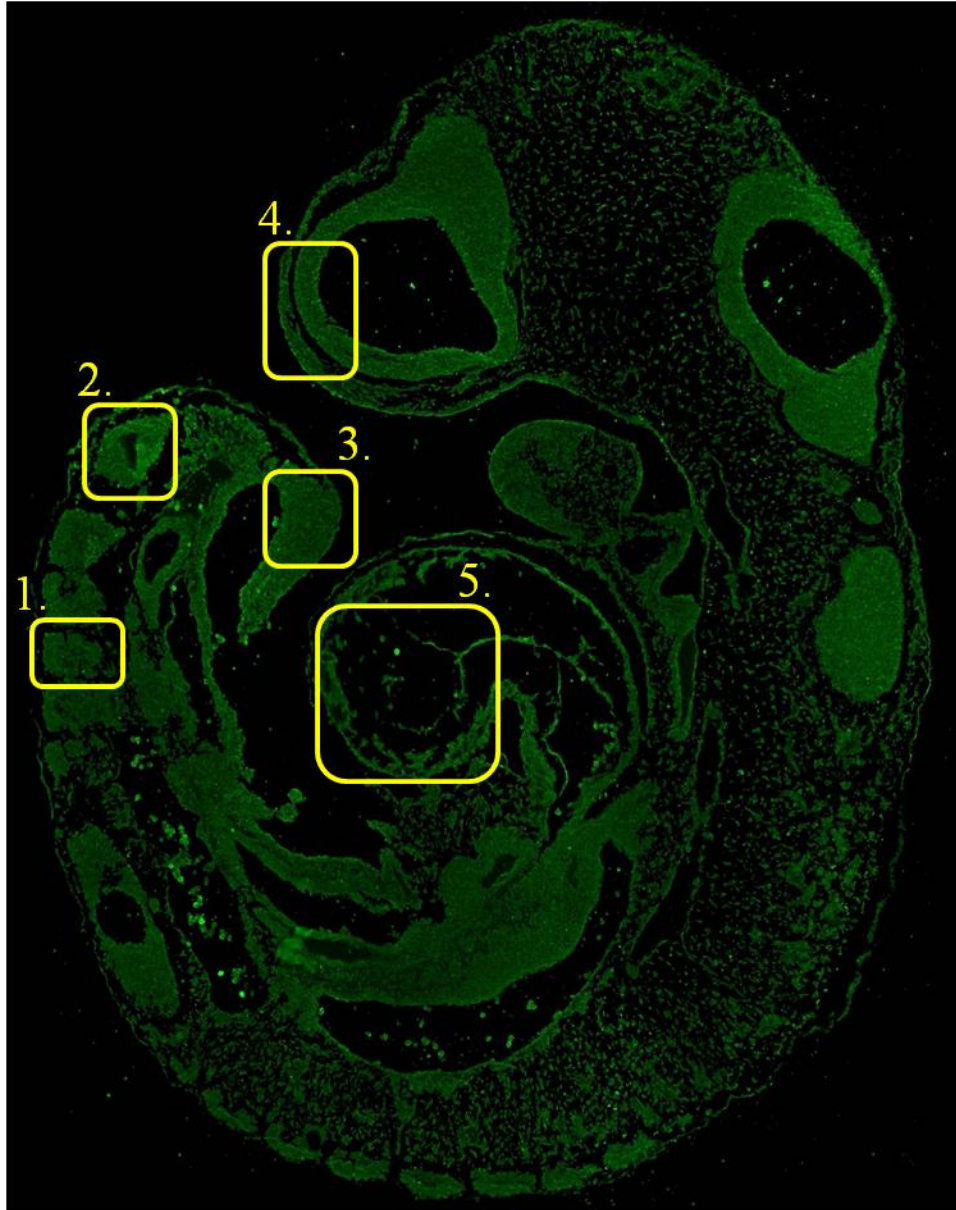


**Figure S2. The five different regions of the whole embryo targeted for quantitative analysis.**

The image displays a whole embryo with the five regions targeted for analysis in this study. (1) Somite, (2) Neural tube, (3) Caudal neuroepithelium, (4) Rostral neuroepithelium and (5) Heart.

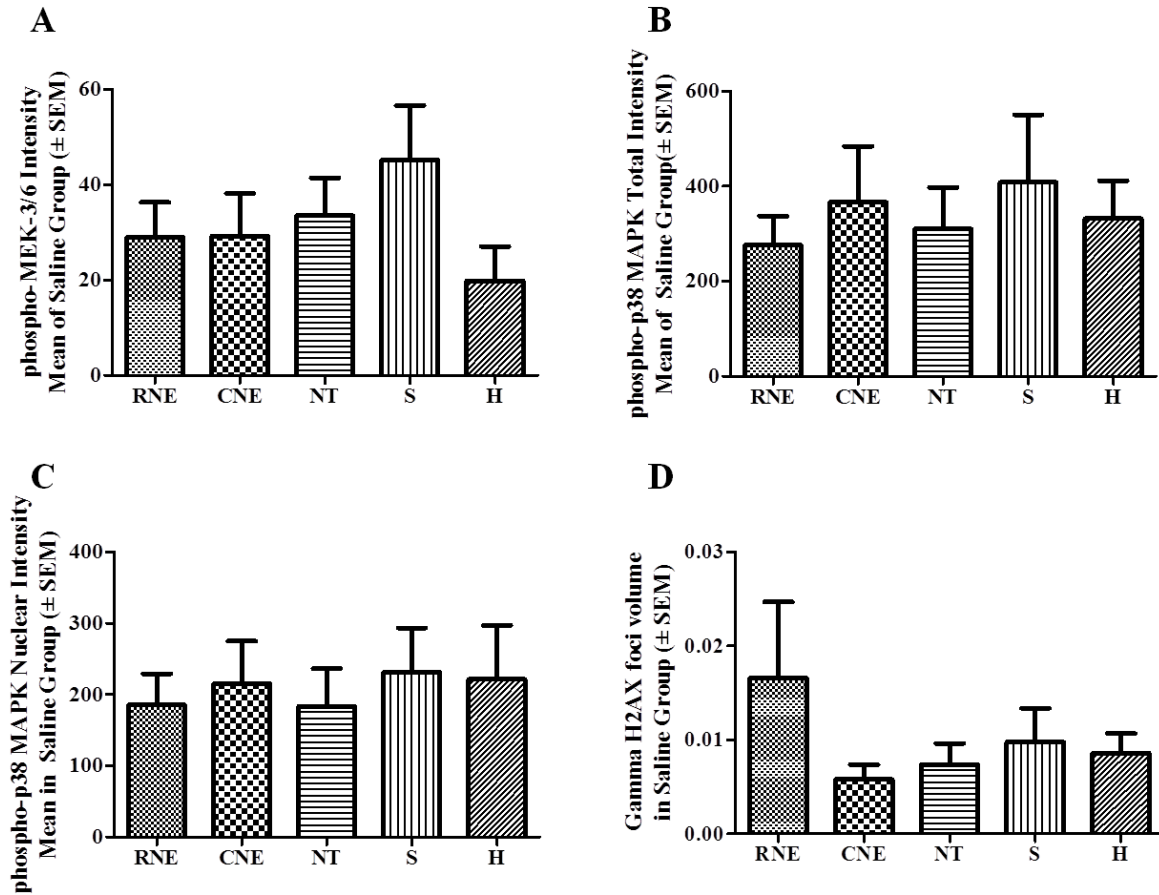


**Figure S3. Basal level expression of markers in saline-treated embryos in the five different regions targeted for analysis.**

Quantification of basal level expression in saline-treated embryos. A) phospho-MEK-3/6 intensity means, B) total phospho-p38 MAPK intensity means, C) nuclear phospho-p38 MAPK intensity means and D)  $\gamma$ H2AX focal volumes. In control embryos, there were no significant differences among the five regions in these measurements.

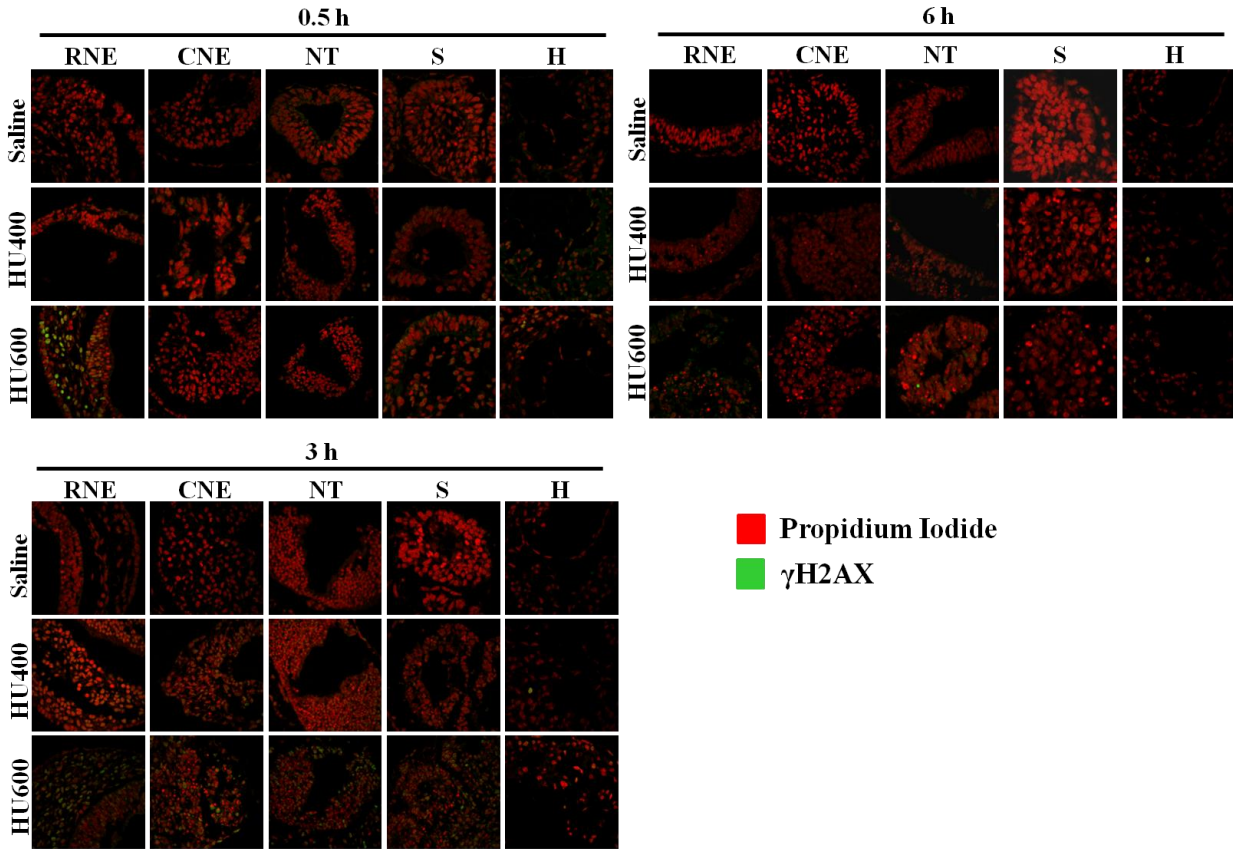


**Figure S4. Original images of  $\gamma$ H2AX staining of GD 9 embryos**

Confocal z-stack images of  $\gamma$ H2AX staining of the five regions taken at 63x/1.4 oil DIC objective.

**Table S1: Summary of immunofluorescence analysis of phospho-MEK-3/6**

Time Point	Dose	Structure	Number of embryos analyzed <sup>a</sup>	Statistical Analysis <sup>b</sup> (Dunnett's Test)	Regional Difference (Tukey's Test)
0.5 h	Saline	RNE	13		
		CNE			
		NT			
		S			
		H			
	HU400 mg/kg	RNE	15	ns	
CNE		ns			
NT		ns			
S		*, p < 0.05			
H		ns			
HU600mg/kg	RNE	15	ns		
	CNE		ns		
	NT		ns		
	S		ns		
	H		*, p < 0.05		
3 h	Saline	RNE	14		non-significant
		CNE			
		NT			
		S			
		H			
	HU400 mg/kg	RNE	14	ns	non-significant
CNE		*, p < 0.05			
NT		ns			
S		ns			

		H		*, p < 0.05	
	HU600 mg/kg	RNE	14	†, p < 0.01	non-significant
		CNE		‡, p < 0.001	
		NT		†, p < 0.01	
		S		ns	
		H		‡, p < 0.001	
6 h	Saline	RNE	14		
		CNE			
		NT			
		S			
		H			
	HU 400 mg/kg	RNE	14	ns	
		CNE		ns	
		NT		ns	
		S		*, p < 0.05	
		H		ns	
	HU600m g/kg	RNE	14	*, p < 0.05	
		CNE		ns	
NT		†, p < 0.01			
S		*, p < 0.05			
H		ns			

<sup>a</sup>The number is the total number of embryos analyzed among n=5 females. A minimum of 2 embryos were analyzed from each litter.

<sup>b</sup>Comparisons were made between the saline-treated and HU-treated groups.

**Table S2: Summary of immunofluorescence analysis of total phospho-p38 MAPK**

<b>Time Point</b>	<b>Dose</b>	<b>Structure</b>	<b>Number of embryos analyzed<sup>a</sup></b>	<b>Statistical Analysis<sup>b</sup> (Dunnett's Test)</b>	<b>Regional Difference<sup>c</sup> (Tukey's Test)</b>
0.5 h	Saline	RNE	10		
		CNE			
		NT			
		S			
		H			
	HU400 mg/kg	RNE	10	ns	
		CNE		ns	
		NT		ns	
		S		ns	
H		ns			
HU600mg/kg	RNE	10	ns		
	CNE		ns		
	NT		ns		
	S		ns		
	H		ns		
3 h	Saline	RNE	10		non-significant
		CNE			
		NT			
		S			
		H			
	HU400 mg/kg	RNE	10	ns	non-significant
CNE	ns				
NT	ns				
S	ns				

		H		ns	
	HU600 mg/kg	RNE	10	†, p < 0.01	‡, p < 0.001, S and H
		CNE		†, p < 0.01	*, p < 0.05, H
		NT		†, p < 0.01	*, p < 0.05, H
		S		ns	
		H		ns	
6 h	Saline	RNE	10		
		CNE			
		NT			
		S			
		H			
	HU 400 mg/kg	RNE	10	*, p < 0.05	
		CNE		ns	
		NT		ns	
		S		ns	
		H		ns	
	HU600m g/kg	RNE	10	ns	
		CNE		*, p < 0.05	
		NT		†, p < 0.01	
		S		ns	
		H		ns	

<sup>a</sup>Number is the total number of embryos analyzed among n=5 females. A minimum of 2 embryos were analyzed from each litter.

<sup>b</sup>Comparisons were made between saline-treated group to HU-treated groups.

<sup>c</sup>Comparisons were made between all five structures. Structures that were significantly different from each other are indicated after the p value.

**Table S3: Summary of immunofluorescence analysis of nuclear phospho-p38 MAPK**

Time Point	Dose	Structure	Number of embryos analyzed <sup>a</sup>	Statistical Analysis <sup>b</sup> (Dunnett's Test)	Regional Difference <sup>c</sup> (Tukey's Test)
0.5 h	Saline	RNE	10		
		CNE			
		NT			
		S			
		H			
	HU400 mg/kg	RNE	10	ns	
		CNE		ns	
		NT		ns	
		S		ns	
H		ns			
HU600mg/kg	RNE	10	ns		
	CNE		ns		
	NT		‡, p < 0.001		
	S		ns		
	H		ns		
3 h	Saline	RNE	10		non-significant
		CNE			
		NT			
		S			
		H			
	HU400 mg/kg	RNE	10	ns	non-significant
CNE		ns			
NT		ns			
S		ns			

		H		ns	
	HU600 mg/kg	RNE	10	†, p < 0.01	*, NT; †, S and H  *, p < 0.05, H
		CNE		‡, p < 0.001	
		NT		*, p < 0.05	
		S		ns	
		H		ns	
6 h	Saline	RNE	10		
		CNE			
		NT			
		S			
		H			
	HU 400 mg/kg	RNE	10	ns	
		CNE		ns	
		NT		†, p < 0.01	
		S		†, p < 0.01	
		H		ns	
	HU600m g/kg	RNE	10	ns	
		CNE		*, p < 0.05	
		NT		‡, p < 0.001	
		S		‡, p < 0.001	
		H		ns	

<sup>a</sup>Number represents the total number of embryos analyzed among n=5 females. A minimum of 2 embryos were analyzed from each litter.

<sup>b</sup>Comparisons were made between saline-treated group to HU-treated groups.

<sup>c</sup>Comparisons were made between all five structures. Structures that were significantly different from each other are indicated after the p value.

**Table S4: Summary of immunofluorescence analysis of  $\gamma$ H2AX foci volume**

<b>Time Point</b>	<b>Dose</b>	<b>Structure</b>	<b>Number of embryos analyzed<sup>a</sup></b>	<b>Statistical Analysis<sup>b</sup> (Dunnett's Test)</b>	<b>Regional Difference<sup>c</sup> (Tukey's Test)</b>
0.5 h	Saline	RNE	13		
		CNE			
		NT			
		S			
		H			
	HU400 mg/kg	RNE	15	ns	
		CNE		ns	
		NT		ns	
		S		ns	
H		ns			
HU600mg/kg	RNE	15	ns		
	CNE		ns		
	NT		*, p < 0.05		
	S		ns		
	H		ns		
3 h	Saline	RNE	14		non-significant
		CNE			
		NT			
		S			
		H			
	HU400 mg/kg	RNE	12	*, p < 0.05	non-significant
CNE	†, p < 0.01				
NT	ns				
S	ns				

		H		ns	
	HU600 mg/kg	RNE	13	‡, p < 0.001	*, p < 0.05, RNE
		CNE		‡, p < 0.001	
		NT		‡, p < 0.001	
		S		‡, p < 0.001	
		H		‡, p < 0.001	
6 h	Saline	RNE	15		
		CNE			
		NT			
		S			
		H			
	HU 400 mg/kg	RNE	15	ns	
		CNE		ns	
		NT		ns	
		S		ns	
		H		ns	
	HU600m g/kg	RNE	14	ns	
		CNE		ns	
		NT		ns	
		S		ns	
		H		ns	

<sup>a</sup>Number is the total number of embryos analyzed among n=5 females. A minimum of 2 embryos were analyzed from each litter.

<sup>b</sup>Comparisons were made between saline-treated group to HU-treated groups.

<sup>c</sup>Comparisons were made between all five structures. Structures that were significantly different from each other are indicated after the p value.

## **Chapter Three**

### **Discussion**

### **3.1 Summary**

The major goal of this study was to elucidate the embryonic stress-response pathways involved in mediating HU-induced developmental toxicity during organogenesis. Exposure of CD1 mouse embryos to HU induced dramatic activation of the p38 MAPK pathway, including both MEK-3/6 and p38 MAPK. While activated MEK-3/6 was expressed ubiquitously in the embryo, activated p38 MAPK had a more regional expression, specifically in malformation-sensitive tissues in the embryo. These findings suggested that p38 MAPK may play a role in inducing specific malformations observed after HU exposure.

HU treatment of pregnant mice dramatically induced DSBs in their embryos, as assessed by the formation of  $\gamma$ H2AX foci. The DDR elicited was widespread within the embryo, but more enhanced in malformation-sensitive tissues. In addition, pyknotic nuclei were observed in most tissues of the embryo, except the heart, a region which is resistant to HU-induced toxicity. This suggests that DDR response is spatially regulated in the embryo, which may contribute to the specific malformation induced by HU. The following subsections will discuss further the roles of p38 MAPK pathway and DDR in HU-induced developmental toxicity.

### **3.2 Role of p38 MAPKs in hydroxyurea induced developmental toxicity**

*In utero* exposure to HU, at a dose of 400mg/kg or 600mg/kg, did not alter the total protein expression of MEK-3/6, but triggered a dramatic increase in the expression of activated MEK-3/6 at 0.5h, 3h and 6h post-treatment. The distribution of activated MEK-3/6 was widespread in the embryos, including in the rostral neural epithelium, caudal neural epithelium, neural tube, somites and heart. HU exposure induced a dose-dependent increase in the activation of MEK-3/6 in all regions; however, there were no significant differences in the expression of

phospho-MEK-3/6 among the five regions. The activation of p38 MAPK was also affected by HU exposure, even more so since its increase exceeded that of MEK-3/6. Similar to phospho-MEK-3/6, total phospho-p38 MAPK was distributed globally in the embryo. However, HU induced a region specific localization of phospho-p38 MAPK, with enhanced expression in the neural tube, rostral and caudal neuroepithelium. More interestingly, upon HU exposure, preferential nuclear localization of phospho-p38 MAPK was observed in the rostral and caudal neural epithelium only. Thus, maternal exposure to HU induced a spatially regulated activation of the p38 MAPK pathway in organogenesis-stage embryos.

Although MEK-3/6 had a widespread activation in embryos compared to the region-specific activation of p38 MAPK, it is important to note that MEK-3/6 is likely to play an essential role in HU-induced developmental toxicity. Although other MAP2Ks, such as MEK-4, can activate p38 MAPK, maximal activation of p38 MAPK is achieved through MEK-3/6 *in vivo* (Raman et al., 2007). Therefore, MEK-3/6 is crucial in mediating the activation of p38 MAPK. Several studies have dissected the roles of MEK-3 and MEK-6; these studies show that the major MAP2K required for p38 MAPK activation is dependent on the stimulus as well as the cell type. For example, MEK-3 is the major activator of p38 MAPK in mesangial cells stimulated by transforming growth factor, while MEK-6 is the predominant activator in thymocytes (Wang et al., 2002). Whether MEK-3 and MEK-6 have differential expression amongst embryonic tissues remains elusive. Moreover, differential activation of p38 MAPK in embryos may affect the outcome in HU-induced effects. Individual detection of their activation and localization in embryos after HU exposure may help in understanding their separate and distinct functions. In addition, using antisense techniques or knock-out animals may provide more information about their roles in HU-induced developmental toxicity.

As the activation of p38 MAPK was enhanced in malformation-sensitive tissues, mainly the caudal neuroepithelium, one may postulate that such induction may lead to the caudal defects induced by HU. However, based on a previous study, selective inhibition of p38 MAPK enhanced HU-induced fetal mortality rather than caudal defects (Yan and Hales, 2008). This observation led to the suggestion that p38 MAPK plays a role in protecting the embryo from HU insult. It is likely that a defense mechanism is developed in cells to overcome the detrimental effects of cytotoxic drugs, including HU, which can severely compromise DNA integrity. There is evidence from several studies that p38 MAPK plays a strong pro-survival role in response to DNA damage through a coordinated downregulation of pro-apoptotic signals and upregulation of pro-survival genes (Phong et al., 2010). Therefore, contrary to its well-described classical role in apoptosis, p38 MAPK is essential in mediating survival. (Thornton et al., 2008). In response to DNA damage, p38 MAPK may also elicit an indirect mechanism to increase cell survival by inducing a cell cycle checkpoint. Upon damage, it is crucial that the cell cycle is arrested to allow the opportunity for DNA repair prior to mitotic catastrophe. Indeed, in several cell lines HU exposure led to the activation of MAPKs p38 $\alpha$  and p38 $\beta$ , preventing mitotic entry (Rodriguez-Bravo et al., 2007).

Amongst the five regions of embryos analyzed, the heart received significant damage upon HU exposure, yet it had little to no cell death and no any obvious malformations. Interestingly, nuclear expression of phospho-p38 MAPK in the heart is minimal. In contrast, HU-induced caudal malformations are associated with increased nuclear expression of phospho-p38 MAPK. These results suggest that different substrates of p38 MAPK may be targeted depending on the localization of p38 MAPK itself. It is possible that nuclear translocation of p38 MAPK may lead to an upregulation of pro-apoptotic genes, while cytoplasmic accumulation of

p38 MAPK favours a survival response. Reinhardt et al. (2010) discovered a late cytoplasmic cell cycle checkpoint that is controlled by the p38/MK2 pathway. Following DNA damage, the p38/MK2 complex relocates from the nucleus to the cytoplasm. The critical function of the cytoplasmic checkpoint is to prolong the duration of cell cycle arrest through the stabilization of RNA-binding/regulatory proteins, including TIAR, PARN and hnRNPAo. These targets further lead to the accumulation of Gadd45 $\alpha$ , resulting in pronounced cytoplasmic sequestration of mitotic phosphatases such as Cdc25, preventing access to and activation of nuclear cyclin/cdk substrates (Reinhardt et al., 2010). It is possible that sustained cell cycle arrest mediated by p38/MK2 is occurring in the heart, allowing this organ to have more time for DNA repair.

Thus, further studies are needed to determine the mechanism whereby p38 MAPK chooses to execute apoptotic or survival signals in different regions of the embryo. Identification of p38 MAPK substrates in different regions of the embryos is a priority in understanding the differential effects generated by HU exposure in different tissues. Specifically, nuclear substrates will give insight to whether pro-apoptotic or pro-survival genes are regulated after HU exposure. Since the dynamic of p38 MAPK localization is not limited only to nuclear shuttling, cytoplasmic accumulation or translocation should also be explored. Lastly, the p38 MAPK response is executed differently depending on its upstream mediators, therefore MAP3K and MAP4K should be identified to clearly define the p38MAPK axis in HU-developmental toxicity.

### **3.3 DNA damage response in hydroxyurea induced developmental toxicity**

The ability of embryos to detect DNA damage and their capacity to repair DNA have generated a great amount of interest in the field. Although the regulatory mechanisms and signaling pathways controlling DNA repair are well characterized, the precise molecular

strategies whereby embryos detect and implement DNA repair in response to a teratogen exposure are incompletely understood. Our study has highlighted the role of the DNA damage response upon teratogenic insult in early organogenesis staged embryos. A dramatic dose-dependent increase in the formation of  $\gamma$ H2AX foci was detected in all five regions of the embryo following HU exposure at 400 mg/kg and 600 mg/kg. The increase in  $\gamma$ H2AX foci began at 0.5h and peaked at 3h post-treatment. More interestingly,  $\gamma$ H2AX foci formation was the highest in the caudal neuroepithelium. Thus, HU-induced activation of DNA damage signaling pathways in organogenesis stage embryos was enhanced in malformation-sensitive tissue.

While DNA damage-induced  $\gamma$ H2AX formation remains to be the best characterized histone modification, the C-terminal tail of H2AX contains several other amino acid residues that are subject to various post-translational modifications that may play a role in regulating DNA damage response. Therefore, DNA damage response could be regulated through a histone code that is seemingly more complicated than the mere phosphorylation of serine-139 on H2AX. The study conducted by Cook et al. has recently supported this notion by discovering the phosphorylation of tyrosine residue (Y142) of H2AX (Cook et al., 2009). Tyr142 is constitutively phosphorylated in H2AX. Upon the induction of DSBs, Tyr142 is dephosphorylated by tyrosine phosphatases, followed by the phosphorylation of Ser139, which provides a docking site for DNA repair factors at the break sites (Rogakou et al., 1999). Intriguingly, when both Tyr142 and Ser139 are phosphorylated simultaneously, the binding of DNA repair factors was decreased significantly; instead pro-apoptotic factor JNK1 was associated with the dual phosphorylation on H2AX (Cook et al., 2009). This additional phosphorylation-dependent mechanism may function as an active determinant of cell-fate decisions, between apoptotic and repair responses, during mammalian organogenesis. Clearly, it

will be a priority to dissect the contribution of different histone codes in different regions of the embryo in order to understand how these dynamic chromatin modifications influence cell-fate decisions.

The volumes of  $\gamma$ H2AX foci decreased at 6h after HU treatment. The loss of  $\gamma$ H2AX at DSB sites has been thought to reflect the completion of DNA repair (Bouquet et al., 2006). Yet our results do not seem to support this concept, as during the same time period, an obvious increase in pyknotic nuclei and cell fragmentation can be observed in most tissues, reflecting the death of embryonic cells from non-repairable damage. It is possible that DNA damage induced by HU is overwhelming for the embryo, and perhaps the only option is to activate the cell death machinery. Several studies have demonstrated that a variety of teratogens can induce unscheduled and excessive cell death in embryonic tissues that subsequently develop abnormally, leading to structural malformations (Huang and Hales, 2002; Mirkes and Little, 1998; Sulik et al., 1988). It has also been proposed that for teratogens, there exists a critical dose, and when the number of cells affected is below this “threshold”, then there is no permanent effect (Ferguson and Ford, 1997). From our results, the caudal neuroepithelium receives the most damage, as indicated by the highest volume of  $\gamma$ H2AX foci. Based on this “threshold” theory, the caudal neuroepithelium may be the only tissue in which this critical point is exceeded, leading to excessive cell death and resulting in caudal defects in HU-induced developmental toxicity.

Teratogen-induced cell death is a common event in the pathogenesis associated with malformed tissues and it is known that different cells and tissues within the developing embryo exhibit different sensitivities. In the case of HU and many other teratogens, the heart continues to show extreme resistance to cell death. Therefore, embryonic heart cells possess some molecular mechanisms to prevent cell death that other cells lack. It has been shown that the absence of cell

death in heart is accompanied by complete lack of DNA fragmentation, activation of caspase-3 or the cleavage of PARP (Mirkes and Little, 1998). Moreover, studies have shown that while teratogens induce the release of cytochrome c and caspase-9 activation in malformation-sensitive tissues, the mitochondrial apoptotic pathway is blocked in heart cells (Mirkes and Little, 2000). Soleman et al. (2003) have proposed that heart cell resistance and neuroepithelial cell sensitivity is arguably natural. Cell death in the neuroepithelial cells is tolerable. They are highly proliferative and continue to develop, although abnormally. In contrast, any level of cell death to the heart is detrimental and is likely to result in embryolethality. Therefore, resistance to teratogen-induced cell death is related to functions essential to embryo survival (Soleman et al., 2003). Indeed, extraembryonic yolk sac, which is extremely crucial for embryo survival by providing nutrition and gas exchange, also exhibits the same teratogen-induced cell death resistance as the heart (Soleman et al., 2003).

It is intriguing with respect to the heart that based on our study, albeit the absence of cell death, HU induced significant DNA damage in the heart. Previous studies, from our lab and others, have shown that HU does not induce any obvious malformations to the heart (Yan and Hales, 2006). These results suggest that the heart may have the capacity to undergo sufficient DNA repair to maintain genomic integrity, thereby promoting survival in this organ. As mentioned in the previous subsection, the heart has the least nuclear phospho-p38 MAPK, which may lead to the activation of late and prolonged 'cytoplasmic' cell cycle arrest. Thus, the heart has more time for DNA repair compared to other tissues in the embryo. Moreover, DNA repair gene expression data have also shown that most DNA repair genes in different repair pathways, including base excision repair, nucleotide excision repair, homologous recombination and non-

homologous end-joining, are already expressed in GD9 mouse embryos (Pachkowski et al., 2011).

As the knowledge of the teratogen-induced DNA damage response in the embryo remains limited, future studies are needed. A thorough assessment of chromatin modifications and DNA repair proteins in different regions of the embryo are needed. These studies should not only focus on the expression levels, but more importantly, on functional assessments to demonstrate the active removal of DNA damage by embryonic tissues. Altogether, these studies would shed light on the mechanisms regulating and determining the differential outcome of embryonic tissues in HU-induced developmental toxicity.

### **3.4 The role of oxidative and replication stress in hydroxyurea induced developmental toxicity**

*In utero* exposure to HU induced the activation of p38 MAPK and the formation of  $\gamma$ H2AX foci starting at 0.5 h post-treatment. In previous studies, the formation of 4-HNE protein adducts (Yan and Hales, 2006) and the increase in AP-1 DNA binding activity (Yan and Hales, 2005) also occurred at 0.5h after HU exposure. Both 4-HNE and AP-1 are targets of oxidative stress, and as p38 MAPK is highly activated by stress stimuli, including oxidative stress, these results are indicative of oxidative stress-mediated responses induced by HU. More convincingly, since the inhibition of DNA synthesis does not occur until three to four hours post-treatment with HU (DeSesso and Goeringer, 1990), the increase in formation of  $\gamma$ H2AX foci at 0.5h is most probably induced by free radicals generated by HU. In addition, previous studies have also shown that 4-HNE protein adducts were detected at higher level in caudal regions (Yan and Hales, 2006). Therefore, region-specific oxidative stress may be the basis of enhanced sensitivity

in the caudal region that is seen in this study, including the nuclear translocation of phospho-p38 and  $\gamma$ H2AX foci. Both the formation of  $\gamma$ H2AX foci and the activation of p38 MAPK peaked at 3 h post-HU treatment, the time corresponding to DNA synthesis inhibition induced by HU (Wells and Winn, 1996). As replication stress can induce further DNA strand breaks from stalled and collapsed replication forks, DNA damage can further drive the activation and nuclear translocation of p38 MAPK, as well as the formation of  $\gamma$ H2AX foci. Therefore, peak in these endpoints induced by HU is attributed to both oxidative stress and replication stress.

HU-induced oxidative stress has been found to be region-specific in organogenesis stage embryos; whether replication stress also specifically targets the caudal region under the influence of HU is unknown. Replication stress mainly affects cells in the replication stage; therefore, cells that are highly proliferative will be most affected by HU. During organogenesis, the embryo grows caudally, as stem cells in the primitive streak and tail bud divide rapidly to produce a new pair of somites every 90-120 minutes (Maroto and Pourquie, 2001). In contrast, the heart has been shown to have much lower proliferative activity than the surrounding embryonic tissues. On GD9, cell quiescence can already be found in the heart, with a remarkable paucity of DNA-synthesizing cells. In fact, the heart appears to be the most differentiated organ in the embryo at this developmental stage (Sedmera et al., 2003). Thus, HU-induced teratogenicity mediated by replication stress could be associated with the proliferation rate of the tissue.

If both oxidative and replication stress preferentially target the caudal regions, then to what extent does each mechanism contribute to cell death and HU-induced teratogenicity? To dissect the DNA damage that is caused by individual mechanisms, several markers can be evaluated. Oxidative stress can initiate a plethora of oxidative DNA damage, with the 8-oxoguanine (8-oxoG) lesion being the most prevalent lesion that causes nucleotide transversion

mutations, capable of initiating cancer development (Wells et al., 2010). 8-oxoG lesions have also been shown to have a casual implication in structural and functional teratogenesis by altering gene transcription in embryos (Wells et al., 2009). To assess the contribution of replication stress to the observed formation of  $\gamma$ H2AX foci, markers such as Chk1 activation, Rad17 phosphorylation or replication protein A foci can be evaluated in organogenesis stage mouse embryos exposed to HU (Bartkova et al., 2010). In summary, further studies are needed to elucidate the mechanisms of oxidative stress and replication stress-mediated developmental toxicity.

### **3.5 Conclusions**

In this study, the expression, activation and localization of members of the p38 MAPK signaling pathway and the DNA damage response were examined in early organogenesis stage embryos in response to maternal exposure of HU.

1) Maternal exposure to HU induces a dramatic increase in the activation of p38 MAPK and its upstream mediator, MEK-3/6, in organogenesis stage embryos, without affecting their total protein levels. MEK-3/6 activation was widespread in the embryo, whereas activated p38 MAPK was localized to the neural tube, rostral and caudal neuroepithelium. Moreover, phospho-p38 MAPK was found to preferentially translocate into the nucleus in only the rostral and caudal neuroepithelium. Therefore, the p38 MAPK pathway is activated in response to HU insult in the embryo, with activation of the downstream target kinase (p38 MAPK) being more region-specific.

2) HU-treated embryos exhibited a dramatic increase in overall  $\gamma$ H2AX intensity and focal volumes, starting at 0.5h and peaking at 3h post-treatment. Significant increases occurred

in each of the five regions in embryos exposed to HU. Within the embryo, the caudal neuroepithelium received the most DNA damage, as indicated by the greatest increase in  $\gamma$ H2AX focal volumes. Thus, HU-induced activation of the DNA damage signaling pathway in the embryo during organogenesis was enhanced in malformation-sensitive tissues. Moreover, we hypothesize that HU-induced DNA damage in the embryos is mediated by both oxidative and replication stress.

3) Exposure to HU induced cell death, as assessed by the appearance of pyknotic nuclei and cell fragmentation in HU-treated embryos. The increase of pyknotic nuclei was most significant at 6h in all regions of the embryo except the heart. The determination of whether embryonic heart cells are capable of efficient DNA repair will require further experiments.

## References

- Adams RH, Porras A, Alonso G, Jones M, Vintersten K, Panelli S, Valladares A, Perez L, Klein R and Nebreda AR (2000) Essential role of p38alpha MAP kinase in placental but not embryonic cardiovascular development. *Molecular cell* **6**:109-116.
- Allen M, Svensson L, Roach M, Hambor J, McNeish J and Gabel CA (2000) Deficiency of the stress kinase p38alpha results in embryonic lethality: characterization of the kinase dependence of stress responses of enzyme-deficient embryonic stem cells. *The Journal of experimental medicine* **191**:859-870.
- Askari N, Beenstock J, Livnah O and Engelberg D (2009) p38 alpha Is Active in Vitro and in Vivo When Monophosphorylated at Threonine 180. *Biochemistry* **48**:2497-2504.
- Ayoub N, Jeyasekharan AD, Bernal JA and Venkitaraman AR (2008) HP1-beta mobilization promotes chromatin changes that initiate the DNA damage response. *Nature* **453**:682-686.
- Balaban RS, Nemoto S and Finkel T (2005) Mitochondria, oxidants, and aging. *Cell* **120**:483-495.
- Bard J (1994) *Embryos: Color Atlas of Development*, Wolfe Publishing London, England.
- Barnes DE, Stamp G, Rosewell I, Denzel A and Lindahl T (1998) Targeted disruption of the gene encoding DNA ligase IV leads to lethality in embryonic mice. *Current biology : CB* **8**:1395-1398.
- Bartkova J, Hamerlik P, Stockhausen MT, Ehrmann J, Hlobilkova A, Laursen H, Kalita O, Kolar Z, Poulsen HS, Broholm H, Lukas J and Bartek J (2010) Replication stress and oxidative damage contribute to aberrant constitutive activation of DNA damage signalling in human gliomas. *Oncogene* **29**:5095-5102.

- Beardmore VA, Hinton HJ, Eftychi C, Apostolaki M, Armaka M, Darragh J, McIlrath J, Carr JM, Armit LJ, Clacher C, Malone L, Kollias G and Arthur JS (2005) Generation and characterization of p38beta (MAPK11) gene-targeted mice. *Molecular and cellular biology* **25**:10454-10464.
- Beckman DA and Brent RL (1984) Mechanisms of teratogenesis. *Annual review of pharmacology and toxicology* **24**:483-500.
- Ben-Levy R, Hooper S, Wilson R, Paterson HF and Marshall CJ (1998) Nuclear export of the stress-activated protein kinase p38 mediated by its substrate MAPKAP kinase-2. *Current biology : CB* **8**:1049-1057.
- Bergink S and Jentsch S (2009) Principles of ubiquitin and SUMO modifications in DNA repair. *Nature* **458**:461-467.
- Berlett BS and Stadtman ER (1997) Protein oxidation in aging, disease, and oxidative stress. *The Journal of biological chemistry* **272**:20313-20316.
- Bester AC, Roniger M, Oren YS, Im MM, Sarni D, Chaoat M, Bensimon A, Zamir G, Shewach DS and Kerem B (2011) Nucleotide deficiency promotes genomic instability in early stages of cancer development. *Cell* **145**:435-446.
- Bouquet F, Muller C and Salles B (2006) The loss of gammaH2AX signal is a marker of DNA double strand breaks repair only at low levels of DNA damage. *Cell Cycle* **5**:1116-1122.
- Bradham CA and McClay DR (2006) p38 MAPK is essential for secondary axis specification and patterning in sea urchin embryos. *Development* **133**:21-32.
- Brancho D, Tanaka N, Jaeschke A, Ventura JJ, Kelkar N, Tanaka Y, Kyuuma M, Takeshita T, Flavell RA and Davis RJ (2003) Mechanism of p38 MAP kinase activation in vivo. *Genes & development* **17**:1969-1978.

- Brugmans L, Kanaar R and Essers J (2007) Analysis of DNA double-strand break repair pathways in mice. *Mutation research* **614**:95-108.
- Bulavin DV, Higashimoto Y, Popoff IJ, Gaarde WA, Basrur V, Potapova O, Appella E and Fornace AJ, Jr. (2001) Initiation of a G2/M checkpoint after ultraviolet radiation requires p38 kinase. *Nature* **411**:102-107.
- Bulavin DV, Phillips C, Nannenga B, Timofeev O, Donehower LA, Anderson CW, Appella E and Fornace AJ, Jr. (2004) Inactivation of the Wip1 phosphatase inhibits mammary tumorigenesis through p38 MAPK-mediated activation of the p16(Ink4a)-p19(Arf) pathway. *Nature genetics* **36**:343-350.
- Bulavin DV, Saito S, Hollander MC, Sakaguchi K, Anderson CW, Appella E and Fornace AJ, Jr. (1999) Phosphorylation of human p53 by p38 kinase coordinates N-terminal phosphorylation and apoptosis in response to UV radiation. *The EMBO journal* **18**:6845-6854.
- Burhans WC and Weinberger M (2007) DNA replication stress, genome instability and aging. *Nucleic acids research* **35**:7545-7556.
- Buschmann T, Potapova O, Bar-Shira A, Ivanov VN, Fuchs SY, Henderson S, Fried VA, Minamoto T, Alarcon-Vargas D, Pincus MR, Gaarde WA, Holbrook NJ, Shiloh Y and Ronai Z (2001) Jun NH2-terminal kinase phosphorylation of p53 on Thr-81 is important for p53 stabilization and transcriptional activities in response to stress. *Molecular and cellular biology* **21**:2743-2754.
- Cappellini A, Tazzari PL, Mantovani I, Billi AM, Tassi C, Ricci F, Conte R and Martelli AM (2005) Antiapoptotic role of p38 mitogen activated protein kinase in Jurkat T cells and

- normal human T lymphocytes treated with 8-methoxypsoralen and ultraviolet-A radiation. *Apoptosis : an international journal on programmed cell death* **10**:141-152.
- Celeste A, Petersen S, Romanienko PJ, Fernandez-Capetillo O, Chen HT, Sedelnikova OA, Reina-San-Martin B, Coppola V, Meffre E, Difilippantonio MJ, Redon C, Pilch DR, Oлару A, Eckhaus M, Camerini-Otero RD, Tessarollo L, Livak F, Manova K, Bonner WM, Nussenzweig MC and Nussenzweig A (2002) Genomic instability in mice lacking histone H2AX. *Science* **296**:922-927.
- Chabes A, Georgieva B, Domkin V, Zhao X, Rothstein R and Thelander L (2003) Survival of DNA damage in yeast directly depends on increased dNTP levels allowed by relaxed feedback inhibition of ribonucleotide reductase. *Cell* **112**:391-401.
- Chan KL, Palmai-Pallag T, Ying S and Hickson ID (2009) Replication stress induces sister-chromatid bridging at fragile site loci in mitosis. *Nature cell biology* **11**:753-760.
- Ciccia A and Elledge SJ (2010) The DNA damage response: making it safe to play with knives. *Molecular cell* **40**:179-204.
- Cook PJ, Ju BG, Telese F, Wang X, Glass CK and Rosenfeld MG (2009) Tyrosine dephosphorylation of H2AX modulates apoptosis and survival decisions. *Nature* **458**:591-596.
- Cuadrado A and Nebreda AR (2010) Mechanisms and functions of p38 MAPK signalling. *The Biochemical journal* **429**:403-417.
- D'Autreaux B and Toledano MB (2007) ROS as signalling molecules: mechanisms that generate specificity in ROS homeostasis. *Nature reviews Molecular cell biology* **8**:813-824.
- Davison D and Baldock R EMAP eMouse Atlas Project.

- de Boer J, Donker I, de Wit J, Hoeijmakers JH and Weeda G (1998) Disruption of the mouse xeroderma pigmentosum group D DNA repair/basal transcription gene results in preimplantation lethality. *Cancer research* **58**:89-94.
- Deacon K, Mistry P, Chernoff J, Blank JL and Patel R (2003) p38 Mitogen-activated protein kinase mediates cell death and p21-activated kinase mediates cell survival during chemotherapeutic drug-induced mitotic arrest. *Molecular biology of the cell* **14**:2071-2087.
- Dean JL, Brook M, Clark AR and Saklatvala J (1999) p38 mitogen-activated protein kinase regulates cyclooxygenase-2 mRNA stability and transcription in lipopolysaccharide-treated human monocytes. *The Journal of biological chemistry* **274**:264-269.
- Dennery PA (2007) Effects of oxidative stress on embryonic development. *Birth defects research Part C, Embryo today : reviews* **81**:155-162.
- DeSesso JM (1979) Cell death and free radicals: a mechanism for hydroxyurea teratogenesis. *Medical hypotheses* **5**:937-951.
- DeSesso JM (1981) Amelioration of teratogenesis. I. Modification of hydroxyurea-induced teratogenesis by the antioxidant propyl gallate. *Teratology* **24**:19-35.
- DeSesso JM and Goeringer GC (1990) The nature of the embryo-protective interaction of propyl gallate with hydroxyurea. *Reprod Toxicol* **4**:145-152.
- DeSesso JM and Jordan RL (1977) Drug-induced limb dysplasias in fetal rabbits. *Teratology* **15**:199-211.
- Desesso JM, Scialli AR and Goeringer GC (1994) D-mannitol, a specific hydroxyl free radical scavenger, reduces the developmental toxicity of hydroxyurea in rabbits. *Teratology* **49**:248-259.

- El-Benna J, Dang PM, Gougerot-Pocidallo MA, Marie JC and Braut-Boucher F (2009) p47phox, the phagocyte NADPH oxidase/NOX2 organizer: structure, phosphorylation and implication in diseases. *Experimental & molecular medicine* **41**:217-225.
- Enslin H, Branch DM and Davis RJ (2000) Molecular determinants that mediate selective activation of p38 MAP kinase isoforms. *The EMBO journal* **19**:1301-1311.
- Enslin H, Raingeaud J and Davis RJ (1998) Selective activation of p38 mitogen-activated protein (MAP) kinase isoforms by the MAP kinase kinases MKK3 and MKK6. *The Journal of biological chemistry* **273**:1741-1748.
- Fantel AG and Person RE (2002) Further evidence for the role of free radicals in the limb teratogenicity of L-NAME. *Teratology* **66**:24-32.
- Farber E and Baserga R (1969) Differential effects of hydroxyurea on survival of proliferating cells in vivo. *Cancer research* **29**:136-139.
- Feng W, Bachant J, Collingwood D, Raghuraman MK and Brewer BJ (2009) Centromere replication timing determines different forms of genomic instability in *Saccharomyces cerevisiae* checkpoint mutants during replication stress. *Genetics* **183**:1249-1260.
- Feng W, Di Rienzi SC, Raghuraman MK and Brewer BJ (2011) Replication stress-induced chromosome breakage is correlated with replication fork progression and is preceded by single-stranded DNA formation. *G3 (Bethesda)* **1**:327-335.
- Ferguson LR and Ford JH (1997) Overlap between mutagens and teratogens. *Mutation research* **396**:1-8.
- Ferm VH (1966) Severe Developmental Malformations - Malformations Induced by Urethane and Hydroxyurea in Hamster. *Arch Pathol* **81**:174-&.

- Fernandez-Capetillo O, Chen HT, Celeste A, Ward I, Romanienko PJ, Morales JC, Naka K, Xia Z, Camerini-Otero RD, Motoyama N, Carpenter PB, Bonner WM, Chen J and Nussenzweig A (2002) DNA damage-induced G2-M checkpoint activation by histone H2AX and 53BP1. *Nature cell biology* **4**:993-997.
- Filosto M, Tonin P, Vattei G, Savio C, Rizzuto N and Tomelleri G (2003) Transcription factors c-Jun/activator protein-1 and nuclear factor-kappa B in oxidative stress response in mitochondrial diseases. *Neuropathology and applied neurobiology* **29**:52-59.
- Franklin CC and Kraft AS (1997) Conditional expression of the mitogen-activated protein kinase (MAPK) phosphatase MKP-1 preferentially inhibits p38 MAPK and stress-activated protein kinase in U937 cells. *The Journal of biological chemistry* **272**:16917-16923.
- Fujino G, Noguchi T, Matsuzawa A, Yamauchi S, Saitoh M, Takeda K and Ichijo H (2007) Thioredoxin and TRAF family proteins regulate reactive oxygen species-dependent activation of ASK1 through reciprocal modulation of the N-terminal homophilic interaction of ASK1. *Molecular and cellular biology* **27**:8152-8163.
- Grawunder U, Zimmer D, Fugmann S, Schwarz K and Lieber MR (1998) DNA ligase IV is essential for V(D)J recombination and DNA double-strand break repair in human precursor lymphocytes. *Molecular cell* **2**:477-484.
- Greenblatt MB, Shim JH, Zou W, Sitara D, Schweitzer M, Hu D, Lotinun S, Sano Y, Baron R, Park JM, Arthur S, Xie M, Schneider MD, Zhai B, Gygi S, Davis R and Glimcher LH (2010) The p38 MAPK pathway is essential for skeletogenesis and bone homeostasis in mice. *The Journal of clinical investigation* **120**:2457-2473.
- Guardavaccaro D and Pagano M (2006) Stabilizers and destabilizers controlling cell cycle oscillators. *Molecular cell* **22**:1-4.

- Han J, Lee JD, Bibbs L and Ulevitch RJ (1994) A MAP kinase targeted by endotoxin and hyperosmolarity in mammalian cells. *Science* **265**:808-811.
- Hansen JM (2006) Oxidative stress as a mechanism of teratogenesis. *Birth defects research Part C, Embryo today : reviews* **78**:293-307.
- Hansen JM, Carney EW and Harris C (1999) Differential alteration by thalidomide of the glutathione content of rat vs. rabbit conceptuses in vitro. *Reprod Toxicol* **13**:547-554.
- Hansen JM and Harris C (2004) A novel hypothesis for thalidomide-induced limb teratogenesis: redox misregulation of the NF-kappaB pathway. *Antioxidants & redox signaling* **6**:1-14.
- Hansen JM, Harris KK, Philbert MA and Harris C (2002) Thalidomide modulates nuclear redox status and preferentially depletes glutathione in rabbit limb versus rat limb. *The Journal of pharmacology and experimental therapeutics* **300**:768-776.
- He TC, Sparks AB, Rago C, Hermeking H, Zawel L, da Costa LT, Morin PJ, Vogelstein B and Kinzler KW (1998) Identification of c-MYC as a target of the APC pathway. *Science* **281**:1509-1512.
- Hempstock J, Jauniaux E, Greenwold N and Burton GJ (2003) The contribution of placental oxidative stress to early pregnancy failure. *Human pathology* **34**:1265-1275.
- Hu JH, Chen T, Zhuang ZH, Kong L, Yu MC, Liu Y, Zang JW and Ge BX (2007) Feedback control of MKP-1 expression by p38. *Cellular signalling* **19**:393-400.
- Hu MC, Wang YP, Mikhail A, Qiu WR and Tan TH (1999) Murine p38-delta mitogen-activated protein kinase, a developmentally regulated protein kinase that is activated by stress and proinflammatory cytokines. *The Journal of biological chemistry* **274**:7095-7102.

- Huang C and Hales BF (2002) Role of caspases in murine limb bud cell death induced by 4-hydroperoxycyclophosphamide, an activated analog of cyclophosphamide. *Teratology* **66**:288-299.
- Kang YH and Lee SJ (2008) Role of p38 MAPK and JNK in enhanced cervical cancer cell killing by the combination of arsenic trioxide and ionizing radiation. *Oncology reports* **20**:637-643.
- Karin M and Shaulian E (2001) AP-1: linking hydrogen peroxide and oxidative stress to the control of cell proliferation and death. *IUBMB life* **52**:17-24.
- Karran P (2000) DNA double strand break repair in mammalian cells. *Current opinion in genetics & development* **10**:144-150.
- Kaufman MH (1992) *The Atlas of Mouse Development*, Elsevier Academic Press London, UK.
- Kennedy BJ (1972) Hydroxyurea therapy in chronic myelogenous leukemia. *Cancer* **29**:1052-1056.
- Keogh MC, Kim JA, Downey M, Fillingham J, Chowdhury D, Harrison JC, Onishi M, Datta N, Galicia S, Emili A, Lieberman J, Shen X, Buratowski S, Haber JE, Durocher D, Greenblatt JF and Krogan NJ (2006) A phosphatase complex that dephosphorylates gammaH2AX regulates DNA damage checkpoint recovery. *Nature* **439**:497-501.
- Khanna KK and Jackson SP (2001) DNA double-strand breaks: signaling, repair and the cancer connection. *Nature genetics* **27**:247-254.
- Khera KS (1979) A teratogenicity study on hydroxyurea and diphenylhydantoin in cats. *Teratology* **20**:447-452.
- Kim PM, Winn LM, Parman T and Wells PG (1997) UDP-glucuronosyltransferase-mediated protection against in vitro DNA oxidation and micronucleus formation initiated by

- phenytoin and its embryotoxic metabolite 5-(p-hydroxyphenyl)-5-phenylhydantoin. *The Journal of pharmacology and experimental therapeutics* **280**:200-209.
- Kinner A, Wu W, Staudt C and Iliakis G (2008) Gamma-H2AX in recognition and signaling of DNA double-strand breaks in the context of chromatin. *Nucleic acids research* **36**:5678-5694.
- Kishi H, Nakagawa K, Matsumoto M, Suga M, Ando M, Taya Y and Yamaizumi M (2001) Osmotic shock induces G1 arrest through p53 phosphorylation at Ser33 by activated p38MAPK without phosphorylation at Ser15 and Ser20. *The Journal of biological chemistry* **276**:39115-39122.
- Kleine H and Luscher B (2009) Learning how to read ADP-ribosylation. *Cell* **139**:17-19.
- Knobloch J, Shaughnessy JD, Jr. and Ruther U (2007) Thalidomide induces limb deformities by perturbing the Bmp/Dkk1/Wnt signaling pathway. *FASEB journal : official publication of the Federation of American Societies for Experimental Biology* **21**:1410-1421.
- Krakoff IH, Brown NC and Reichard P (1968) Inhibition of ribonucleoside diphosphate reductase by hydroxyurea. *Cancer research* **28**:1559-1565.
- Kuma Y, Campbell DG and Cuenda A (2004) Identification of glycogen synthase as a new substrate for stress-activated protein kinase 2b/p38beta. *The Biochemical journal* **379**:133-139.
- Kumar S, McDonnell PC, Gum RJ, Hand AT, Lee JC and Young PR (1997) Novel homologues of CSBP/p38 MAP kinase: activation, substrate specificity and sensitivity to inhibition by pyridinyl imidazoles. *Biochemical and biophysical research communications* **235**:533-538.

- Kurosu T, Takahashi Y, Fukuda T, Koyama T, Miki T and Miura O (2005) p38 MAP kinase plays a role in G2 checkpoint activation and inhibits apoptosis of human B cell lymphoma cells treated with etoposide. *Apoptosis : an international journal on programmed cell death* **10**:1111-1120.
- Lavin MF and Shiloh Y (1997) The genetic defect in ataxia-telangiectasia. *Annual review of immunology* **15**:177-202.
- Lee NK, Choi YG, Baik JY, Han SY, Jeong DW, Bae YS, Kim N and Lee SY (2005) A crucial role for reactive oxygen species in RANKL-induced osteoclast differentiation. *Blood* **106**:852-859.
- Lee Y, Barnes DE, Lindahl T and McKinnon PJ (2000) Defective neurogenesis resulting from DNA ligase IV deficiency requires Atm. *Genes & development* **14**:2576-2580.
- Lenz W and Knapp K (1962) Thalidomide embryopathy. *Archives of environmental health* **5**:100-105.
- Li J, Stouffs M, Serrander L, Banfi B, Bettiol E, Charnay Y, Steger K, Krause KH and Jaconi ME (2006) The NADPH oxidase NOX4 drives cardiac differentiation: Role in regulating cardiac transcription factors and MAP kinase activation. *Molecular biology of the cell* **17**:3978-3988.
- Lu G, Kang YJ, Han J, Herschman HR, Stefani E and Wang Y (2006) TAB-1 modulates intracellular localization of p38 MAP kinase and downstream signaling. *The Journal of biological chemistry* **281**:6087-6095.
- Mac Auley A, Werb Z and Mirkes PE (1993) Characterization of the unusually rapid cell cycles during rat gastrulation. *Development* **117**:873-883.

- Madaan K, Kaushik D and Verma T (2012) Hydroxyurea: a key player in cancer chemotherapy. *Expert review of anticancer therapy* **12**:19-29.
- Mah LJ, El-Osta A and Karagiannis TC (2010) gammaH2AX: a sensitive molecular marker of DNA damage and repair. *Leukemia : official journal of the Leukemia Society of America, Leukemia Research Fund, UK* **24**:679-686.
- Mahaney BL, Meek K and Lees-Miller SP (2009) Repair of ionizing radiation-induced DNA double-strand breaks by non-homologous end-joining. *The Biochemical journal* **417**:639-650.
- Maroto M and Pourquie O (2001) A molecular clock involved in somite segmentation. *Current topics in developmental biology* **51**:221-248.
- Matsuzawa A and Ichijo H (2008) Redox control of cell fate by MAP kinase: physiological roles of ASK1-MAP kinase pathway in stress signaling. *Biochimica et biophysica acta* **1780**:1325-1336.
- McManus KJ and Hendzel MJ (2005) ATM-dependent DNA damage-independent mitotic phosphorylation of H2AX in normally growing mammalian cells. *Molecular biology of the cell* **16**:5013-5025.
- Mirkes PE and Little SA (1998) Teratogen-induced cell death in postimplantation mouse embryos: differential tissue sensitivity and hallmarks of apoptosis. *Cell death and differentiation* **5**:592-600.
- Mirkes PE and Little SA (2000) Cytochrome c release from mitochondria of early postimplantation murine embryos exposed to 4-hydroperoxycyclophosphamide, heat shock, and staurosporine. *Toxicology and applied pharmacology* **162**:197-206.

- Moallem SA and Hales BF (1998) The role of p53 and cell death by apoptosis and necrosis in 4-hydroperoxycyclophosphamide-induced limb malformations. *Development* **125**:3225-3234.
- Morris MC, Heitz A, Mery J, Heitz F and Divita G (2000) An essential phosphorylation-site domain of human cdc25C interacts with both 14-3-3 and cyclins. *The Journal of biological chemistry* **275**:28849-28857.
- Mudgett JS, Ding J, Guh-Siesel L, Chartrain NA, Yang L, Gopal S and Shen MM (2000) Essential role for p38alpha mitogen-activated protein kinase in placental angiogenesis. *Proceedings of the National Academy of Sciences of the United States of America* **97**:10454-10459.
- Nagata S and Golstein P (1995) The Fas death factor. *Science* **267**:1449-1456.
- Nishitoh H, Saitoh M, Mochida Y, Takeda K, Nakano H, Rothe M, Miyazono K and Ichijo H (1998) ASK1 is essential for JNK/SAPK activation by TRAF2. *Molecular cell* **2**:389-395.
- Noguchi T, Ishii K, Fukutomi H, Naguro I, Matsuzawa A, Takeda K and Ichijo H (2008) Requirement of reactive oxygen species-dependent activation of ASK1-p38 MAPK pathway for extracellular ATP-induced apoptosis in macrophage. *The Journal of biological chemistry* **283**:7657-7665.
- Ornoy A (2007) Embryonic oxidative stress as a mechanism of teratogenesis with special emphasis on diabetic embryopathy. *Reprod Toxicol* **24**:31-41.
- Owens DM and Keyse SM (2007) Differential regulation of MAP kinase signalling by dual-specificity protein phosphatases. *Oncogene* **26**:3203-3213.

- Pachkowski BF, Guyton KZ and Sonawane B (2011) DNA repair during in utero development: a review of the current state of knowledge, research needs, and potential application in risk assessment. *Mutation research* **728**:35-46.
- Parker CG, Hunt J, Diener K, McGinley M, Soriano B, Keesler GA, Bray J, Yao Z, Wang XS, Kohno T and Lichenstein HS (1998) Identification of stathmin as a novel substrate for p38 delta. *Biochemical and biophysical research communications* **249**:791-796.
- Peng Y, Kwok KH, Yang PH, Ng SS, Liu J, Wong OG, He ML, Kung HF and Lin MC (2005) Ascorbic acid inhibits ROS production, NF-kappa B activation and prevents ethanol-induced growth retardation and microencephaly. *Neuropharmacology* **48**:426-434.
- Perera FP, Jedrychowski W, Rauh V and Whyatt RM (1999) Molecular epidemiologic research on the effects of environmental pollutants on the fetus. *Environmental health perspectives* **107 Suppl 3**:451-460.
- Phong MS, Van Horn RD, Li S, Tucker-Kellogg G, Surana U and Ye XS (2010) p38 mitogen-activated protein kinase promotes cell survival in response to DNA damage but is not required for the G(2) DNA damage checkpoint in human cancer cells. *Molecular and cellular biology* **30**:3816-3826.
- Pinkus R, Weiner LM and Daniel V (1996) Role of oxidants and antioxidants in the induction of AP-1, NF-kappaB, and glutathione S-transferase gene expression. *The Journal of biological chemistry* **271**:13422-13429.
- Poli J, Tsaponina O, Crabbe L, Keszthelyi A, Pantesco V, Chabes A, Lengronne A and Pasero P (2012) dNTP pools determine fork progression and origin usage under replication stress. *The EMBO journal* **31**:883-894.

- Puri PL, Wu Z, Zhang P, Wood LD, Bhakta KS, Han J, Feramisco JR, Karin M and Wang JY (2000) Induction of terminal differentiation by constitutive activation of p38 MAP kinase in human rhabdomyosarcoma cells. *Genes & development* **14**:574-584.
- Raingeaud J, Gupta S, Rogers JS, Dickens M, Han J, Ulevitch RJ and Davis RJ (1995) Pro-inflammatory cytokines and environmental stress cause p38 mitogen-activated protein kinase activation by dual phosphorylation on tyrosine and threonine. *The Journal of biological chemistry* **270**:7420-7426.
- Raman M, Chen W and Cobb MH (2007) Differential regulation and properties of MAPKs. *Oncogene* **26**:3100-3112.
- Reinhardt HC, Hasskamp P, Schmedding I, Morandell S, van Vugt MA, Wang X, Linding R, Ong SE, Weaver D, Carr SA and Yaffe MB (2010) DNA damage activates a spatially distinct late cytoplasmic cell-cycle checkpoint network controlled by MK2-mediated RNA stabilization. *Molecular cell* **40**:34-49.
- Remy G, Risco AM, Inesta-Vaquera FA, Gonzalez-Teran B, Sabio G, Davis RJ and Cuenda A (2010) Differential activation of p38MAPK isoforms by MKK6 and MKK3. *Cellular signalling* **22**:660-667.
- Rodriguez-Bravo V, Guaita-Esteruelas S, Salvador N, Bachs O and Agell N (2007) Different S/M checkpoint responses of tumor and non tumor cell lines to DNA replication inhibition. *Cancer research* **67**:11648-11656.
- Rogakou EP, Boon C, Redon C and Bonner WM (1999) Megabase chromatin domains involved in DNA double-strand breaks in vivo. *The Journal of cell biology* **146**:905-916.

- Rogakou EP, Pilch DR, Orr AH, Ivanova VS and Bonner WM (1998) DNA double-stranded breaks induce histone H2AX phosphorylation on serine 139. *The Journal of biological chemistry* **273**:5858-5868.
- Roulston A, Reinhard C, Amiri P and Williams LT (1998) Early activation of c-Jun N-terminal kinase and p38 kinase regulate cell survival in response to tumor necrosis factor alpha. *The Journal of biological chemistry* **273**:10232-10239.
- Ruiz-Gines JA, Lopez-Ongil S, Gonzalez-Rubio M, Gonzalez-Santiago L, Rodriguez-Puyol M and Rodriguez-Puyol D (2000) Reactive oxygen species induce proliferation of bovine aortic endothelial cells. *Journal of cardiovascular pharmacology* **35**:109-113.
- Salas-Vidal E, Lomeli H, Castro-Obregon S, Cuervo R, Escalante-Alcalde D and Covarrubias L (1998) Reactive oxygen species participate in the control of mouse embryonic cell death. *Experimental cell research* **238**:136-147.
- Sanchez-Carbente MR, Castro-Obregon S, Covarrubias L and Narvaez V (2005) Motoneuronal death during spinal cord development is mediated by oxidative stress. *Cell death and differentiation* **12**:279-291.
- Sastre J, Diazrubio E, Blanco J and Cifuentes L (1996a) Experimental study of the protective effect of glutathione against cisplatin-induced nephrotoxicity. *Oncology reports* **3**:1149-1152.
- Sastre J, Pallardo FV and Vina J (1996b) Glutathione, oxidative stress and aging. *Age* **19**:129-139.
- Sauer H, Gunther J, Hescheler J and Wartenberg M (2000a) Thalidomide inhibits angiogenesis in embryoid bodies by the generation of hydroxyl radicals. *The American journal of pathology* **156**:151-158.

- Sauer H, Rahimi G, Hescheler J and Wartenberg M (2000b) Role of reactive oxygen species and phosphatidylinositol 3-kinase in cardiomyocyte differentiation of embryonic stem cells. *FEBS letters* **476**:218-223.
- Savic V, Yin B, Maas NL, Bredemeyer AL, Carpenter AC, Helmink BA, Yang-Iott KS, Sleckman BP and Bassing CH (2009) Formation of dynamic gamma-H2AX domains along broken DNA strands is distinctly regulated by ATM and MDC1 and dependent upon H2AX densities in chromatin. *Molecular cell* **34**:298-310.
- Schlisser AE, Yan J and Hales BF (2010) Teratogen-induced oxidative stress targets glyceraldehyde-3-phosphate dehydrogenase in the organogenesis stage mouse embryo. *Toxicological sciences : an official journal of the Society of Toxicology* **118**:686-695.
- Schnabel D, Salas-Vidal E, Narvaez V, Sanchez-Carbente Mdel R, Hernandez-Garcia D, Cuervo R and Covarrubias L (2006) Expression and regulation of antioxidant enzymes in the developing limb support a function of ROS in interdigital cell death. *Developmental biology* **291**:291-299.
- Schreiber M, Kolbus A, Piu F, Szabowski A, Mohle-Steinlein U, Tian J, Karin M, Angel P and Wagner EF (1999) Control of cell cycle progression by c-Jun is p53 dependent. *Genes & development* **13**:607-619.
- Sedelnikova OA, Rogakou EP, Panyutin IG and Bonner WM (2002) Quantitative detection of (125)IdU-induced DNA double-strand breaks with gamma-H2AX antibody. *Radiation research* **158**:486-492.
- Sedmera D, Reckova M, DeAlmeida A, Coppin SR, Kubalak SW, Gourdie RG and Thompson RP (2003) Spatiotemporal pattern of commitment to slowed proliferation in the embryonic mouse heart indicates progressive differentiation of the cardiac conduction

- system. *The anatomical record Part A, Discoveries in molecular, cellular, and evolutionary biology* **274**:773-777.
- Shackelford RE, Innes CL, Sieber SO, Heinloth AN, Leadon SA and Paules RS (2001) The Ataxia telangiectasia gene product is required for oxidative stress-induced G1 and G2 checkpoint function in human fibroblasts. *The Journal of biological chemistry* **276**:21951-21959.
- She QB, Chen N and Dong Z (2000) ERKs and p38 kinase phosphorylate p53 protein at serine 15 in response to UV radiation. *The Journal of biological chemistry* **275**:20444-20449.
- Sneedden JL and Loeb LA (2004) Mutations in the R2 subunit of ribonucleotide reductase that confer resistance to hydroxyurea. *The Journal of biological chemistry* **279**:40723-40728.
- Soleman D, Cornel L, Little SA and Mirkes PE (2003) Teratogen-induced activation of the mitochondrial apoptotic pathway in the yolk sac of day 9 mouse embryos. *Birth defects research Part A, Clinical and molecular teratology* **67**:98-107.
- Stiff T, O'Driscoll M, Rief N, Iwabuchi K, Lobrich M and Jeggo PA (2004) ATM and DNA-PK function redundantly to phosphorylate H2AX after exposure to ionizing radiation. *Cancer research* **64**:2390-2396.
- Stucki M, Clapperton JA, Mohammad D, Yaffe MB, Smerdon SJ and Jackson SP (2005) MDC1 directly binds phosphorylated histone H2AX to regulate cellular responses to DNA double-strand breaks. *Cell* **123**:1213-1226.
- Sulik KK, Cook CS and Webster WS (1988) Teratogens and craniofacial malformations: relationships to cell death. *Development* **103 Suppl**:213-231.
- Sung P (1997) Function of yeast Rad52 protein as a mediator between replication protein A and the Rad51 recombinase. *The Journal of biological chemistry* **272**:28194-28197.

- Suzanne M, Irie K, Glise B, Agnes F, Mori E, Matsumoto K and Noselli S (1999) The Drosophila p38 MAPK pathway is required during oogenesis for egg asymmetric development. *Genes & development* **13**:1464-1474.
- Takekawa M, Maeda T and Saito H (1998) Protein phosphatase 2 $\alpha$  inhibits the human stress-responsive p38 and JNK MAPK pathways. *The EMBO journal* **17**:4744-4752.
- Tamura K, Sudo T, Senfleben U, Dadak AM, Johnson R and Karin M (2000) Requirement for p38 $\alpha$  in erythropoietin expression: a role for stress kinases in erythropoiesis. *Cell* **102**:221-231.
- Tao W and Levine AJ (1999) P19(ARF) stabilizes p53 by blocking nucleo-cytoplasmic shuttling of Mdm2. *Proceedings of the National Academy of Sciences of the United States of America* **96**:6937-6941.
- Thornton TM, Pedraza-Alva G, Deng B, Wood CD, Aronshtam A, Clements JL, Sabio G, Davis RJ, Matthews DE, Doble B and Rincon M (2008) Phosphorylation by p38 MAPK as an alternative pathway for GSK3 $\beta$  inactivation. *Science* **320**:667-670.
- Tobiume K, Matsuzawa A, Takahashi T, Nishitoh H, Morita K, Takeda K, Minowa O, Miyazono K, Noda T and Ichijo H (2001) ASK1 is required for sustained activations of JNK/p38 MAP kinases and apoptosis. *EMBO reports* **2**:222-228.
- Uhlik MT, Abell AN, Johnson NL, Sun W, Cuevas BD, Lobel-Rice KE, Horne EA, Dell'Acqua ML and Johnson GL (2003) Rac-MEKK3-MKK3 scaffolding for p38 MAPK activation during hyperosmotic shock. *Nature cell biology* **5**:1104-1110.
- Unal E, Arbel-Eden A, Sattler U, Shroff R, Lichten M, Haber JE and Koshland D (2004) DNA damage response pathway uses histone modification to assemble a double-strand break-specific cohesin domain. *Molecular cell* **16**:991-1002.

- Vasudevan SA, Skoko J, Wang K, Burlingame SM, Patel PN, Lazo JS, Nuchtern JG and Yang J (2005) MKP-8, a novel MAPK phosphatase that inhibits p38 kinase. *Biochemical and biophysical research communications* **330**:511-518.
- Vinson RK and Hales BF (2002) DNA repair during organogenesis. *Mutation research* **509**:79-91.
- Walker AL, Steward S, Howard TA, Mortier N, Smeltzer M, Wang YD and Ware RE (2011) Epigenetic and molecular profiles of erythroid cells after hydroxyurea treatment in sickle cell anemia. *Blood* **118**:5664-5670.
- Wang L, Ma R, Flavell RA and Choi ME (2002) Requirement of mitogen-activated protein kinase kinase 3 (MKK3) for activation of p38alpha and p38delta MAPK isoforms by TGF-beta 1 in murine mesangial cells. *The Journal of biological chemistry* **277**:47257-47262.
- Ward IM and Chen J (2001) Histone H2AX is phosphorylated in an ATR-dependent manner in response to replicational stress. *The Journal of biological chemistry* **276**:47759-47762.
- Warr N, Carre GA, Siggers P, Faleato JV, Brixey R, Pope M, Bogani D, Childers M, Wells S, Scudamore CL, Tedesco M, Barrantes ID, Nebreda AR, Trainor PA and Greenfield A (2012) Gadd45 gamma and Map3k4 Interactions Regulate Mouse Testis Determination via p38 MAPK-Mediated Control of Sry Expression. *Dev Cell* **23**:1020-1031.
- Wells PG, McCallum GP, Chen CS, Henderson JT, Lee CJ, Perstin J, Preston TJ, Wiley MJ and Wong AW (2009) Oxidative stress in developmental origins of disease: teratogenesis, neurodevelopmental deficits, and cancer. *Toxicological sciences : an official journal of the Society of Toxicology* **108**:4-18.

- Wells PG, McCallum GP, Lam KC, Henderson JT and Ondovcik SL (2010) Oxidative DNA damage and repair in teratogenesis and neurodevelopmental deficits. *Birth defects research Part C, Embryo today : reviews* **90**:103-109.
- Wells PG and Winn LM (1996) Biochemical toxicology of chemical teratogenesis. *Critical reviews in biochemistry and molecular biology* **31**:1-40.
- Wiese AG, Pacifici RE and Davies KJ (1995) Transient adaptation of oxidative stress in mammalian cells. *Archives of biochemistry and biophysics* **318**:231-240.
- Wilson JG, Scott WJ, Ritter EJ and Fradkin R (1975) Comparative distribution and embryotoxicity of hydroxyurea in pregnant rats and rhesus monkeys. *Teratology* **11**:169-178.
- Winn LM and Wells PG (1995) Phenytoin-initiated DNA oxidation in murine embryo culture, and embryo protection by the antioxidative enzymes superoxide dismutase and catalase: evidence for reactive oxygen species-mediated DNA oxidation in the molecular mechanism of phenytoin teratogenicity. *Molecular pharmacology* **48**:112-120.
- Wolter KG, Hsu YT, Smith CL, Nechushtan A, Xi XG and Youle RJ (1997) Movement of Bax from the cytosol to mitochondria during apoptosis. *The Journal of cell biology* **139**:1281-1292.
- Wong AW, McCallum GP, Jeng W and Wells PG (2008) Oxoguanine glycosylase 1 protects against methamphetamine-enhanced fetal brain oxidative DNA damage and neurodevelopmental deficits. *The Journal of neuroscience : the official journal of the Society for Neuroscience* **28**:9047-9054.

- Wood CD, Thornton TM, Sabio G, Davis RA and Rincon M (2009) Nuclear localization of p38 MAPK in response to DNA damage. *International journal of biological sciences* **5**:428-437.
- Wu GS, Burns TF, McDonald ER, 3rd, Jiang W, Meng R, Krantz ID, Kao G, Gan DD, Zhou JY, Muschel R, Hamilton SR, Spinner NB, Markowitz S, Wu G and el-Deiry WS (1997) KILLER/DR5 is a DNA damage-inducible p53-regulated death receptor gene. *Nature genetics* **17**:141-143.
- Wubah JA, Ibrahim MM, Gao X, Nguyen D, Pisano MM and Knudsen TB (1996) Teratogen-induced eye defects mediated by p53-dependent apoptosis. *Current biology : CB* **6**:60-69.
- Wyman C and Kanaar R (2006) DNA double-strand break repair: all's well that ends well. *Annual review of genetics* **40**:363-383.
- Xie A, Puget N, Shim I, Odate S, Jarzyna I, Bassing CH, Alt FW and Scully R (2004) Control of sister chromatid recombination by histone H2AX. *Molecular cell* **16**:1017-1025.
- Yan J and Hales BF (2005) Activator protein-1 (AP-1) DNA binding activity is induced by hydroxyurea in organogenesis stage mouse embryos. *Toxicological sciences : an official journal of the Society of Toxicology* **85**:1013-1023.
- Yan J and Hales BF (2006) Depletion of glutathione induces 4-hydroxynonenal protein adducts and hydroxyurea teratogenicity in the organogenesis stage mouse embryo. *The Journal of pharmacology and experimental therapeutics* **319**:613-621.
- Yan J and Hales BF (2008) p38 and c-Jun N-terminal kinase mitogen-activated protein kinase signaling pathways play distinct roles in the response of organogenesis-stage embryos to a teratogen. *The Journal of pharmacology and experimental therapeutics* **326**:764-772.

Yarbro JW (1968) Further studies on the mechanism of action of hydroxyurea. *Cancer research* **28**:1082-1087.

Young PR, McLaughlin MM, Kumar S, Kassis S, Doyle ML, McNulty D, Gallagher TF, Fisher S, McDonnell PC, Carr SA, Huddleston MJ, Seibel G, Porter TG, Livi GP, Adams JL and Lee JC (1997) Pyridinyl imidazole inhibitors of p38 mitogen-activated protein kinase bind in the ATP site. *The Journal of biological chemistry* **272**:12116-12121.

Zhan Q, Antinore MJ, Wang XW, Carrier F, Smith ML, Harris CC and Fornace AJ, Jr. (1999) Association with Cdc2 and inhibition of Cdc2/Cyclin B1 kinase activity by the p53-regulated protein Gadd45. *Oncogene* **18**:2892-2900.

Zuzarte-Luis V, Montero JA, Rodriguez-Leon J, Merino R, Rodriguez-Rey JC and Hurle JM (2004) A new role for BMP5 during limb development acting through the synergic activation of Smad and MAPK pathways. *Developmental biology* **272**:39-52.